SSSU 87
ISSN 0140 3818

THE THEORETICAL INVESTIGATION OF A SERIES OF HIGH SPEED DISPLACEMENT CATAMARAN FORMS: VARIATION OF PRISMATIC COEFFICIENT

A.F. Molland and A.R. Lee

Ship Science Report 87

February 1995

THE THEORETICAL INVESTIGATION OF A SERIES OF HIGH SPEED DISPLACEMENT CATAMARAN FORMS: VARIATION OF PRISMATIC COEFFICIENT

A.F. Molland and Adrian R. Lee

Ship Science Report No. 87
University of Southampton

February 1995

CONTENTS

NOMENCLATURE

The nomenclature follows the terms given by the 'ITTC Dictionary of Ship Hydrodynamics' [1], except for some additional terms which are as follows;

"CATAMARAN" refers to any ship with two hulls, side by side and joined to each other by means of a bridge structure above the free surface.

A "DEMIHULL" is one of the hulls which make up the catamaran vessel.

"SEPARATION", (S), is the distance between the centrelines of the demihulls of a catamaran.

C_T	: Total Resistance Coefficient	
C_F	: Frictional Resistance Coefficient	
C_{FO}	: Form Resistance Coefficient	: KC_F
C_V	: Viscous Resistance Coefficient	: $(1+K)C_F$
C_{WT}	: Wake Traverse Resistance Coefficient	
C_R	: Residuary Resistance Coefficient	: C_T-C_F
C_W	: Wave Resistance Coefficient	: C_T-C_V
C_{WP}	: Wave Pattern Resistance Coefficient	
C_I	: Induced Drag Coefficient	
C_{WTHE}	: Theoretical Wave Resistance Coefficient	
C_{TS}	: Transom Stern Resistance Coefficient	
$(1+K)$	: Form Factor	: C_V/C_F
$(1+K_{WP})$	: Form Factor	: $(C_T-C_{WP})/C_F$
L, LWL	: Length on Waterline	
LOA	: Length Overall	
B	: Beam	
T	: Draught	
D	: Depth	
S	: Separation distance between the centrelines of the demihulls of a catamaran.	
W	: Width of a Catamaran	
C_B	: Block Coefficient	
C_P	: Prismatic Coefficient	
C_W	: Waterplane Coefficient	
C_M	: Midship Section Coefficient	
∇	: Displacement Volume	
V	: Ship Speed	
Fn	: Froude Number	
Re	: Reynolds Number	
R_{TS}	: Hydrostatic Transom Resistance	
R_{TSC}	: Hydrostatic Transom Resistance Corrected	
Ω	: Residuary Resistance Interference Factor	
β	: Form Resistance Interference Factor	
τ	: Wave Resistance Interference Factor	

1 INTRODUCTION

The effect of hull spacing (S/L), length to displacement ratio and breadth to draught ratio (B/T) have been investigated experimentally and theoretically at the University of Southampton using a systematic series of semi-displacement round bilge hulls [2,3,4].

Previous research [2] involving parametric studies of Prismatic coefficient (C_P) had indicated that this was an area worthy of further study. The importance of C_P on residuary resistance has been long recognised [5]. Changing the C_P of a hull changes the pressure distribution and therefore the flow around a demihull. It affects the wave resistance and the form resistance. However, no systematic study of prismatic coefficient for high speed transom sterned catamarans appears to have been carried out or published.

This research expands the existing catamaran series by investigating the effect of Prismatic coefficient on demihull interaction. This report describes the theoretical investigation; experimental testing is the subject of a separate Ship Science report [6].

2 HULL FORMS USED IN THE INVESTIGATION

The range of models used in the overall investigation are shown in Table 1. The hulls are of round bilge form and symmetrical about the centre line. The base vessel used for this particular study was model 5b with a prismatic coefficient of 0.693. From this parent hull two hulls were derived, 5d with a C_P of 0.653 and 5e with a C_P of 0.733. Theoretical parametric studies were performed on these demihulls in isolation and in catamaran form with hull separations of S/L 0.2, 0.3, 0.4, and 0.5, for beam draught ratios of 1.5, 2.0 and 2.5 as well as length to displacement ratios of 11 and 13.

Model 4b was also studied in its original condition and for a lower displacement. The lower displacement case coincided with the 5 series and produced a C_P close to 5d.

3 THEORETICAL WAVE RESISTANCE

3.1 Thin Ship Theory

One method developed at Southampton uses linearised wave resistance theory [7,8]. This defines a body with a source sink distribution along the centreplane. The method can only model slender hull forms satisfactorily and assumes the following:

1) The fluid is inviscid, incompressible and homogeneous.
2) The fluid motion is steady and irrotational.
3) Surface tension can be neglected.
4) Wave height at the free surface is small compared with the wave length.

Due to the relatively high length to breadth ratios of catamaran hulls thin ship theory should be capable of producing reasonable predictions of wave resistance. The basic theory, however, does not account for immersed transom effects. The immersed transom which is a feature of most catamaran designs has a significant effect on the wave resistance.

The original program, developed by Insel [2], divided the hull into a series of rectangular panels defined by a uniform grid of stations and waterlines, and the source strengths were calculated from the hull offsets. A hydrostatic adjustment for the transom was then added as employed by several other researchers.

3.2 Program Modifications

The main objects of this work have been to improve the method of incorporating running sinkage and trim, defining the panels and modelling the transom stern.

An investigation was first carried out into the effect on the calculated resistance of changing the number of harmonics and maximum wave angle. Investigations were also carried out to establish the sensitivity of wave resistance to channel depth and width.

The program was modified to work with planes set at varying angles to the horizontal, in the fore and aft direction, referred to as 'fanned waterlines' (Figure 1). This would allow the number of panels along the length of the craft to be kept near constant. Due to the fanned waterlines, panels were no longer of constant size or rectangular in shape.

A different hull definition program was developed that was capable of generating fanned waterlines.

After the first modification was completed to enable fanned waterlines to be used, a series of test cases were run to check the following:

I) Accuracy of the program.

II) Effect of changing the number of equally spaced parallel waterlines.

III) Effect of using unequally spaced parallel waterlines.

IV) Effect of changing the number of fanned waterlines.

V) Difference in wave resistance results between parallel and fanned waterlines.

VI) Change in resistance due to sinkage compared with the change in resistance due to the associated change in panel size.

VII) Change in resistance due to trim compared with the change in resistance due to the associated change in panel size.

3.3 Transom Resistance

A second modification to the program was undertaken to further improve the mathematical modelling of the transom effects. This was because the study of prismatic would necessitate a variation in transom to maximum area ratio, and the transom resistance would be a significant component. The original program, like several used by other researchers, makes a hydrostatic adjustment for the transom. This predicted the experimental results reasonably well above a Froude number of approximately 0.5, but below Fn 0.5 the transom resistance was poorly modelled by the correction.

The hydrostatic correction is a simple addition to the wave resistance:

$$R_{TS} = \int \rho g z \, dz dy$$

The area and depth of immersion of each of the final hull panels is used to determine the transom resistance.

A transom when immersed at low speed causes eddying in the water and a large amount of entrained water moving with the craft increases the resistance. As the craft increases speed the transom progressively comes clear of the water, thus reducing the amount of turbulence. At high speed the transom is totally clear and leaves a surface depression which increases in length with speed. The water flows back into the depression and forms a rooster's tail breaking wave. SHIN et. al.[9] describe the stern wave as " a type of hydraulic jump drastically generated behind the transom stern". The wave formed by the transom when clear is initially steep and breaking but as speed increases the slope of the wave decreases and at certain speeds has little breaking water.

Other researchers in the field have attempted to model the transom in different ways using various source

distributions but there has been little systematical appraisal of the reasons why their particular method has been adopted.

3.3.1 Source Strengths

The source strengths and the total source strength over the entire body were investigated in order to support a simple but effective way of modelling the transom.

For a hull without a transom stern the total net source strength over the entire hull should be zero i.e. no water passes through the hull. For the Wigley hull this was found to be the case and, as predicted, a plot of source strength against hull length produced a straight line (Figure 2) for each waterline and therefore also for the entire body.

On plotting the source strengths for the transom sterned hulls an 'S' shaped curve was produced with a net positive source strength (Figure 3) for each waterline. The amount of curve and the degree of imbalance in the source strengths varied with each waterline. The curves showed a spike at the bow which was considered to be incorrect. The spike was smoothed out by manual manipulation of the file and the calculations rerun (Figure 4). The result was a minimal change in wave resistance.

Further aft as the hull profile crossed a waterline, thereby reducing the hull definition by one panel, a step in the source strength was produced (Figures 3 and 4). The summation of all the horizontal layers produced a curve of total source strength along the hull. This line should be a fair curve but the combination of the steps in the individual source strength curves for each layer introduces either a general unfairness or a spike in the curve for the summation of these source strengths (Figures 5-7).

The lower speeds show a general unfairness in the total source strength curve due to the fact that at the lower trim angles nearly half the panels crossed the profile at varying distances along the hull. At higher speeds the combination of trim and heave produce fewer panels that crossed the profile thus producing a spike in the curve rather than general unfairness, the position of the spike being controlled by the sinkage and trim. Fairing the spike out of the curve for model 4b S/L 0.3 at a Froude number of 0.7 produced a minimal reduction (0.04%) in C_w. These effects demonstrated the need for the number of panels to be as large as possible.

3.3.2 Modelling the Transom Resistance using modified source distributions.

One possible approach to modelling the transom resistance is to measure and analyse the wave pattern and, from this, to reverse the procedure to determine what additional source distribution would be needed to produce that wave pattern. Such an approach is used in Reference 10. This process is extremely complex and an alternative systematic study of source distributions was undertaken. A single trailing source or a number of trailing sources would be investigated which would balance out the net positive strength of the hull and produce a closed body. This was considered to be a logical first attempt.

Two basic approaches were investigated. The first considered the balancing source or sources close to the transom, producing a strong local effect, Yim [11]. The second considered the hull to be extended aft to an imaginary canoe stern, Shin et.al.[9]. This would employ an extrapolation of the hull source strengths to a point where the net source strength was zero.

For each of the two basic approaches there were a number of geometries to be considered (Figures 8-10) which were as follows:

Sources close to the transom

a) A single source one standard panel distance (0.02 LWL) aft of the last hull source at half transom draft (Figure 8a).

b) A single source one standard panel distance aft of the last hull source positioned at the transom bottom (Figure 8b).

c) An array of sources one standard panel distance aft of the last hull source, the number of sources being equal to the number on the last hull panel. The local strength distribution of the sources was in proportion to those on the hull panels but of overall magnitude to produce a net zero source strength (Figure 8c).

d) Three transverse sources of equal strength at one standard panel distance aft at half draft (Figure 9). The sources were distributed transversely using three possible separations; 1/6, 1/5, 1/4 of max waterline beam.

e) Three transverse sources of equal strength at one standard panel distance aft at the transom bottom. The sources were distributed transversely using the same separations as in d; 1/6, 1/5, 1/4 of max waterline beam.

Sources extending aft

f) A single line of sources at standard panel spacings extending aft in the wake at half draft (Figure 10f). The strengths of the sources were determined by extrapolating values from the total source strength of the hull. The number of sources was determined by the requirement to achieve a zero net source strength.

g) As (f) except that the trailing line of sources were moved to the bottom of the transom (Figure 10g).

h) This was similar to cases (f) and (g) except a full vertical array of trailing sources were used up to transom depth with proportional strengths as described in (c) (Figure 10h).

i) The array used in (h) was truncated one panel at a time thus giving an increasing net positive source strength.

These modified source distributions were applied to the fixed sinkage and trim condition. The combinations which produced the most promising results were then run in the free condition and the results compared with experimental results (Figures 12-14). The comparisons were run initially at three Froude numbers 0.3, 0.5, 0.7 in monohull and catamaran configuration.

Due to the poor fit of the results at the lower Froude numbers the more complex transverse transom source distribution was investigated for the catamaran configuration. The transverse distribution increases the range of variables:

1) Number of sources
2) Spacing of sources
3) Relative source strength
4) Deadrise

One transverse spacing was selected for running in monohull and catamaran mode with free sinkage and trim. The sources were positioned on the centre line of each demihull and at 1/4 the maximum demihull beam either side of each demihull centre line. The sources were of equal strength and positioned in a horizontal line at the transom bottom one panel aft of the transom (Figure 15, 16 and 17).

The theoretical work for a single source at the base of the transom was then extended to investigate all the hulls tested experimentally plus breadth to draft and length to displacement variants. The work on model 4b light displacement, 5d and 5e were thought to be of particular interest as the hulls had different transom to midship area ratios and would further validate the method (Figures 24 to 73).

3.3.3 Modelling the Transom Resistance using a modified Hydrostatic correction.

The basic hydrostatic correction had also been tested over the same range of hulls and separations and had failed to satisfactorily model the wave resistance at lower speeds.

In order to provide a more realistic prediction at lower speeds for preliminary and practical design purposes an alternative approach was investigated. In this case a simple empirical modification would be applied to the basic hydrostatic correction at lower speeds in order to provide a closer correlation with the experimental data. The correction needed to be a function of Froude number with the greatest effect at the lowest speed. The final correction was of the form:

$$R_{TSC} = R_{TS} \cdot a \cdot Fn^b$$

Where R_{TS} is the basic hydrostatic transom resistance and R_{TSC} the corrected value.

This approach was applied to all the hulls to determine 'a' and 'b'.

3.4 Investigations

The theoretical work used tank test results where available for sinkage and trim with each hull being run as a monohull and at S/L of 0.3 and 0.5 in catamaran mode. Models 5d and 5e were also run at S/L of 0.2 and 0.4.

Models 5d and 5e were tested theoretically in the first instance using the sinkage and trim obtained from 5b as an estimate of the condition for both the new hulls. This was then compared with the theoretical results using the sinkage and trim obtained from actual tank test data for models 5d and 5e. This was to establish if estimated sinkage and trim values could produce useful design data.

4 DATA REDUCTION AND CORRECTION

The wetted surface area (WSA) used in each case was the static value. Although the WSA for the correct trim and sinkage could be calculated this would not truly reflect the dynamic condition including the influence of the wave elevation.

5 PRESENTATION OF DATA

Figure 1 illustrates the panel distribution for parallel and fanned waterlines.

Figures 2 to 7 show the source strengths produced by the program for various hulls and speeds.

Figures 8 to 11 illustrate the transom source distributions investigated.

Figures 12 to 17 compare the wave resistance produced using the various transom source distributions.

Figure 18 shows the effect of altering the number of harmonics and the wave angle on the calculation of the wave resistance.

Figures 19 and 20 shows the effect of altering the number of waterlines.

Figures 21 and 22 compare the resistance produced using the various different panel definition systems.

Figure 23 compares the form factors produced using theoretical values for C_W with those using C_{WP} from experiment.
Theoretical form factor:

$$(C_{T\,exp} - C_{W\,theory})/C_F$$

Figures 24 to 42 show the comparison between experimental results and theoretical results with the transom represented by a single source, a hydrostatic addition and a hydrostatic addition with a low speed correction.

Figures 43 to 54 and 56 to 82 are the theoretical results for models 4b, 4b light, 5a to 5i, 6d and 6e for both single source and the low speed corrected hydrostatic addition.

Figure 55 is a comparison of theoretical results for models 5b, 5d and 5e for the fanned waterlines system.

Figure 83 compares the transom source strengths for different hulls.

Figures 84-86 compares theoretical results for 6b with the experimental results produced by Molland [4]

6 DISCUSSION OF RESULTS

6.1 Panel Definition

6.1.1 Accuracy of the Program.

The accuracy of the program was checked using a Wigley hull form. This had been generated using a hull fairing program which was different from that used in the earlier analyses. The results proved to be in close agreement with previous work.

6.1.2 An investigation was carried out into the effect on the calculated resistance of changing the number of harmonics and the maximum wave angle.

The input values of harmonic and wave angles used were (30,70), (50,80) and (100,85). Reducing the harmonics and wave angle produced a small underprediction of the wave resistance (Figure 18). The error varied slightly for hydrostatic and transom source versions. This is because the hydrostatic correction has a greater influence on the wave resistance at low speed such that the percentage change in resistance is less than at higher speeds.

6.1.3 Effect of changing the number of equally spaced parallel waterlines.

The original program was written to calculate the source strengths for a maximum of 51 sections and 21 waterlines per hull i.e. 1000 panels. The tests on the Wigley hull for decreasing the number of parallel spaced waterlines and therefore panel density from 20 down to 10 panels per section produced a small but increasing reduction in wave making resistance (Figure 19).

6.1.4 Effect of using unequally spaced parallel waterlines

Decreasing the panel density near the waterline gave an increase in resistance, whilst reducing the panel density near the keel gave a decrease in resistance. This explains the surprisingly small change to wave making resistance for the Wigley hull form when decreasing the number of equally spaced waterlines. This is because increasing resistance values near the load waterline are compensated by the decreasing resistance values near the keel.

6.1.5 Effect of changing the number of fanned waterlines

Tests were then run on the round bilge type hull to see if the rise of floor and non-parabolic sections would change any of the findings. Due to the shape of the hull it is impossible to maintain the same number of panels at each station along the craft even with fanned waterlines. When choosing the pattern of fanned waterlines a set was established that gave a high and reasonably even density.

Decreasing the number of inclined waterlines gave a small but measurable change in calculated wave resistance, initially decreasing but then increasing (Figure 20).

6.1.6 Difference between parallel and fanned waterlines

The comparison between fanned and parallel waterlines on the 5 series hull produced a significant difference in the calculated wave making resistance with the fanned waterlines producing the lower value (Figure 21 and 22).

The fanned waterline system was used for a preliminary study of the effect of prismatic. Models 5b, 5d, and 5e were run as monohulls with fixed trim, and as catamarans with an S/L value of 0.2 over a more limited range of Froude numbers (Figure 55) using trim and sinkage values based on tank test results for model 5b.

6.1.7 Change in resistance due to sinkage compared to the change in resistance due to the associated change in panel size.

When the investigation included sinkage the panel size had to be increased. It was required to demonstrate that the subsequent variation in calculated resistance due to the necessary change in panel size did not overshadow the change in resistance due to the sinkage. The results indicated that the change in resistance due to sinkage was many orders of magnitude greater than that due to panel size.

6.1.8 Change in resistance due to trim compared with the change in resistance due to the associated change in panel size for Fanned waterlines.

There was no systematical way of comparing the results for modifying the fanning of the waterlines due to changes in trim. This would be required in order to determine if changing panel size along the craft would have a significant influence on the resistance values.

It is probable that the panel effect does not mask the true change in wave making resistance due to trim. This is because the hulls trim through a small angle which is then subdivided by the number of waterlines spacings so that each panel changes by only a small amount. Also, when a parametric study is being performed the trim angles between different hulls change by a value significantly smaller than the trim of one of the hulls.

Taken over all, the analysis indicated that inclined parallel waterlines would provide the most acceptable method of modelling trim. The method of fanning the waterlines to maintain a more constant number of panels was not adopted for several reasons: One, as the hulls adopt a running trim the uneven distribution of panels decreases; two, the affect of uneven panel distribution appears to be relatively small; three, the choice of panel distribution produced another variable into the system.

6.1.9 Sensitivity to channel depth and width

A reduction in channel dimensions by 1.5% produced only a small increase in resistance at a Froude number of 0.8 but increased with increasing Froude number to 3.6% for a Froude number of unity. These results indicate how close the models are to the critical Froude number for the onset of shallow water effects.

6.2 Transom Modelling

The results (Figure 13) showed the single source and transverse sources positioned at the bottom of the transom to be the most promising models. The single source showed little improvement in the monohull or catamaran form for the majority of the speed range compared to the hydrostatic correction, the results being a reasonable fit between Fn 0.5-1.0.

The Froude number range 0.3-0.4 was poorly modelled and it is interesting to note that this is the region in which there is partial transom separation.

Moving the sources in the longitudinal direction relative to the transom changed the results at the lower speeds but had little effect at the higher speeds (Figures 11 and 16).

Three transverse sources at a spacing of 1/4 of the maximum beam produced little change from those for the single source (Figure 15, 16 and 17). The modelling of the resistance at low speeds was not improved.

An empirical modification to the hydrostatic transom correction at low speeds led to satisfactory predictions of the wave resistance over the whole speed range. Suitable coefficients are given in Figure 23, and examples of this approach are seen in Figures 24 to 40.

6.3 Results for models 5b, 5d and 5e

The theoretical results (Figures 24 to 42) produced the same general trends as the experimental results [6] apart from the prediction in the main hump region which was poor. There is an obvious phase shift in this region. The theoretical results for model 5d, with the lower C_P and lower transom area, appeared to fit the experimental results better in the Fn range 0.5 to 0.6 than for model 5e. All three hulls had good predictions of wave resistance above this speed. Although the prediction for hull separation of S/L 0.2 was consistently worse than the other separations. The trends between 5d and 5e are generally good (Figures 60-69). The theoretical results using the estimated sinkage and trim also predicted the correct trends (Figures 53,54 and 56, 59).

6.4 Results for models 4b and 4b Light Displacement

There were significant differences between the two theoretical predictions for model 4b light (Figures 40 to 42 and 45,46). The form factor derived from the hydrostatic correction (Figure 23) was closer to the experimental value than the transom source value but the prediction was poor for an S/L of 0.5.

Model 4b at the normal displacement also produced variations between the two methods (Figures 37-39) but with neither method proving to be better for all configurations.

6.5 Results of Parametric Study

6.5.1 Results for Breadth to Draught ratio

A parametric study of B/T (1.5 to 2.5) was undertaken on 5b, 5d and 5e (Figures 47 to 52 and 74 to 79). All models exhibited a reduced resistance for the higher B/T with the effect reducing as the Froude number approached unity. This was true for all configurations tested (monohull, S/L 0.5 and 0.3). The variation was greater and extended further into the higher speed range for the higher prismatic. The higher prismatic had the lower resistance above Fn 0.4 with the combination of high C_P and high B/T being the most advantageous. This is in keeping with the experimental results [Ref 6].

6.5.2 Results for Length to Displacement ratio

A parametric study of L/B (11 to 13) was performed on models 5d and 5e for monohull and S/L 0.5 and 0.3 (Figures 60 to 69 and 80 to 82). The high prismatic produced the lower resistance at the higher speeds

for monohull and S/L 0.5 with the results for S/L 0.5 showing the greatest difference. The results for S/L 0.3 show a smaller difference with a convergence at a Fn of 0.6.

6.5.3 Results for Prismatic Coefficient

Prismatic coefficient was varied from 0.653 to 0.733. The higher C_p produced the lower wave resistance at the higher Froude numbers, except for S/L 0.2 where the curves cross and recross in the region Fn 0.65-0.75.

7 CONCLUSIONS AND RECOMMENDATIONS

7.1 The Thin Ship Theory Program

The program was sensitive to the number of panels used, their shape and size. If a consistent system is adopted for a series of hulls the sensitivity due to sinkage, trim and change in hull shape is not so extreme that it will affect the trends in the resistance results.

Parametric studies employing any given panel arrangement investigated produced consistent trends for the models.

The reliability of the prediction in trends for parametric studies has been demonstrated to be dependant on the accuracy of the trim and sinkage data. It appears that if the variation from a parent hull is not extreme, then the trim and sinkage data for that hull will be adequate for initial studies.

The theoretical results have a tendency to over predict the differences in resistance between different hulls.

The accuracy of prediction appears to vary with hull form. For example model 5d appears to be modelled well over a wider range of Froude number than 5e.

The lower length beam ratio of the 4b models (L/B 9) do not appear to be as well modelled and this may be due to the limitations of thin ship theory.

7.2 Transom Resistance

A single transom source produces as good an approximation to the transom resistance as any source distribution investigated. The transom source should be of a strength that closes the body. It can be situated on the centre line of each demihull at the bottom of the transom. Further work could, however, be carried out to establish whether changes in its longitudinal position, say as a function of speed, would improve the prediction.

A single transom source is an elegant method for correcting for the transom resistance as it is a simple extension to the thin ship theory which can be easily automated with little additional processing time.

Neither the transom source nor basic hydrostatic correction can predict wave resistance satisfactorily for speeds of Fn 0.4 and below. Due to the changing and confused flow around the transom during partial clearance it is thought unlikely that a simple theoretical model would be able to successfully predict transom resistance in this region.

It was found that a simple empirical correction to the hydrostatic transom resistance can produce results of the correct magnitude, and appears to predict the correct trends at low Froude numbers. However, the fit with experimental results is still not good at low speed. This may be due to some phase shift and lack of damping in the thin ship theory. It is likely that improvements in the empirical correction could be made by incorporating the effects of L/B and C_p.

The comparison of the accuracy between the theoretical and the experimental results for one hull configuration and another was dependant on the accuracy of determining the values of $(1+k)$ and $(1+\beta k)$.

7.3 Parametric Investigation

The parametric studies suggest that a catamaran with low prismatic demi-hulls has less hull interaction than a form with a high C_p.

The effect of changing prismatic coefficient is less important to the resistance at higher speeds.

The breadth to draught ratio affects the resistance of monohulls and catamarans at lower speeds with higher B/T being advantageous.

Breadth to draught ratio affects demihulls with a low C_p to a lesser extent than those with a high C_p.

REFERENCES

1) ITTC DICTIONARY OF SHIP HYDRODYNAMICS
MARITIME TECHNOLOGY MONOGRAPH NO 6 RINA 1978

2) INSEL M.
AN INVESTIGATION INTO THE RESISTANCE COMPONENTS OF HIGH SPEED CATAMARANS.

PhD THESIS, UNIVERSITY OF SOUTHAMPTON

3) INSEL M. AND MOLLAND A.F.
AN INVESTIGATION INTO THE RESISTANCE COMPONENTS OF HIGH SPEED DISPLACEMENT CATAMARANS.

TRANS RINA 1992

4) MOLLAND A.F, WELLICOME J.F, COUSER P.
RESISTANCE EXPERIMENTS ON A SYSTEMATIC SERIES OF HIGH SPEED CATAMARAN FORMS: VARIATION OF LENGTH TO DISPLACEMENT RATIO AND BREADTH TO DRAUGHT RATIO.

UNIVERSITY OF SOUTHAMPTON SHIP SCIENCE REPORT NO. 71, 1994

5) TAYLOR D.
THE SPEED AND POWER OF SHIPS

THE UNITED STATES GOVERNMENT PRINTING OFFICE
1943

6) MOLLAND A.F, LEE A.R.
RESISTANCE EXPERIMENTS ON A SERIES OF HIGH SPEED DISPLACEMENT CATAMARAN FORMS: VARIATION OF PRISMATIC COEFFICIENT.

UNIVERSITY OF SOUTHAMPTON SHIP SCIENCE REPORT NO. 86, 1995

7) INSEL M, MOLLAND A.F, WELLICOME J.F.
WAVE RESISTANCE PREDICTION OF A CATAMARAN BY LINEARISED THEORY.

PROCEEDINGS OF CONFERENCE CADMO'94, SOUTHAMPTON, COMPUTATIONAL MECHANICS PUBLICATIONS, 1994.

8) MOLLAND A.F, WELLICOME J.F, COUSER P.
THEORETICAL PREDICTION OF THE WAVE RESISTANCE OF SLENDER HULL FORMS IN CATAMARAN CONFIGURATIONS

UNIVERSITY OF SOUTHAMPTON SHIP SCIENCE REPORT NO. 72, 1994

9) SHIN, MYUNG-SOO, KANG, KUK-JIN, VAN, SUAK-HO, YANG, SEUNG-IL.
NUMERICAL SIMULATION OF FREE SURFACE FLOWS AROUND AN ADVANCING TWIN HULL FORM

10) EVEREST J.T, HOGBEN N.
AN EXPERIMENTAL STUDY OF THE EFFECT OF BEAM VARIATION AND SHALLOW WATER ON 'THIN SHIP' WAVE PREDICTIONS.

TRANS RINA, VOLL 112, 1970.

11) BOHYUN YIM
ANALYSES OF WAVES AND THE WAVE RESISTANCE DUE TO TRANSOM STERN SHIPS

JOURNAL OF SHIP RESEARCH,
JUNE 1969

Table 1 **THE SHIP SCIENCE SYSTEMATIC SERIES**

$L/\nabla^{1/3}$	B/T			C_p
	1.5	2	2.5	
		MODEL		
6.3	-	3b	-	0.693
7.4	4a	4b	4c	0.693
8.5	5a	5b	5c	0.693
9.5	6a	6b	6c	0.693
8.5	5f	5d	5g	0.653
8.5	5h	5e	5i	0.733
9.5		6d		0.653
9.5		6e		0.733

Table 2 **HYDROSTATIC DATA**

HULL	5d	5b	5e	4b LIGHT D'PLMNT.	4b NORMAL D'PLMNT.
Cp	0.653	0.693	0.733	0.657	0.693
C_B	0.396	0.397	0.398	0.334	0.397
C_M	0.606	0.572	0.543	0.509	0.572
C_W	0.756	0.762	0.770	0.737	0.762
L/B	11.0	11.0	11.0	9.4	9.0
B/T	2.0	2.0	2.0	2.3	2.0
L	1.6	1.6	1.6	1.58	1.6
LCB	56.4	56.4	56.4	54.5	56.4
$L/\nabla^{1/3}$	8.479	8.479	8.479	8.504	7.41
WSA	0.2707	0.276	0.2714	0.2745	0.338
TRANSOM A/ MIDSHIP A	0.472	0.524	0.597	0.374	0.524
$L/WSA^{1/2}$	3.07	3.05	3.08	3.016	2.752
$WSA/\nabla^{2/3}$	7.60	7.75	7.62	7.95	7.23
β	1.66	2.00	2.19	1.60	1.50

FIGURE 1

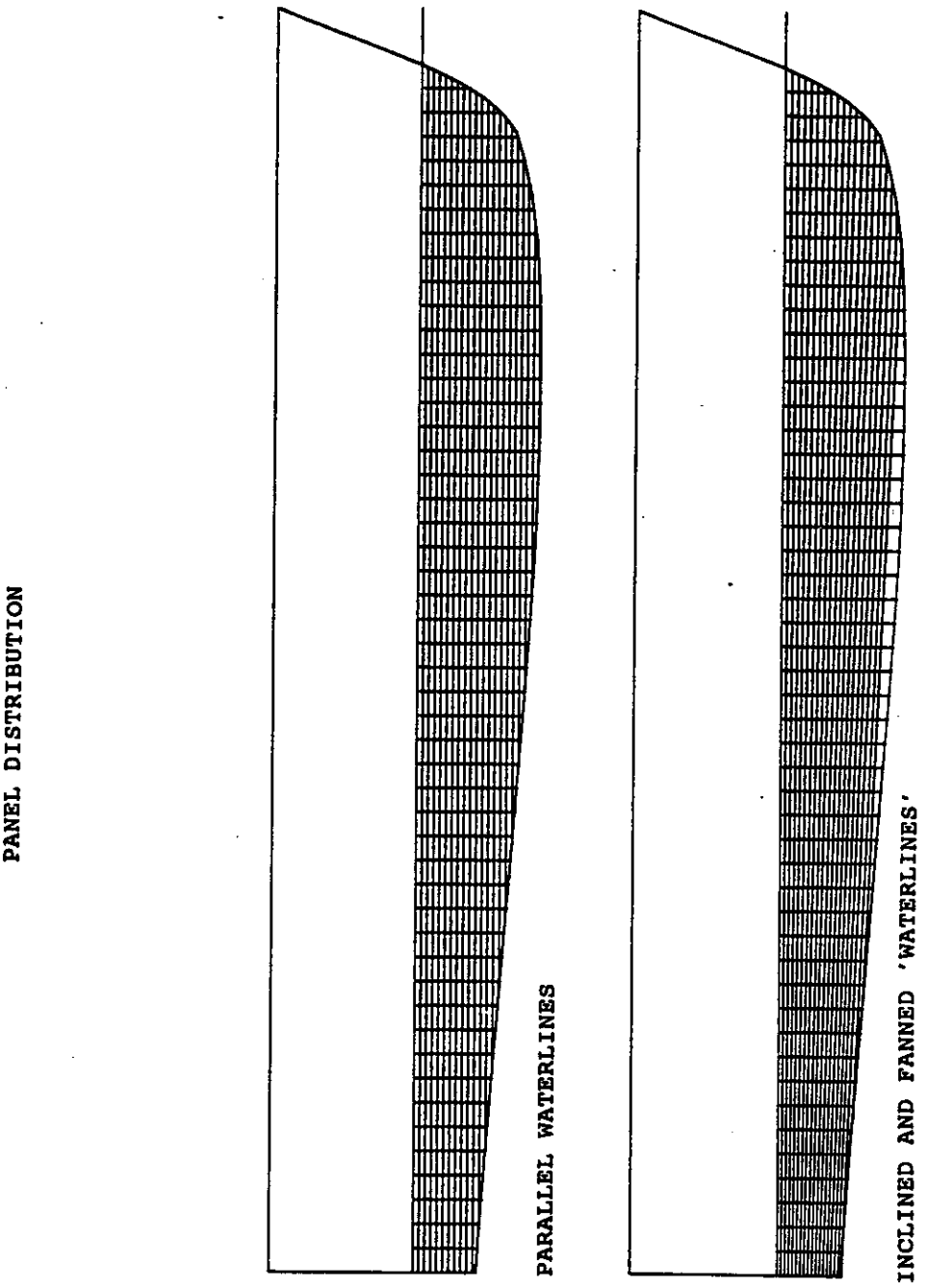
PANEL DISTRIBUTION
PARALLEL WATERLINES
INCLINED AND FANNED 'WATERLINES'

FIGURE 2

SOURCE STRENGTHS
WIGLEY MONOHULL Fn 0.3

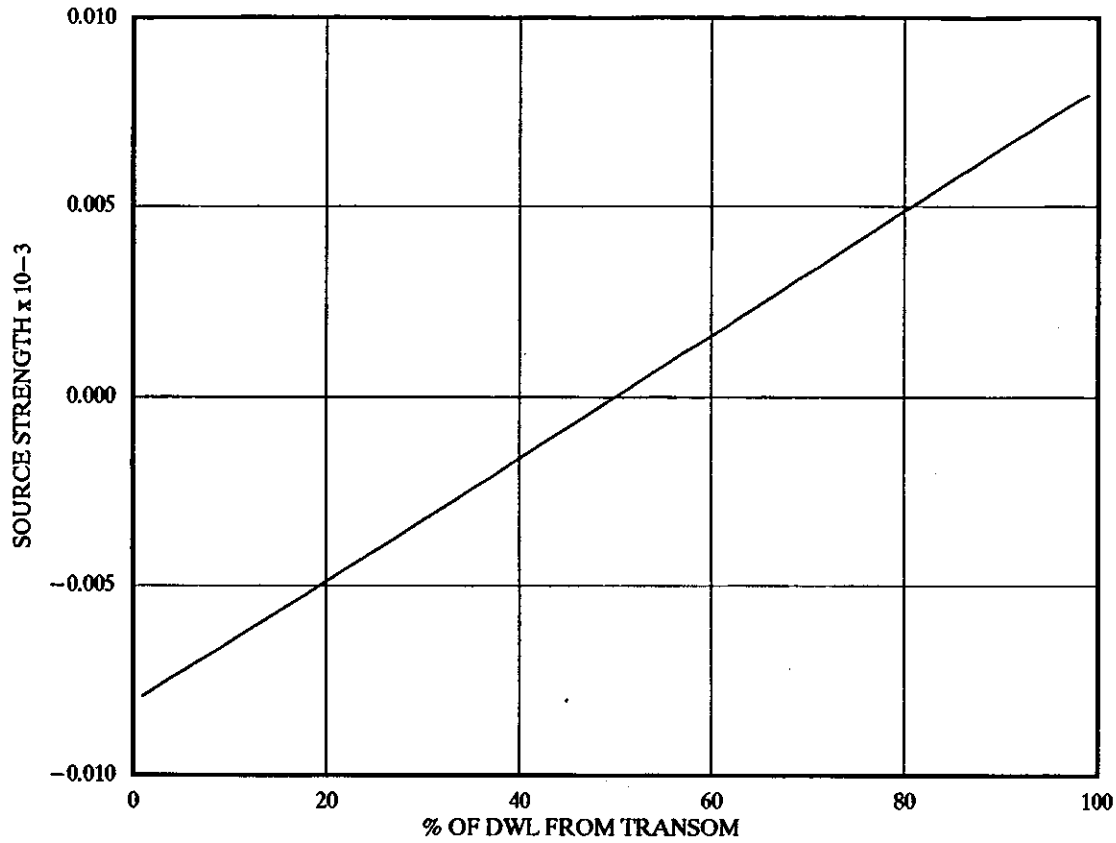

FIGURE 3

SOURCE STRENGTHS
5b MONOHULL Fn 0.3 PARALLEL WATERLINES

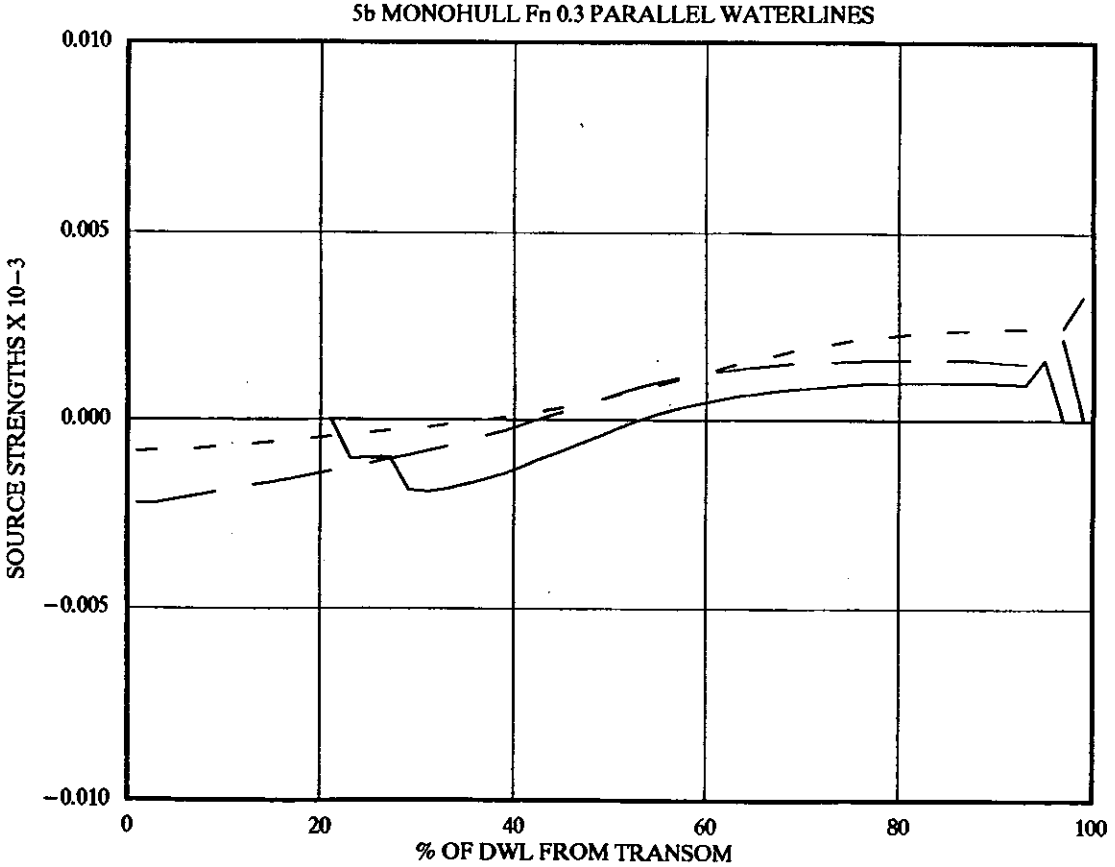

FIGURE 4

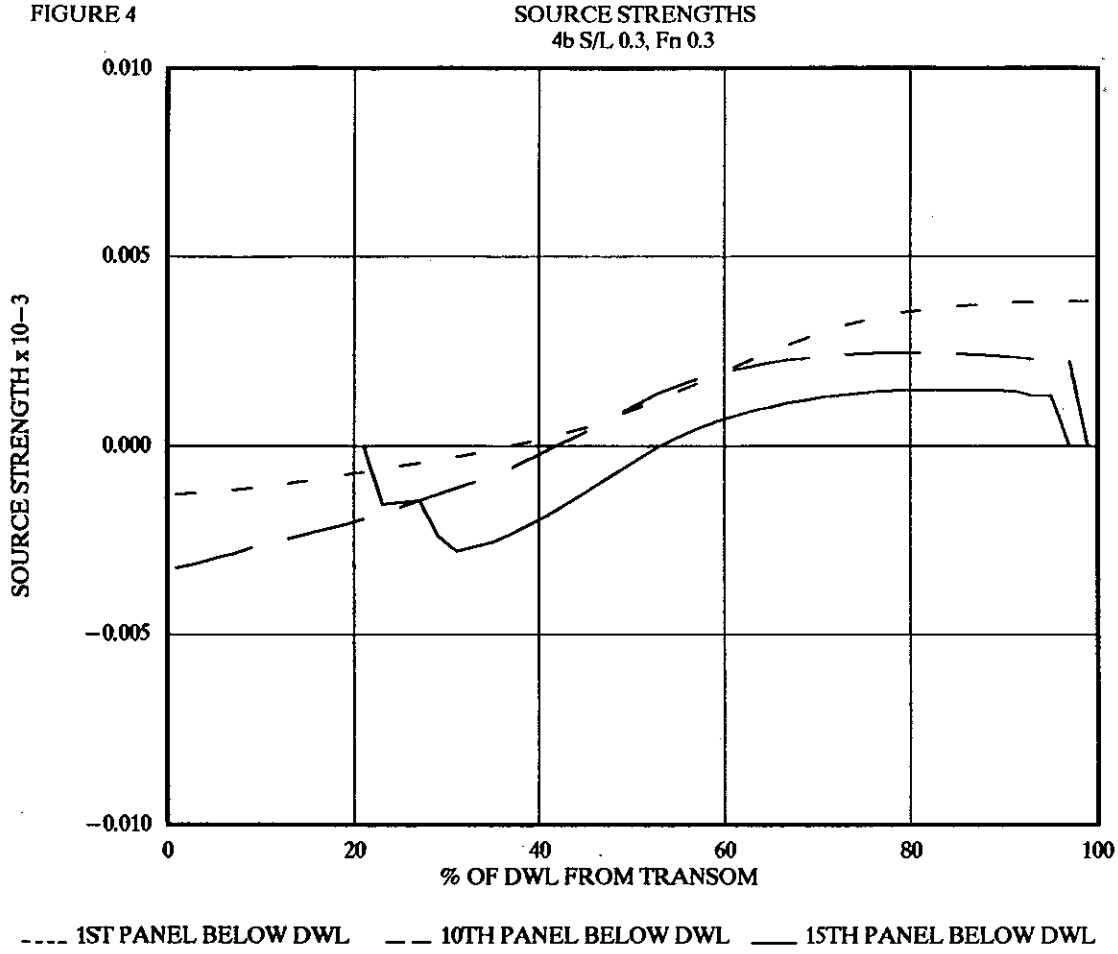

FIGURE 5

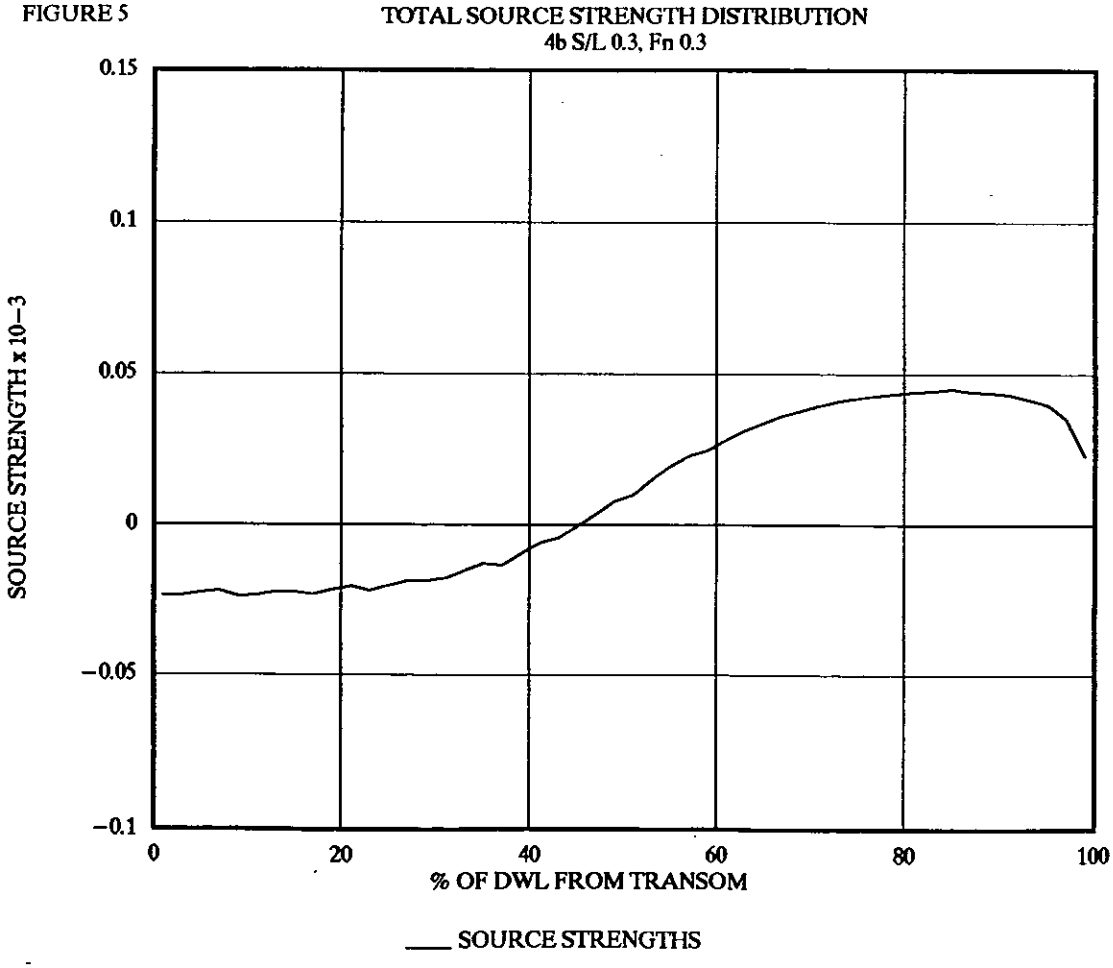

FIGURE 6

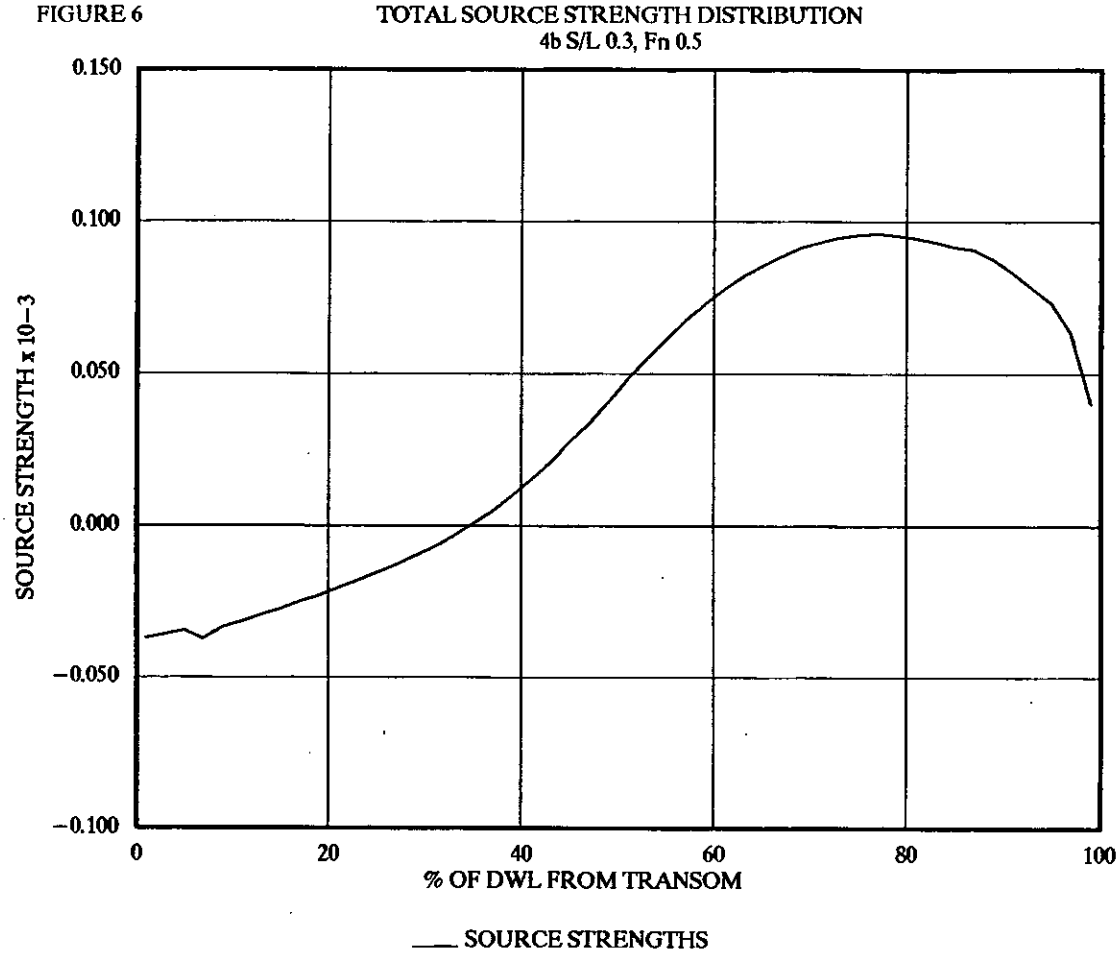

FIGURE 7

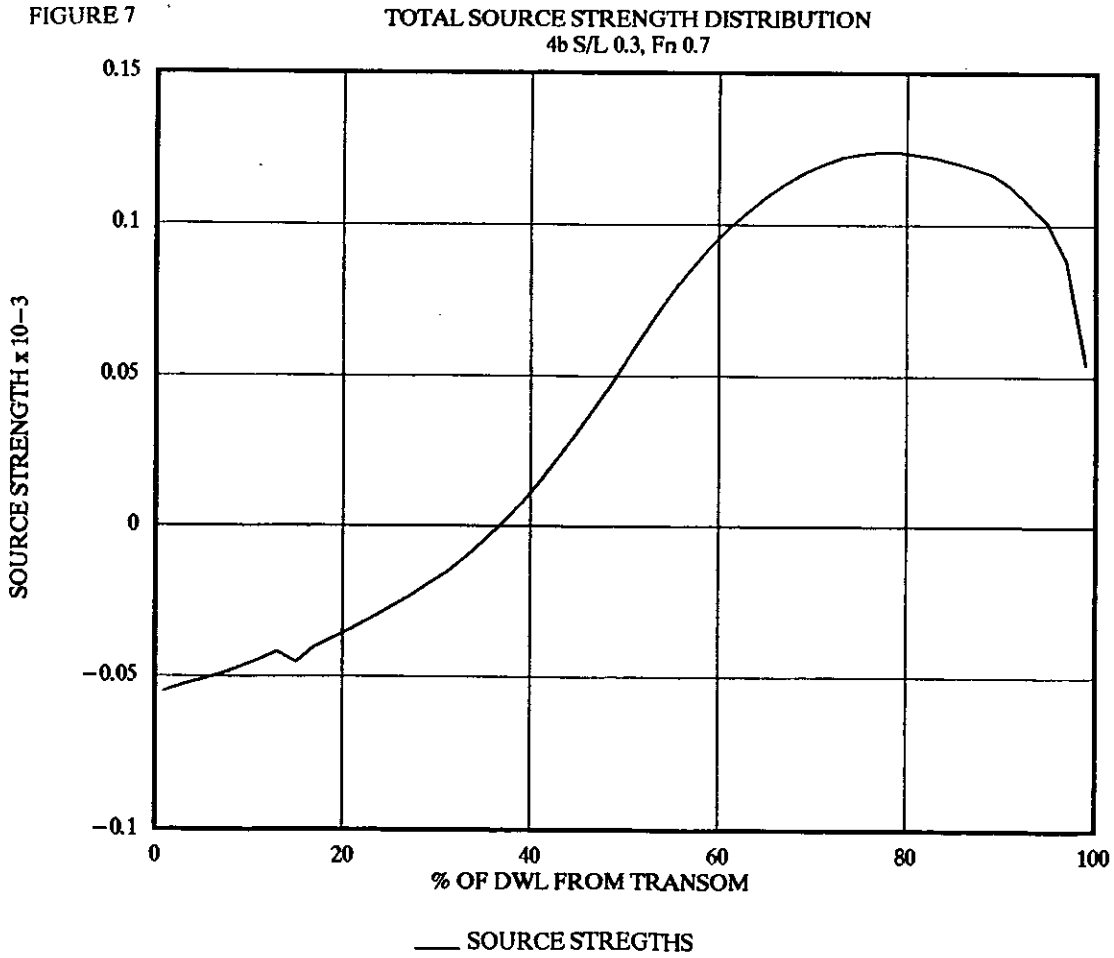

FIGURE 8 DISTRIBUTION OF SOURCES USED TO MODEL TRANSOM RESISTANCE

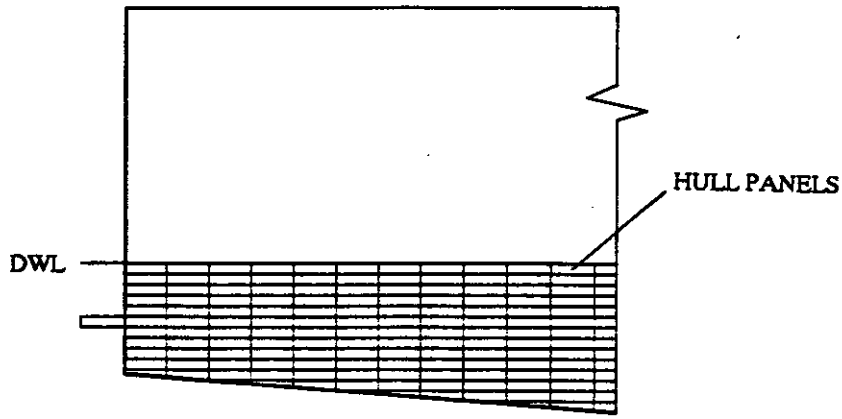

a) A SINGLE SOURCE AT HALF TRANSOM DRAFT

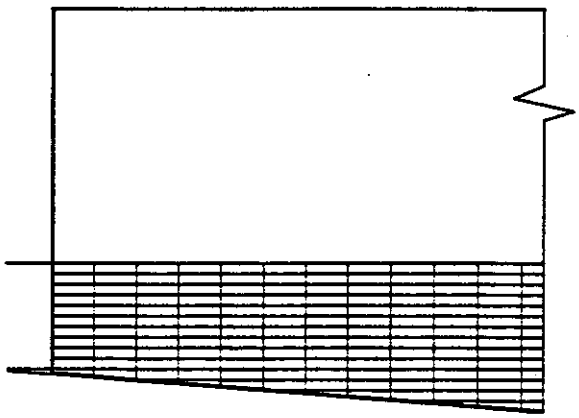

b) A SINGLE SOURCE AT FULL TRANSOM DRAFT

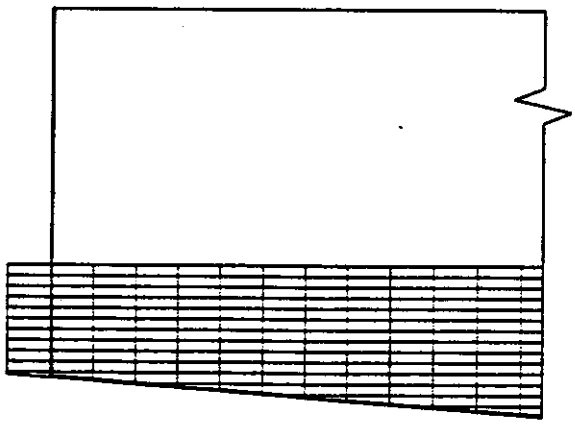

c) A VERTICAL ARRAY OF SOURCES

FIGURE 9 DISTRIBUTION OF SOURCES USED TO MODEL TRANSOM RESISTANCE

d) THREE TRANSVERSE SOURCES

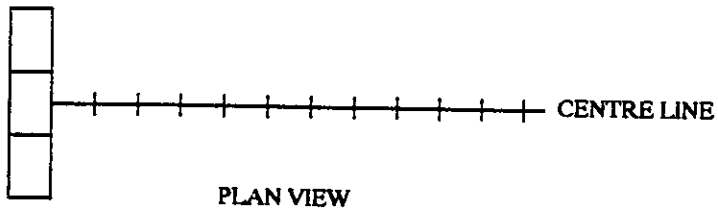

PLAN VIEW

SOURCES POSITIONED AT 1/6 OF MAXIMUM WATERLINE BEAM

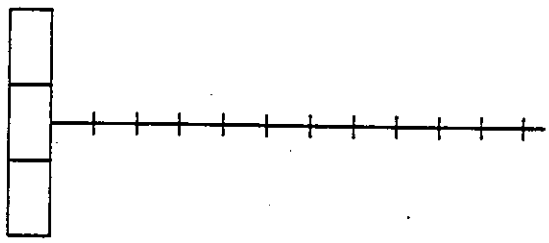

SOURCES POSITIONED AT 1/5 OF MAXIMUM WATERLINE BEAM

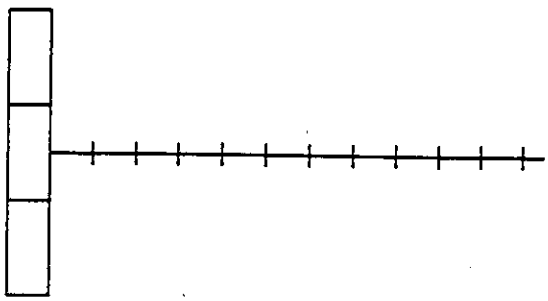

SOURCES POSITIONED AT 1/4 OF MAXIMUM WATERLINE BEAM

FIGURE 10 DISTRIBUTION OF SOURCES USED TO MODEL TRANSOM RESISTANCE

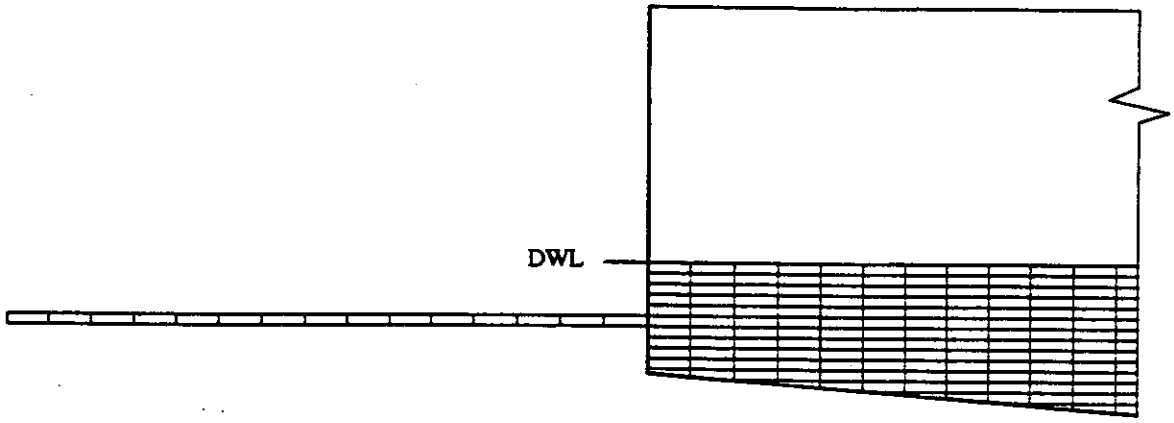

f) A SINGLE TRAILING LINE OF SOURCES AT HALF TRANSOM DRAFT

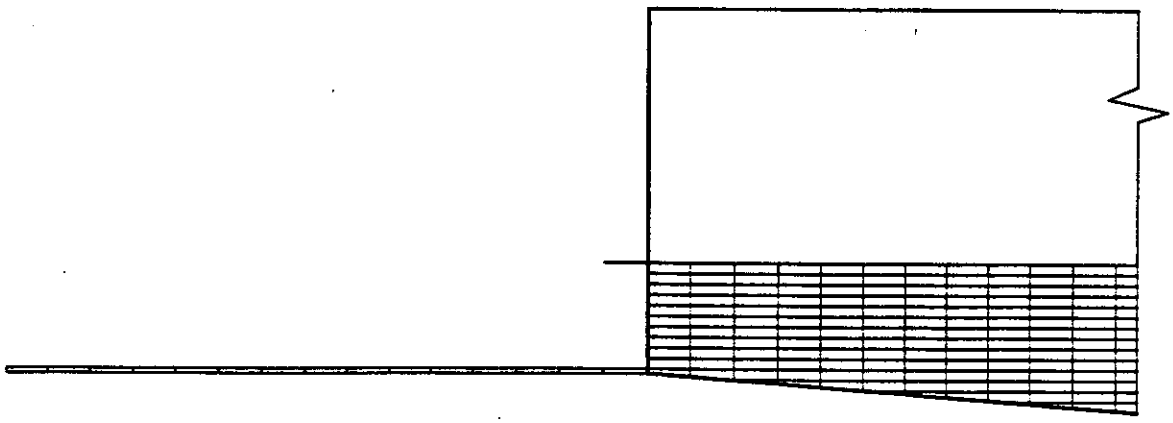

g) A SINGLE TRAILING LINE OF SOURCES AT FULL TRANSOM DRAFT

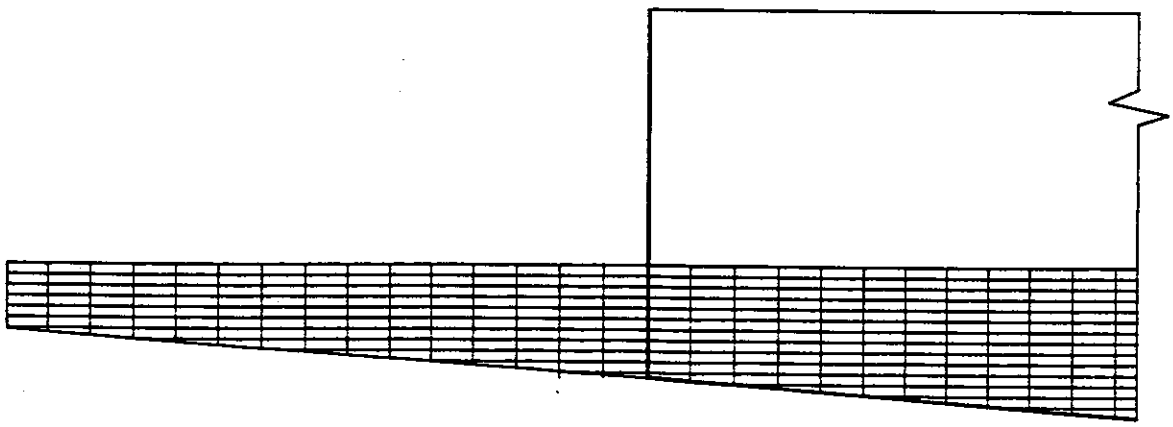

h) ARRAYS OF TRAILING SOURCES

FIGURE 11 DISTRIBUTION OF SOURCES USED TO MODEL TRANSOM RESISTANCE

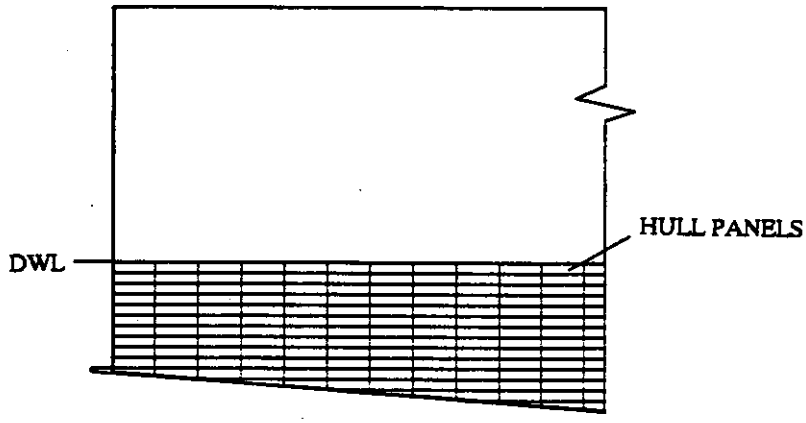

SINGLE SOURCE AT FULL TRANSOM DRAFT AT HALF THE PANEL SPACING

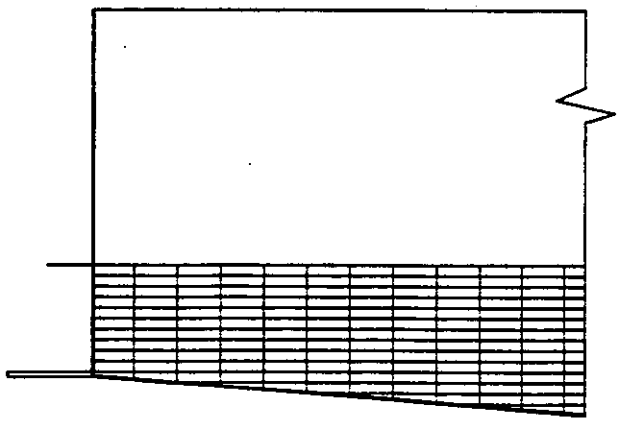

SINGLE SOURCE AT FULL TRANSOM DRAFT AT DOUBLE THE PANEL SPACING

FIGURE 12 COMPARISON OF Cw FOR TRANSVERSE SOURCE OPTIONS
C4b MONOHULL FIXED

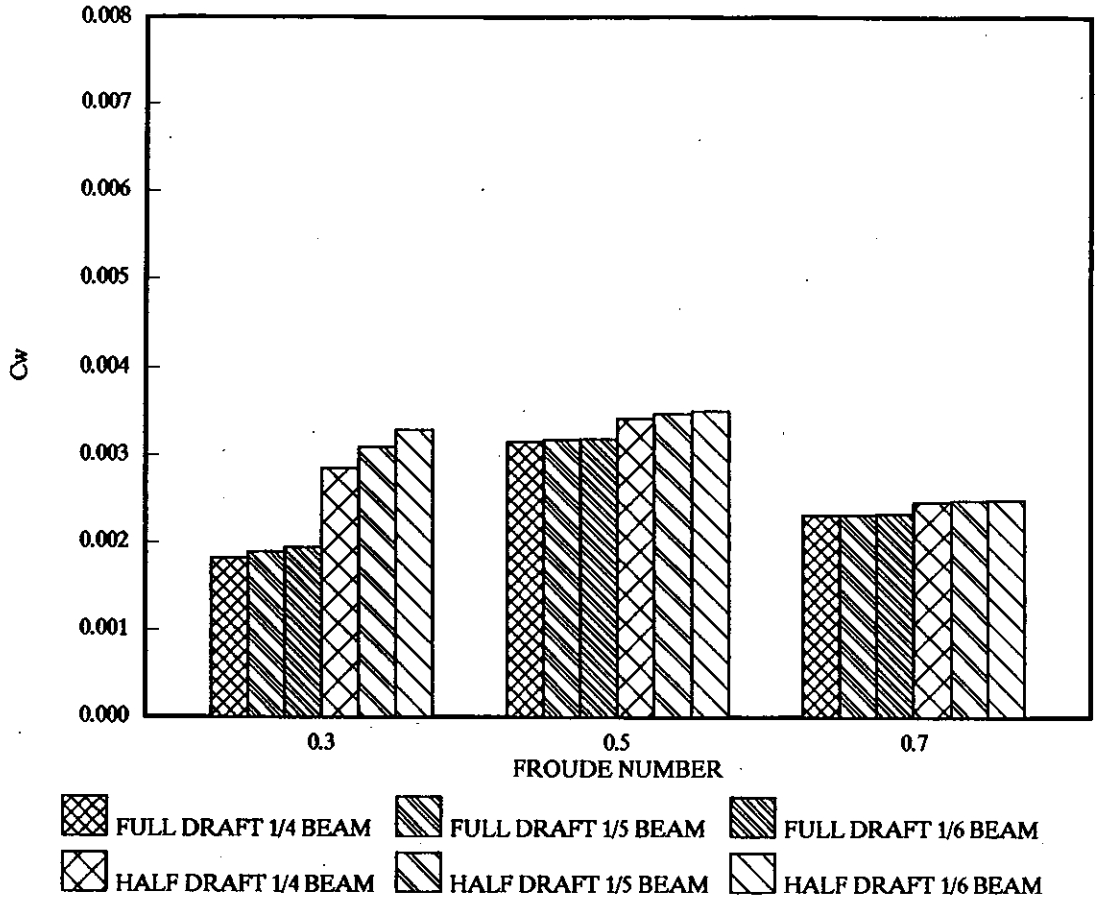

FIGURE 13 COMPARISON OF Cw FOR TRAILING SOURCE OPTIONS
C4b MONOHULL FREE TO SINK AND TRIM

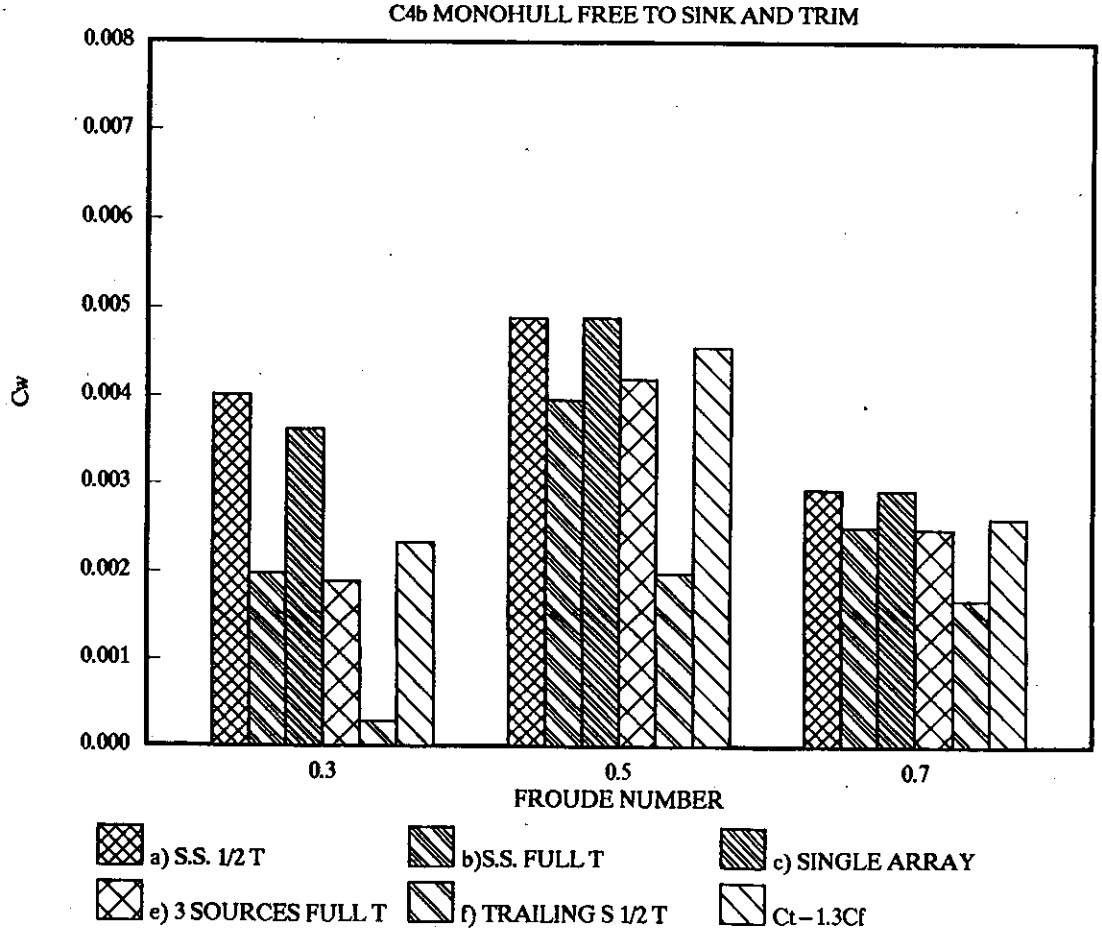

FIGURE 14 COMPARISON OF Cw FOR TRAILING SOURCE OPTIONS
C4b MONOHULL FREE TO SINK AND TRIM

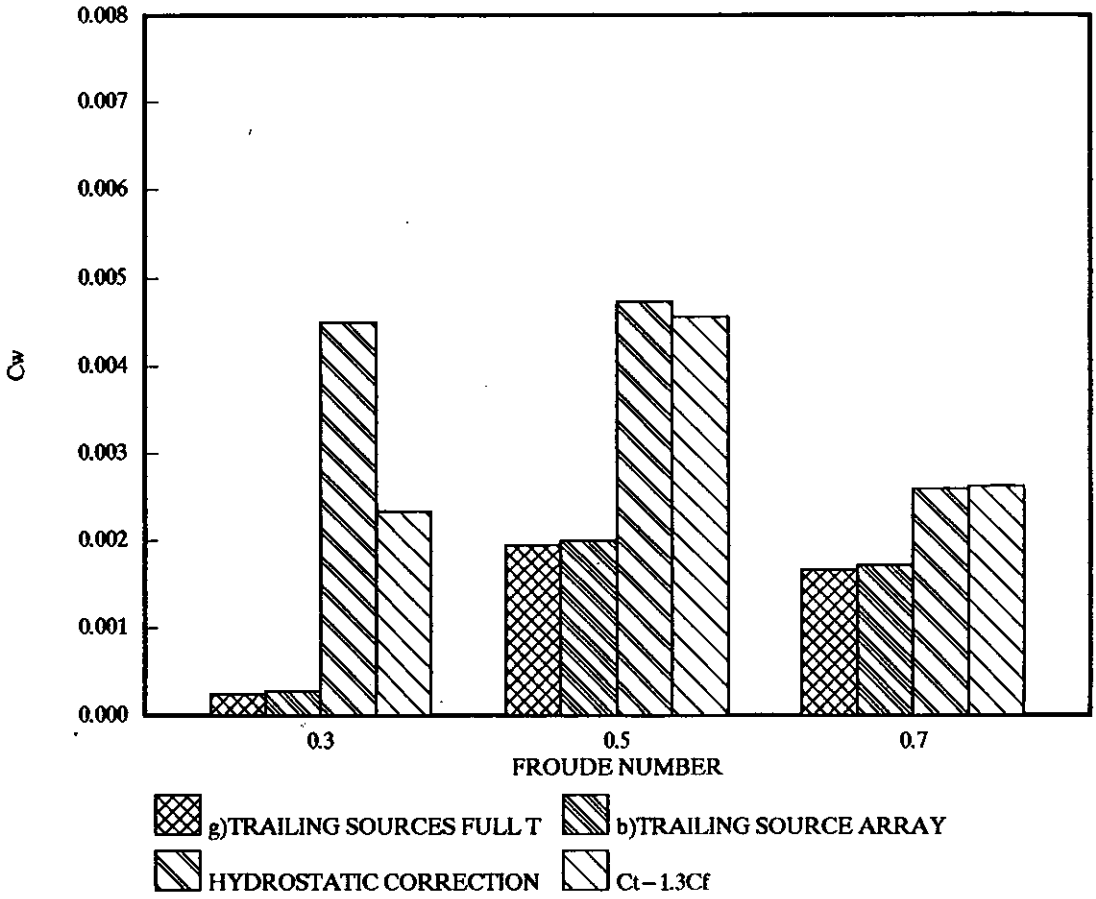

FIGURE 15 COMPARISON OF Cw FOR TRAILING SOURCE OPTIONS
4b MONOHULL FREE TO SINK AND TRIM

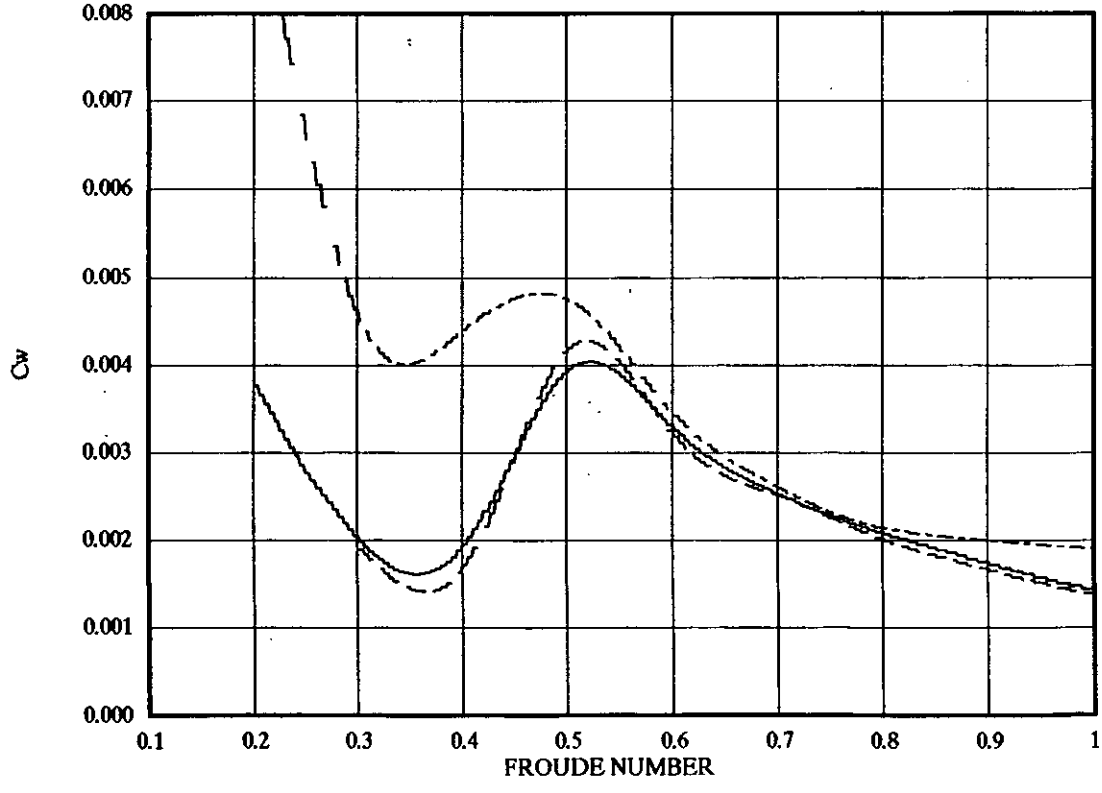

___ a) SINGLE SOURCE FULL T. DRAFT

_ _ e) 3 TRANSVERSE SOURCES FULL T. DRAFT

_ _ _ HYDROSTATIC CORRECTION

FIGURE 16

COMPARISON OF Cw FOR TRAILING SOURCE OPTIONS
C4b S/L 0.3 FREE TO SINK AND TRIM

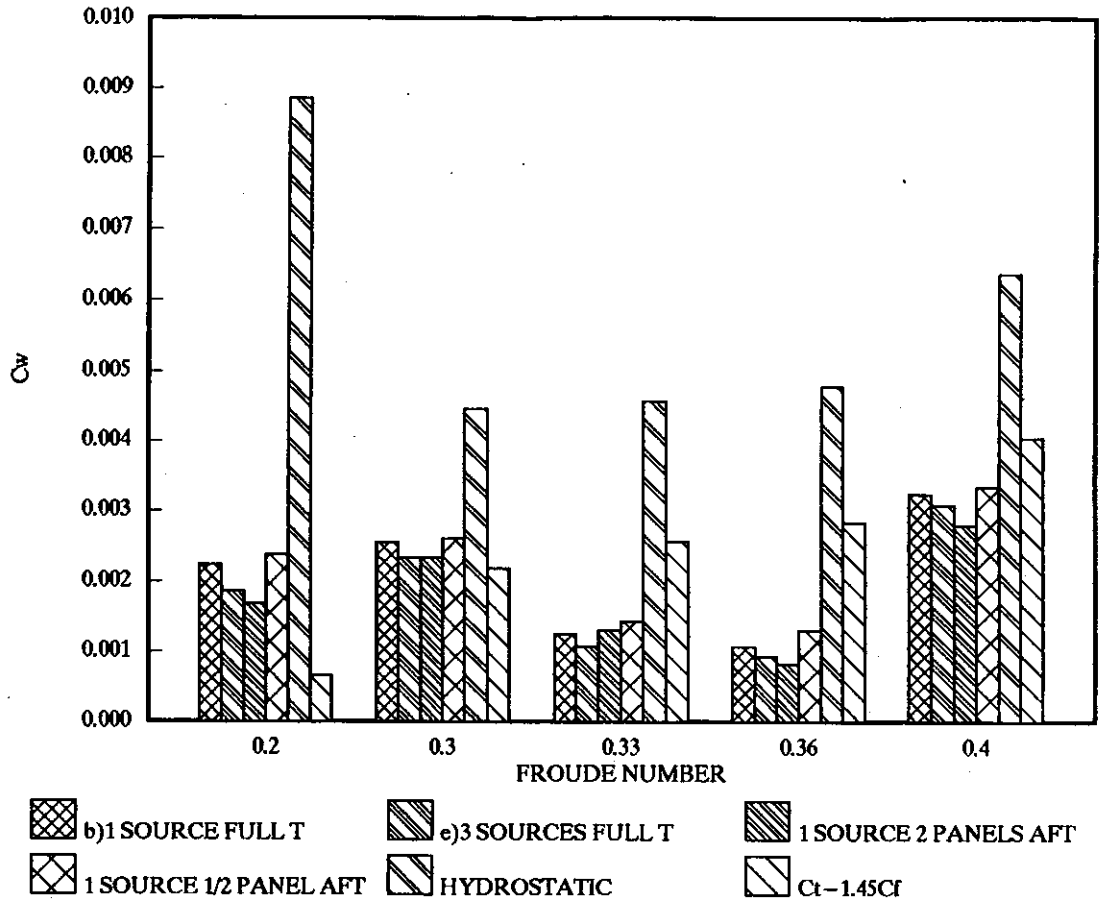

FIGURE 17

THEORETICAL WAVE RESISTANCE 5e MONOHULL
COMPARISON OF THEORETICAL TRANSOM CORRECTIONS

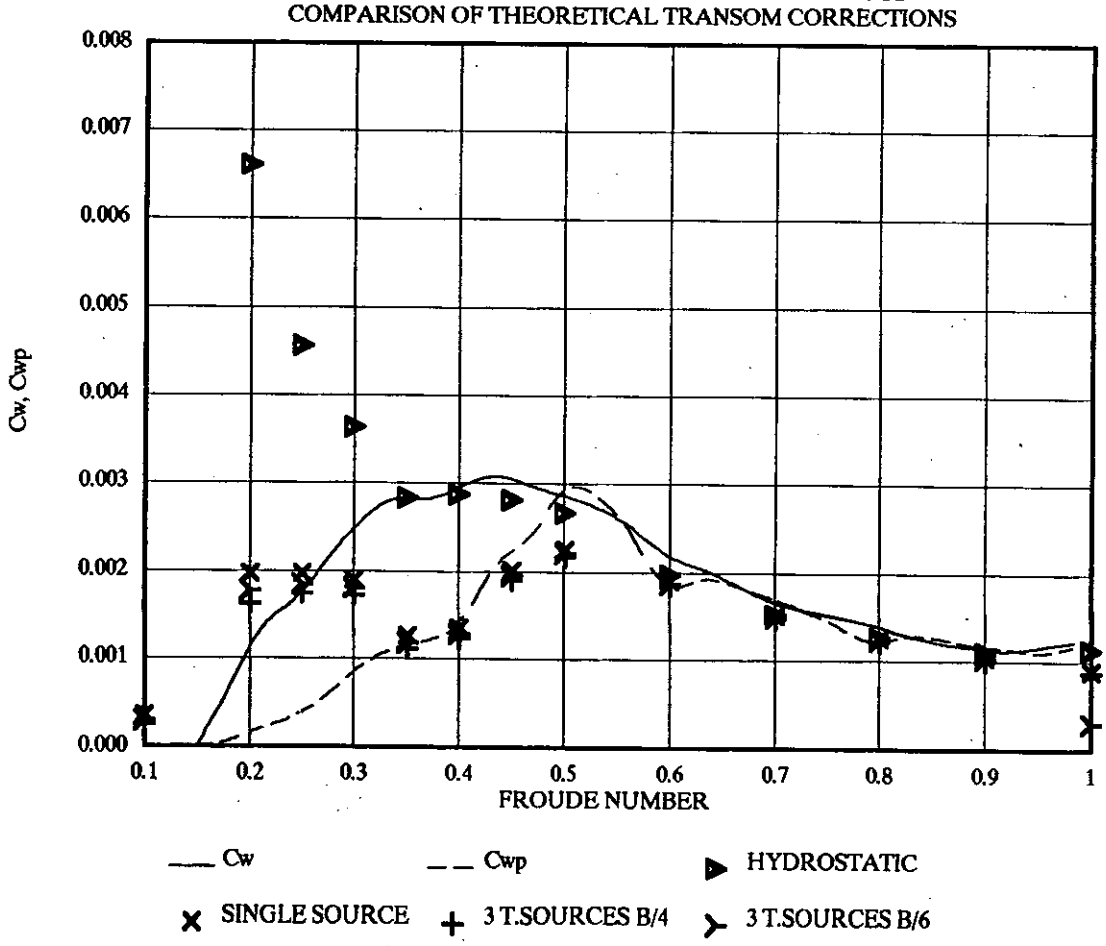

FIGURE 18 THEORETICAL WAVE RESISTANCE
THE EFFECT OF THE NUMBER OF HARMONICS AND WAVE ANGLE

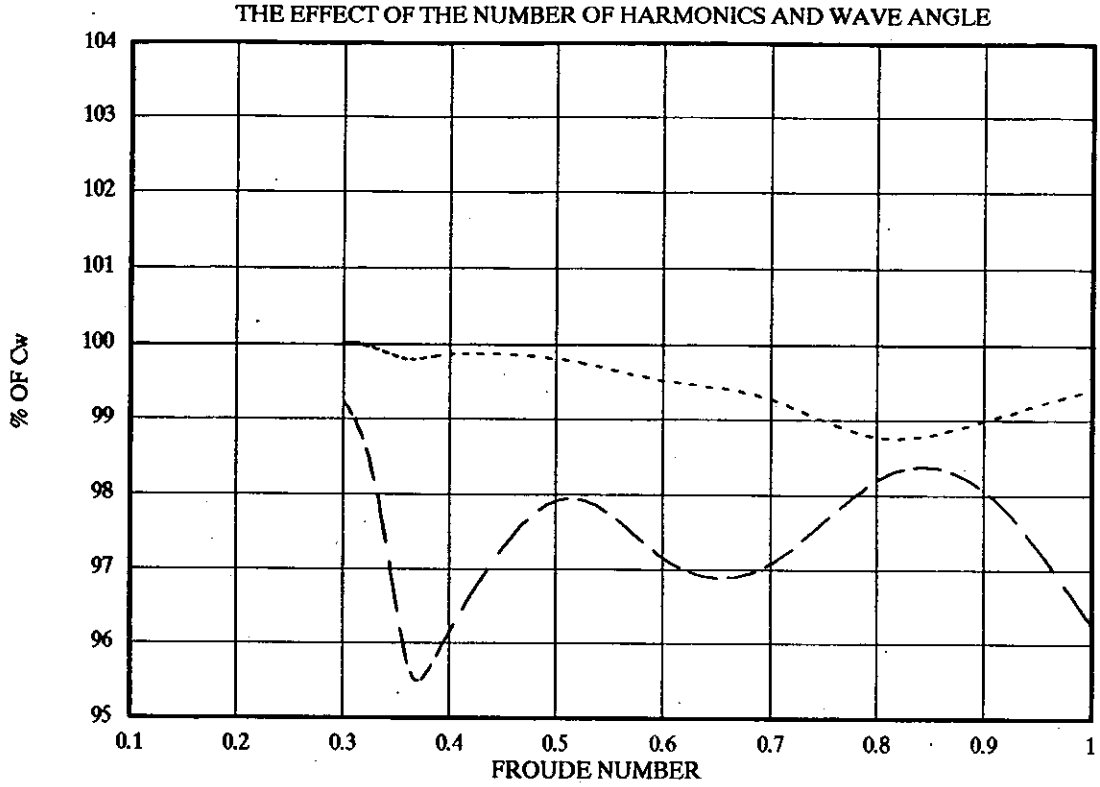

_ _ M = 30, THETA = 70 ---- M = 50, THETA = 80

____ M =100, THETA = 85 (ASSUMED 100%)

FIGURE 19 CHANGE IN Rw WITH NUMBER OF PARALLEL WATERLINES
WIGLEY HULL MONOHULL

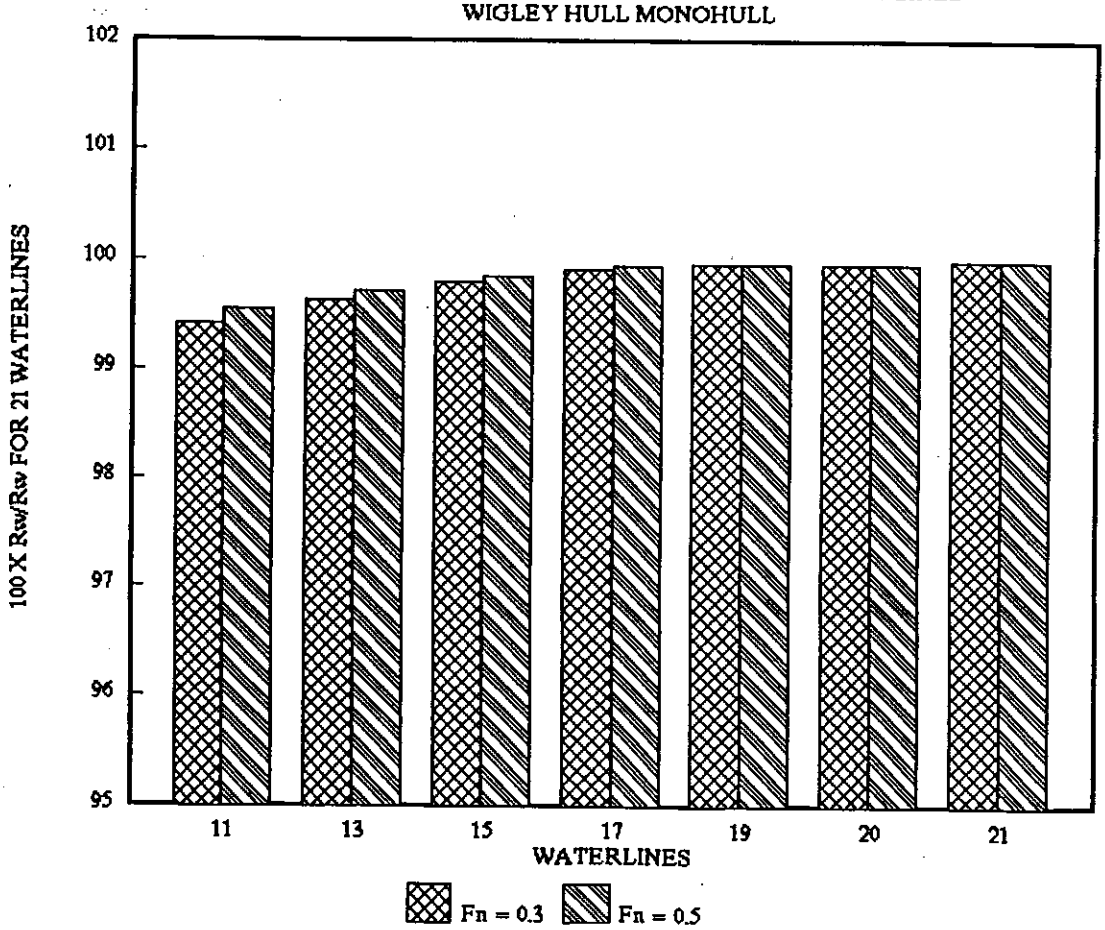

FIGURE 20 CHANGE IN Rw WITH NUMBER OF FANNED WATERLINES
C5b MONOHULL

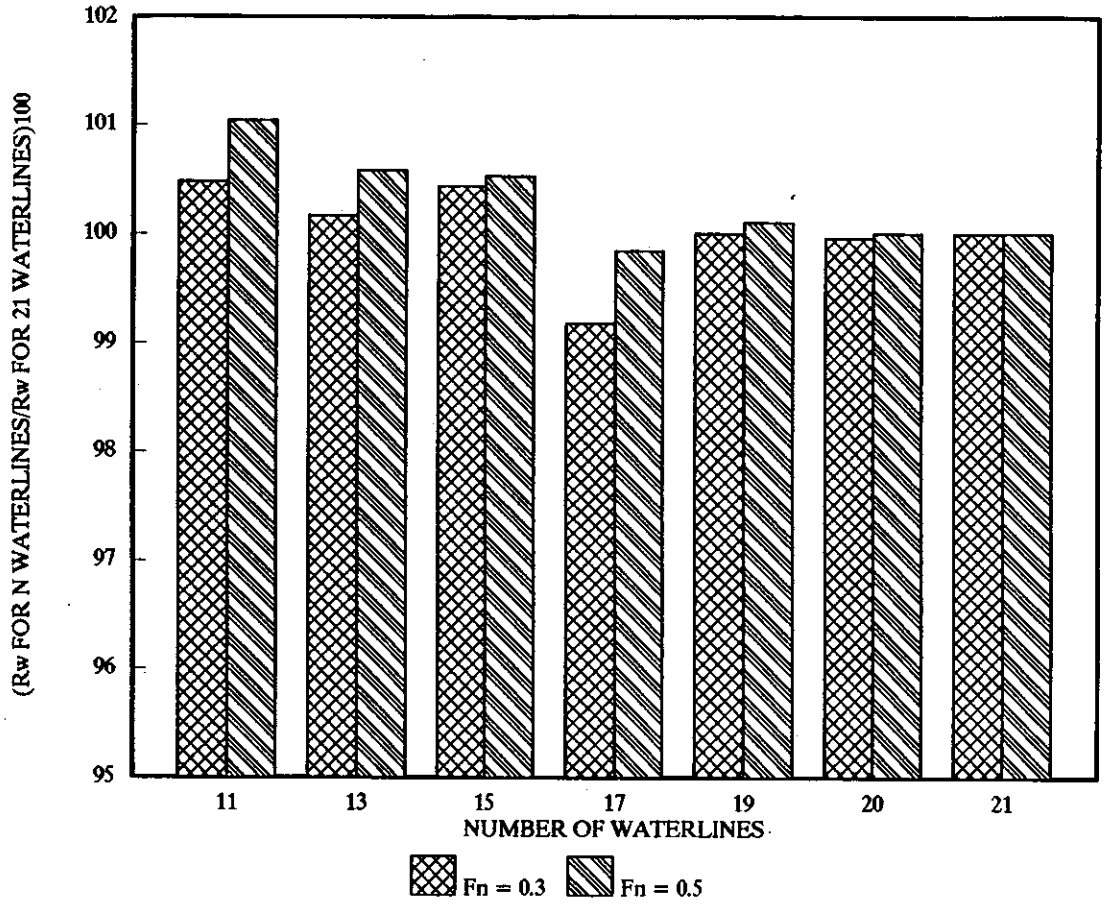

FIGURE 21 THEORETICAL WAVE RESISTANCE 5b MONOHULL WITH HYDROSTATIC TRANSOM
THE EFFECT OF PANNEL DEFINITION (FIXED SINKAGE AND TRIM)

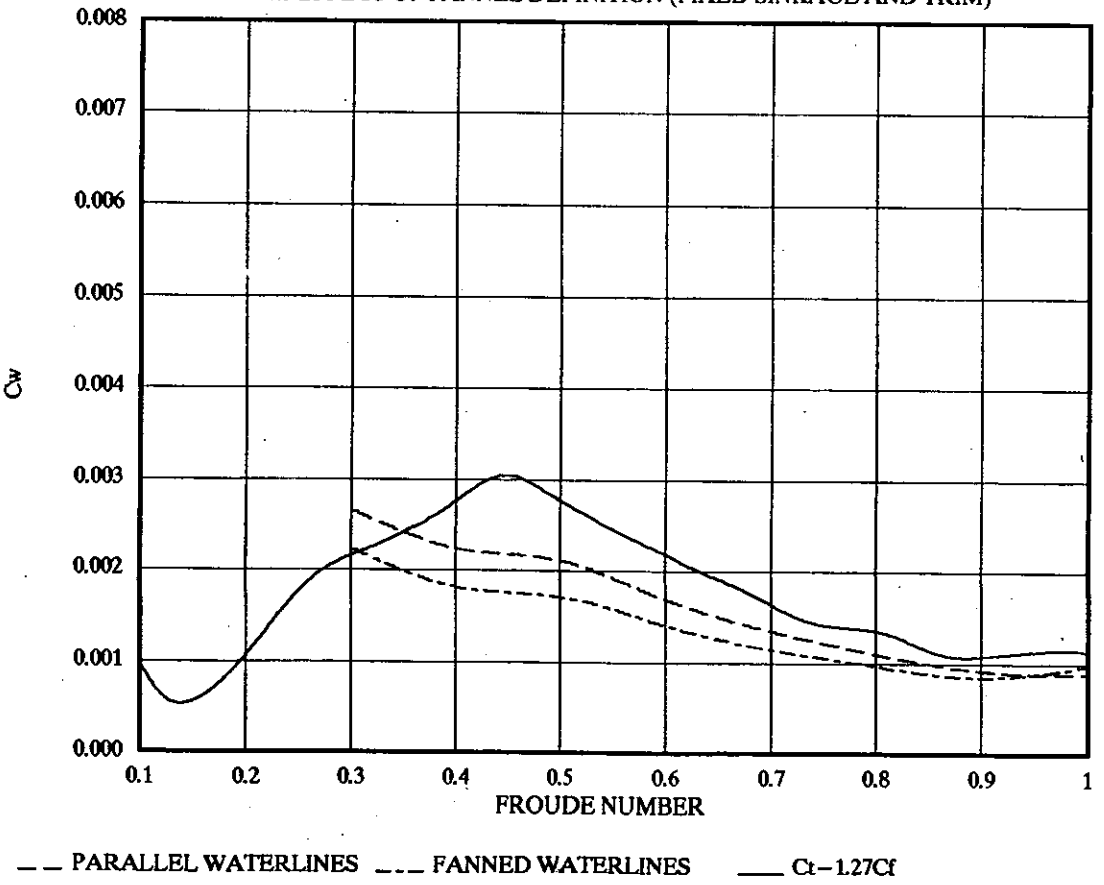

FIGURE 22 THEORETICAL WAVE RESISTANCE 5b S/L 0.2 WITH HYDROSTATIC TRANSOM
THE EFFECT OF PANNEL DEFINITION (FREE SINKAGE AND TRIM)

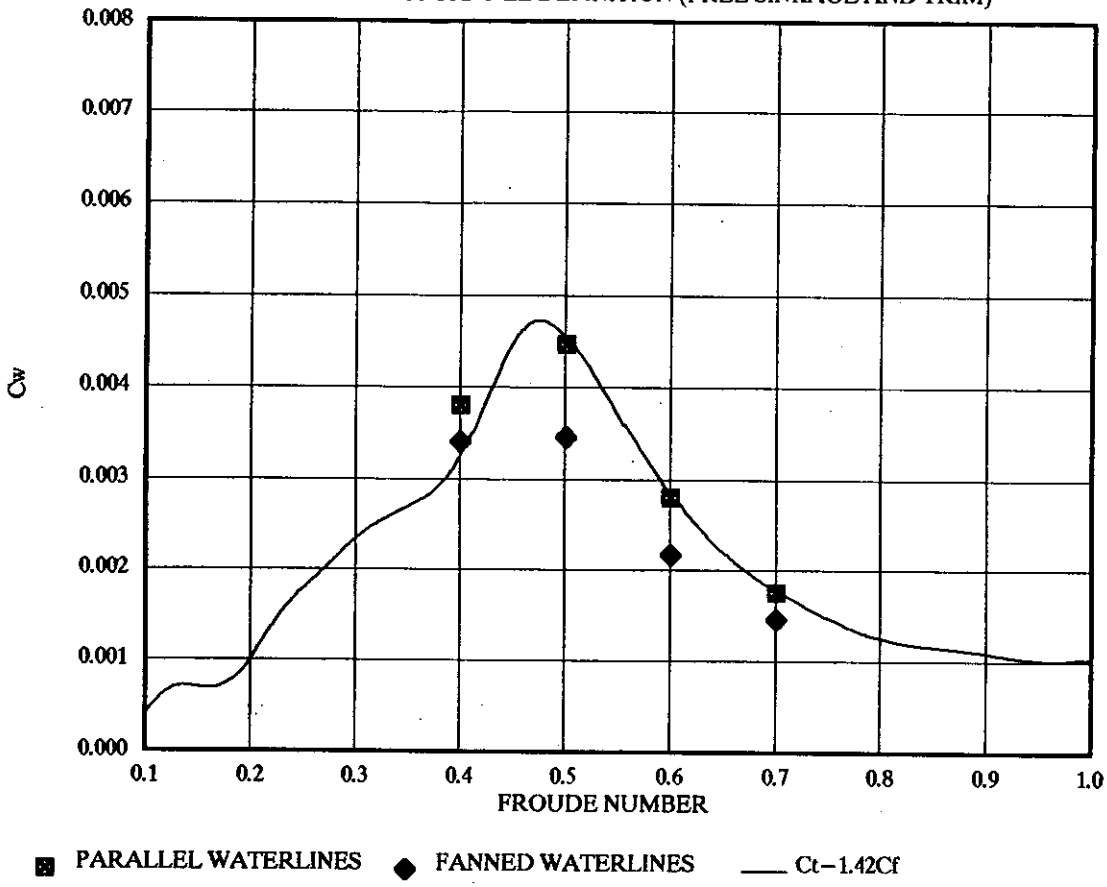

FIGURE 23

FORM FACTORS DERIVED FROM THEORETICAL CALCULATION

MODEL	(Ctexp – Cwtheory)/Cf SINGLE TRANSOM SOURCE	(Ctexp – Cwtheory)/Cf HYDROSTATIC TRANSOM	EXPERIMENTAL
C4b MONO	1.32	*	1.30
C4b S/L O.3	1.44	1.43	1.45
C4b S/L 0.5	1.46	1.43	1.45
C4b LIGHT MONO	1.21	1.26	1.25
C4b LIGHT S/L 0.3	*	*	1.4
C4b LIGHT S/L 0.5	1.30	1.36	1.4
C5d MONO	1.26	1.26	1.26
C5d S/L 0.2	1.41	1.41	1.38
C5d S/L 0.3	1.41	1.41	1.41
C5d S/L 0.4	1.41	1.41	1.43
C5d S/L 0.5	1.44	1.42	1.46
C5b MONO	1.25	1.25	1.27
C5b S/L 0.2			1.42
C5b S/L 0.3	1.44	1.44	1.46
C5b S/L 0.4			
C5b S/L 0.5	1.42	1.41	1.43
C5e MONO	1.23	1.23	1.21
C5e S/L 0.2	1.44	1.44	1.40
C5e S/L 0.3	1.46	1.46	1.46
C5e S/L 0.4	1.46	1.46	1.48
C5e S/L 0.5	1.46	1.46	1.48

* POOR CORRELATION, FORM FACTORS NOT CONSISTANT OVER RANGE

CORRECTION TO HYDROSTATIC TRANSOM RESISTANCE

$Cw = Cw[\text{Thin Ship}] + Cts.a.Fn^{b}$

MODEL	a	b
4b	17	2.95
4b light	17	2.20
5b	20	2.89
5d	18	2.89
5e	20	2.89
6b	20	2.89

FIGURE 24

THEORETICAL WAVE RESISTANCE
5d MONOHULL

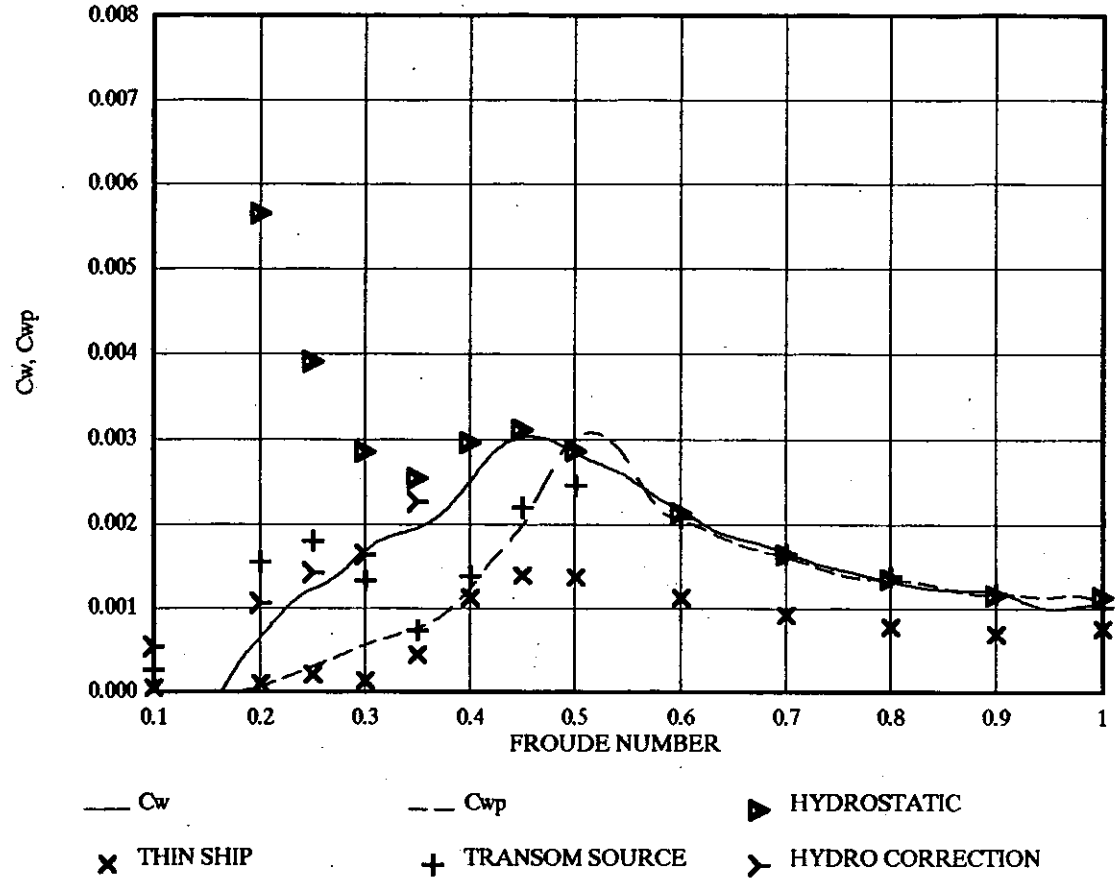

FIGURE 25

THEORETICAL WAVE RESISTANCE
5d S/L 0.2

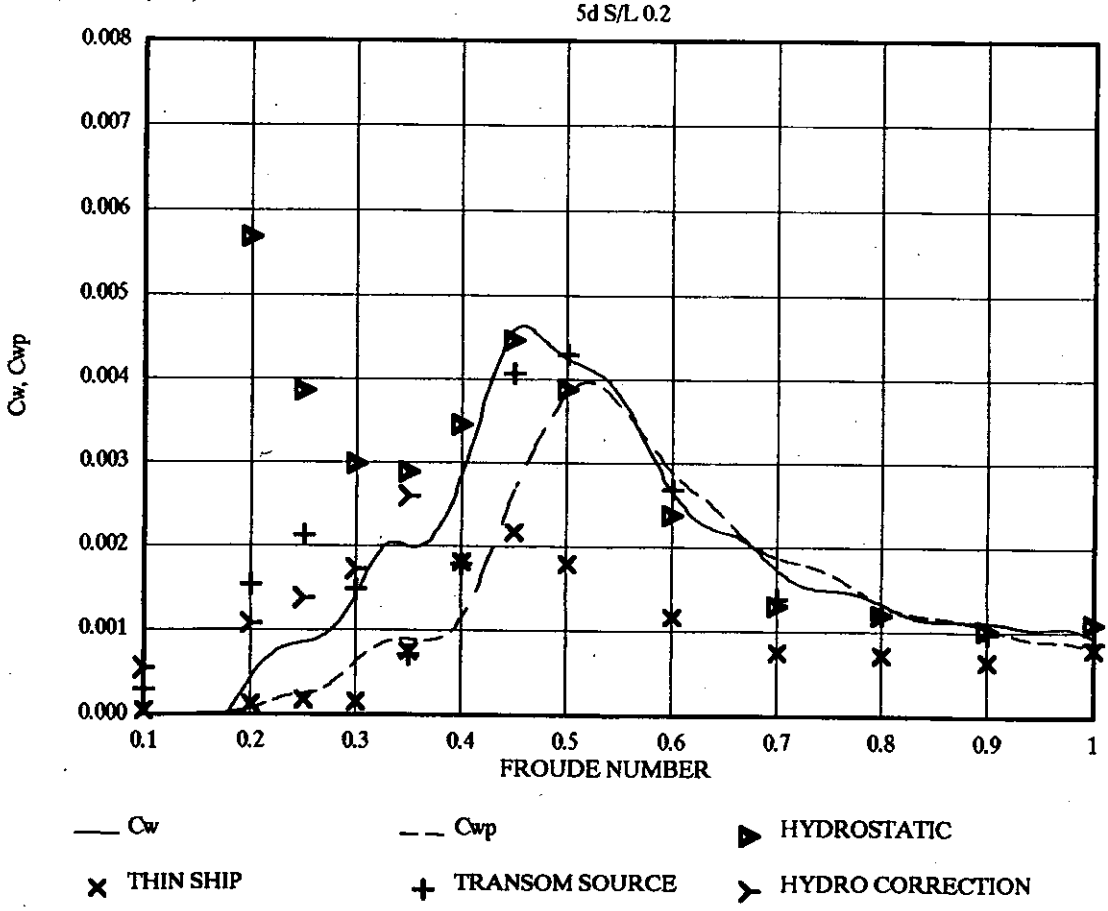

FIGURE 26

THEORETICAL WAVE RESISTANCE
5d S/L 0.3

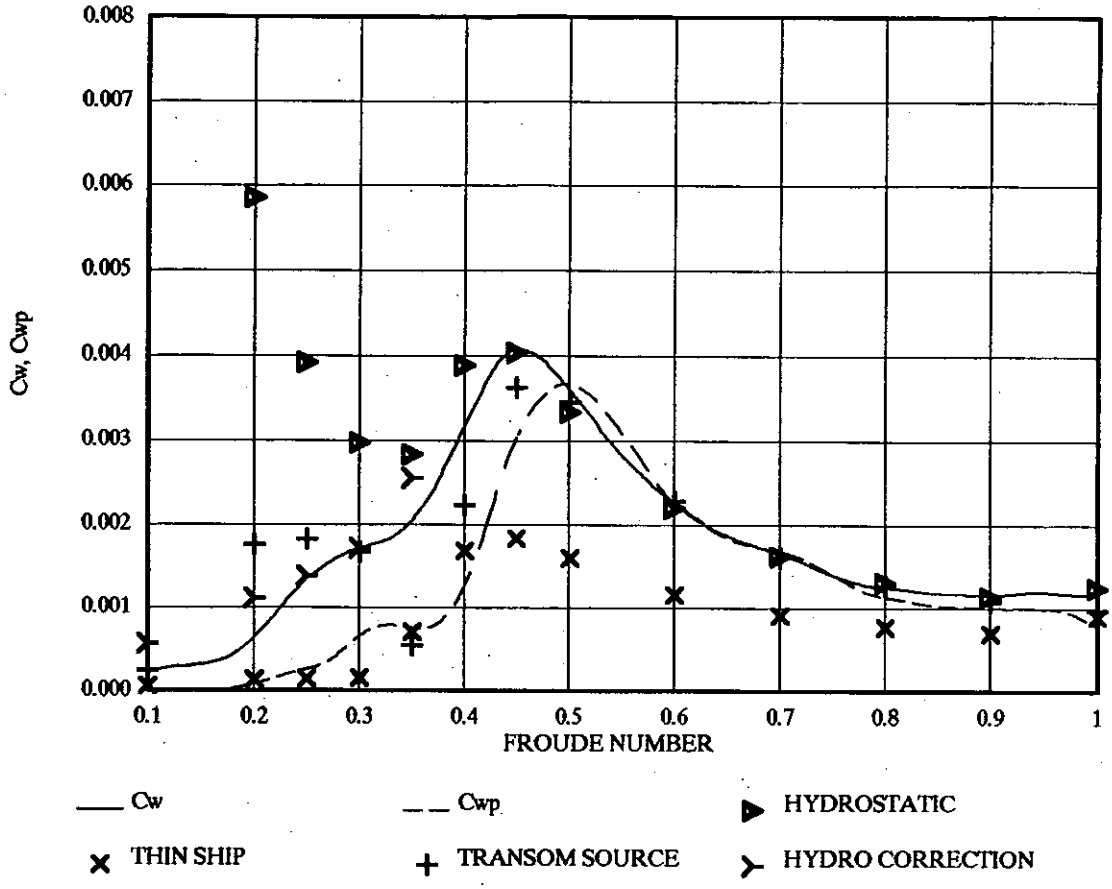

FIGURE 27

THEORETICAL WAVE RESISTANCE
5d S/L 0.4

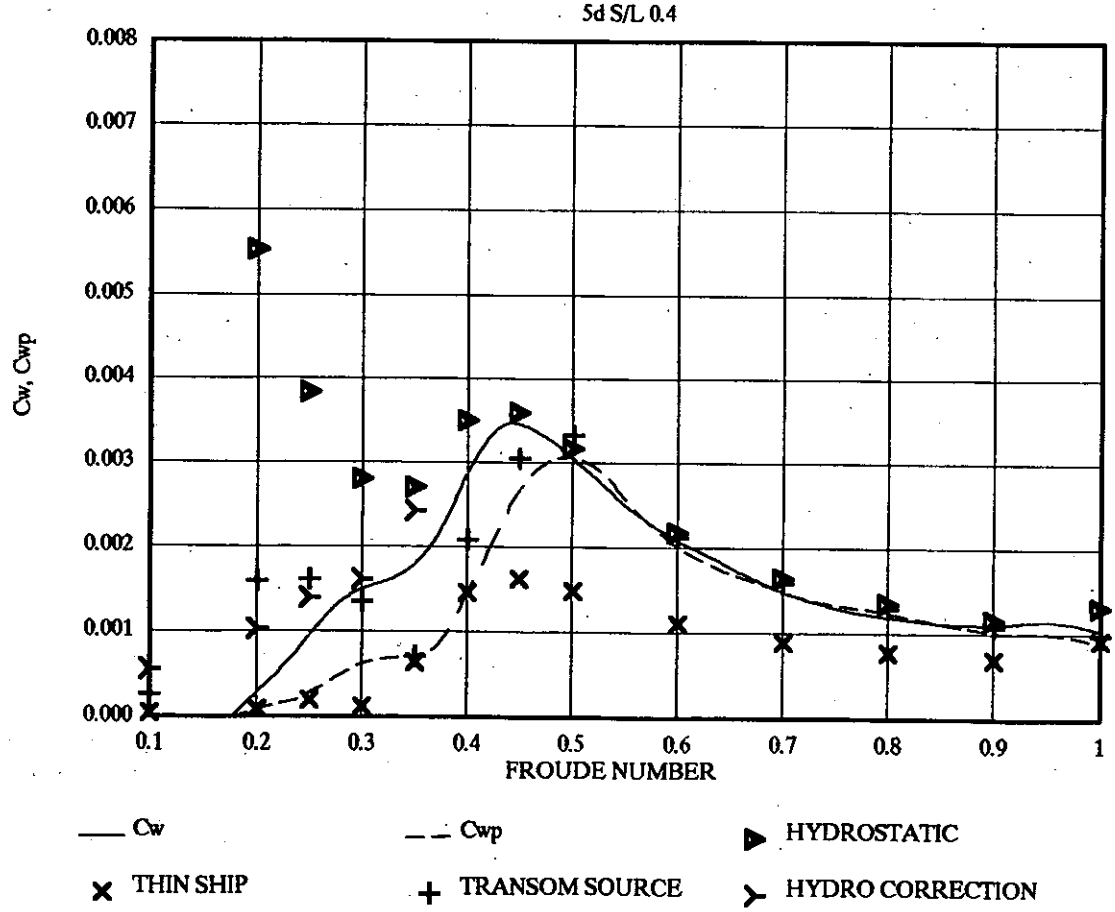

FIGURE 28

THEORETICAL WAVE RESISTANCE
5d S/L 0.5

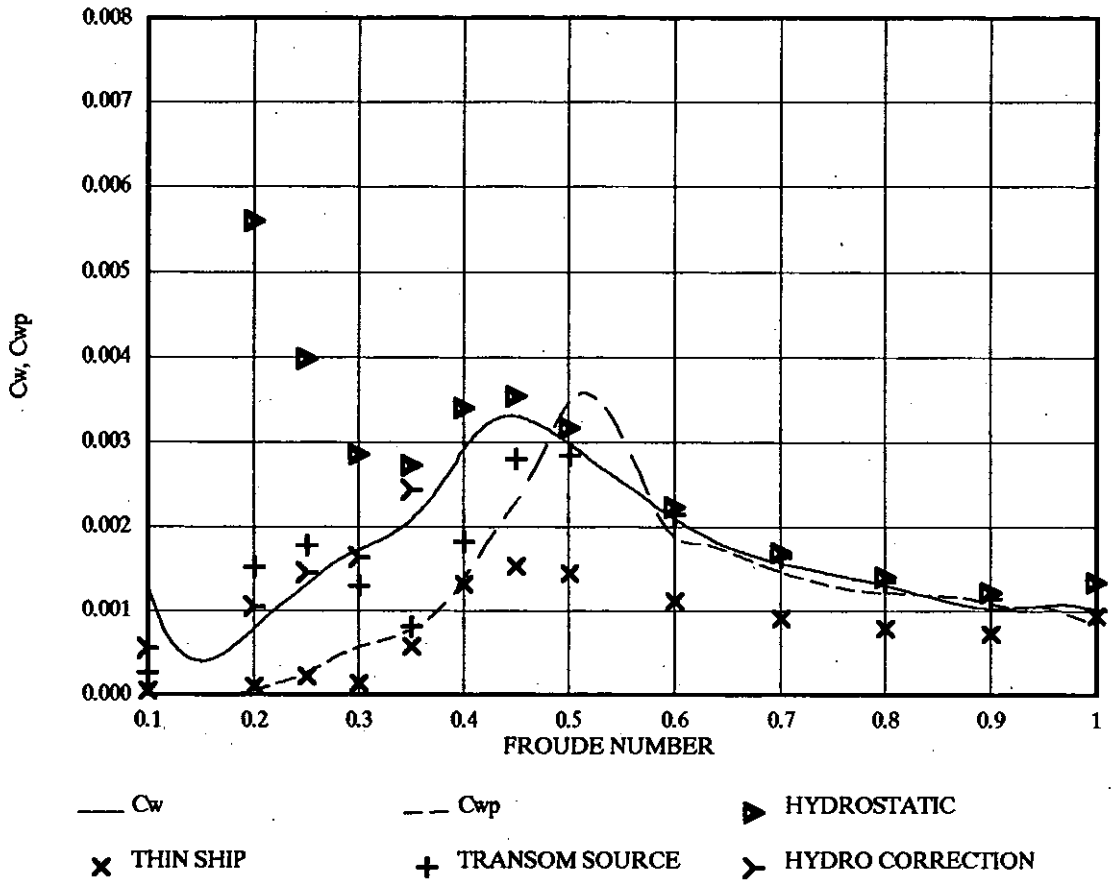

FIGURE 29

THEORETICAL WAVE RESISTANCE
5b MONOHULL

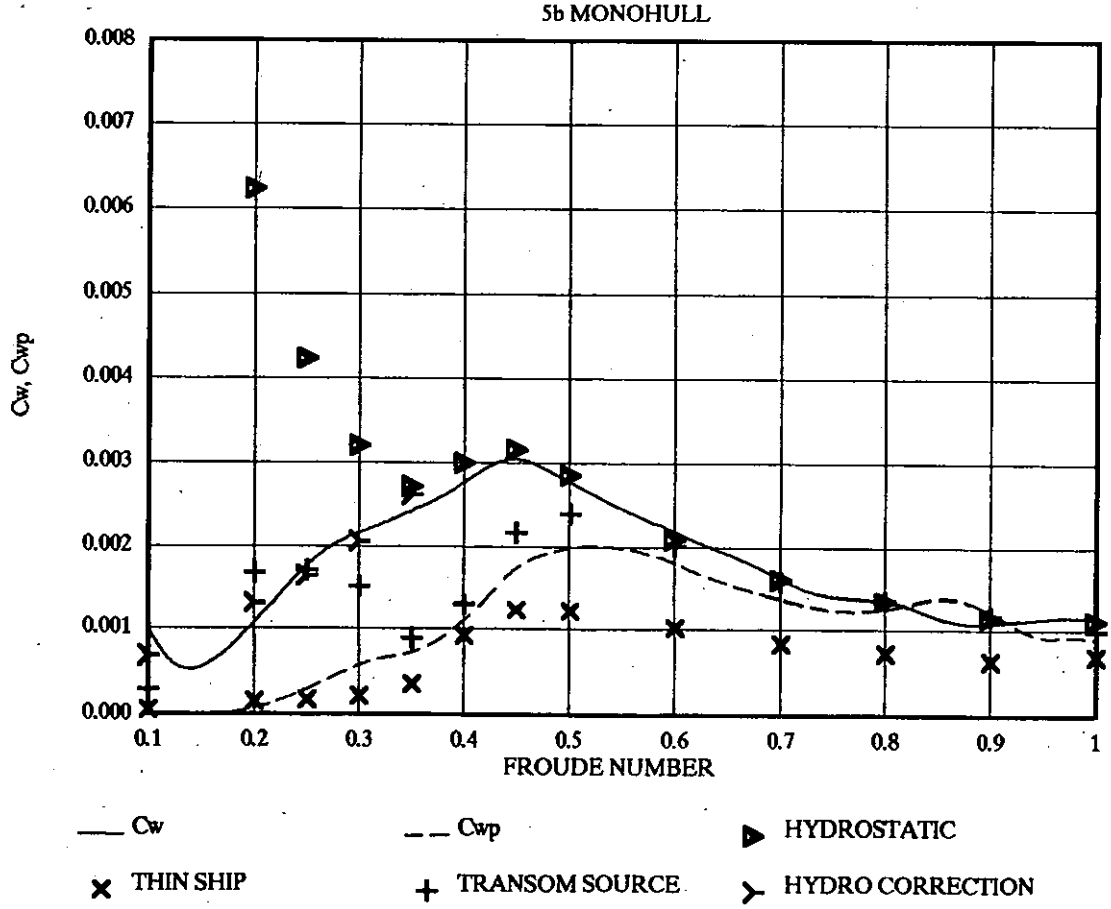

FIGURE 30 THEORETICAL WAVE RESISTANCE 5b S/L 0.3

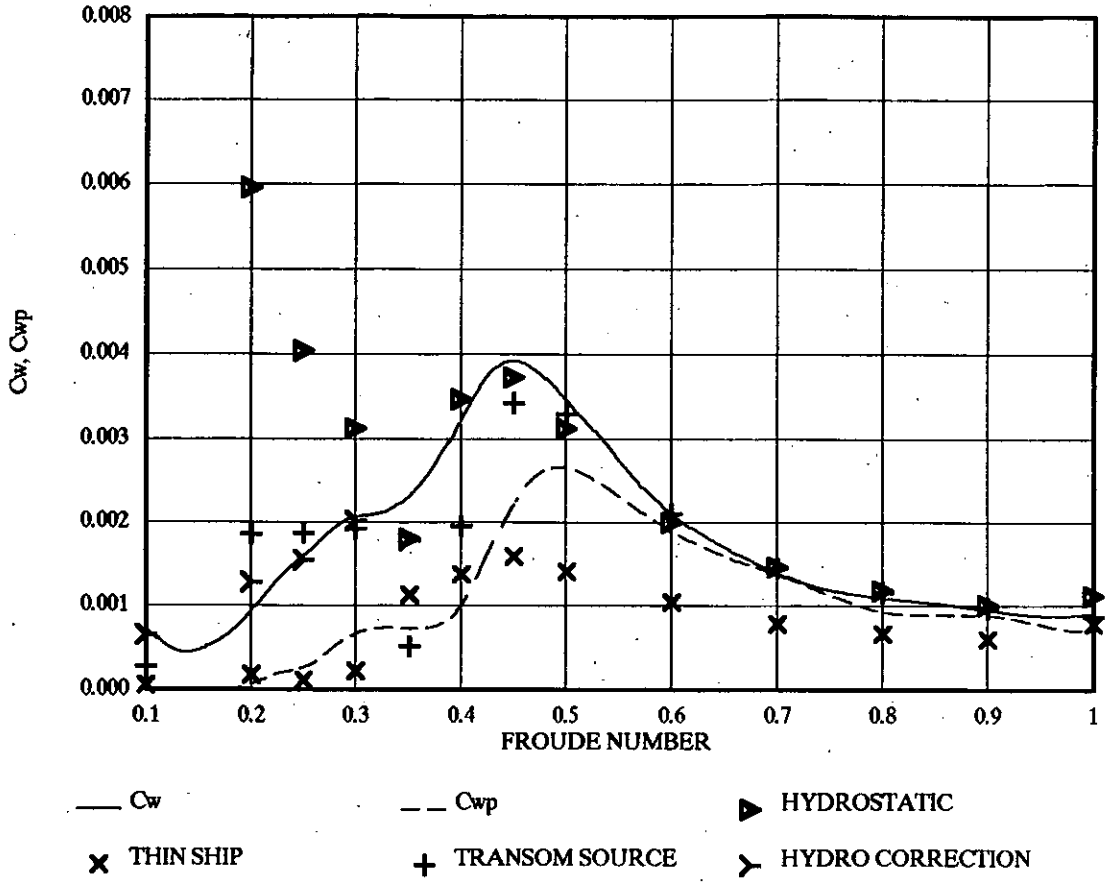

FIGURE 31 THEORETICAL WAVE RESISTANCE 5b S/L 0.5

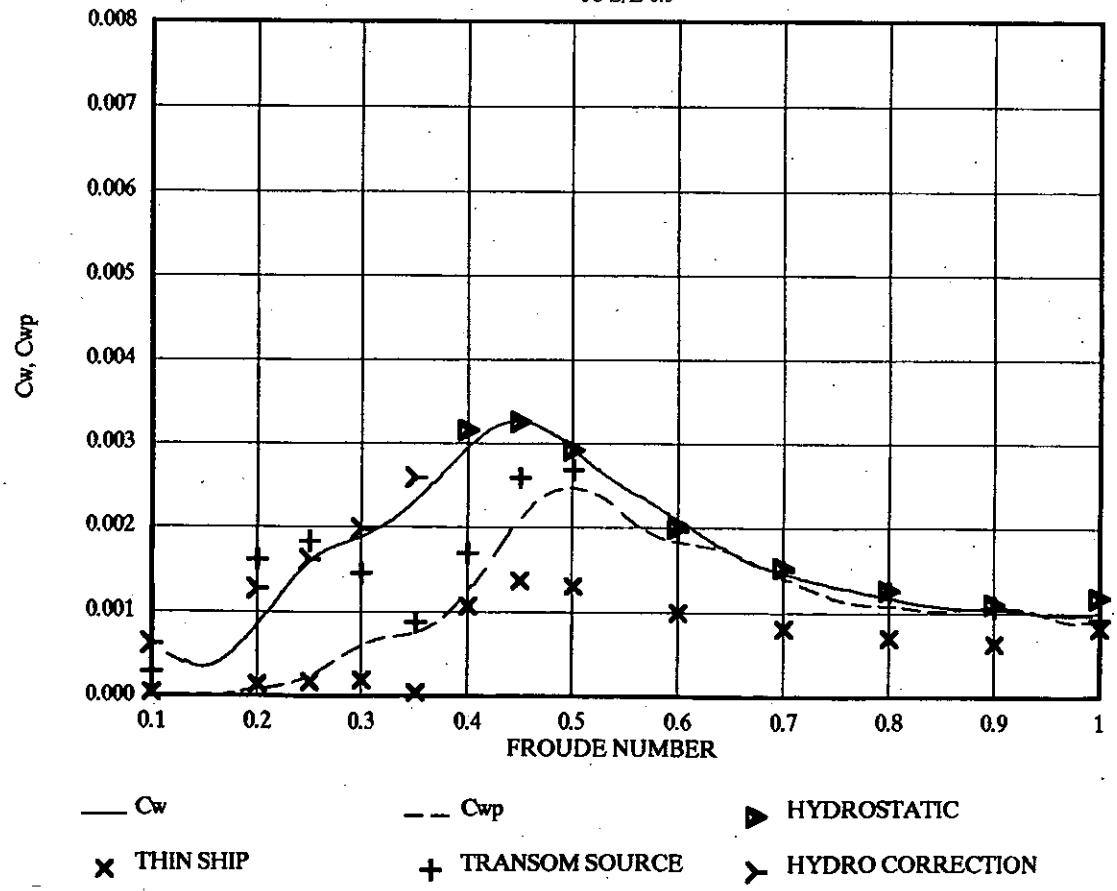

FIGURE 32

THEORETICAL WAVE RESISTANCE
5e MONOHULL

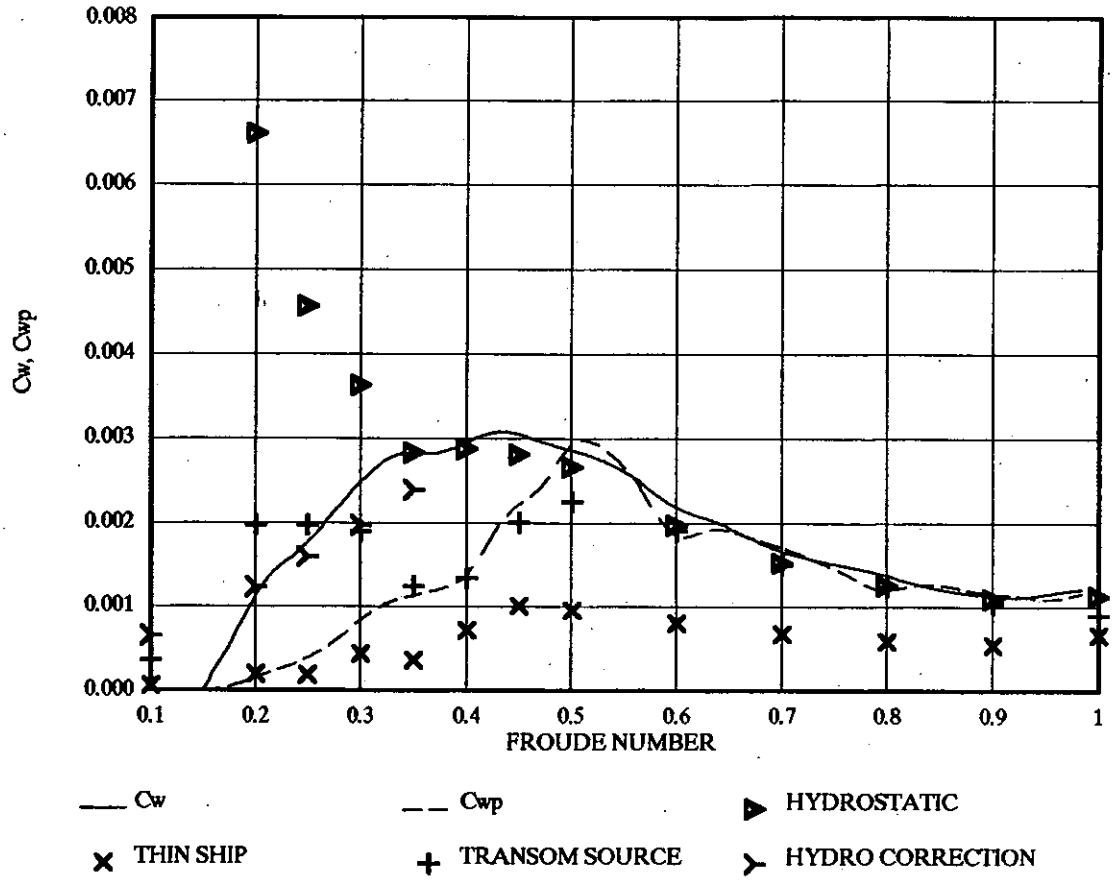

FIGURE 33

THEORETICAL WAVE RESISTANCE
5e S/L 0.2

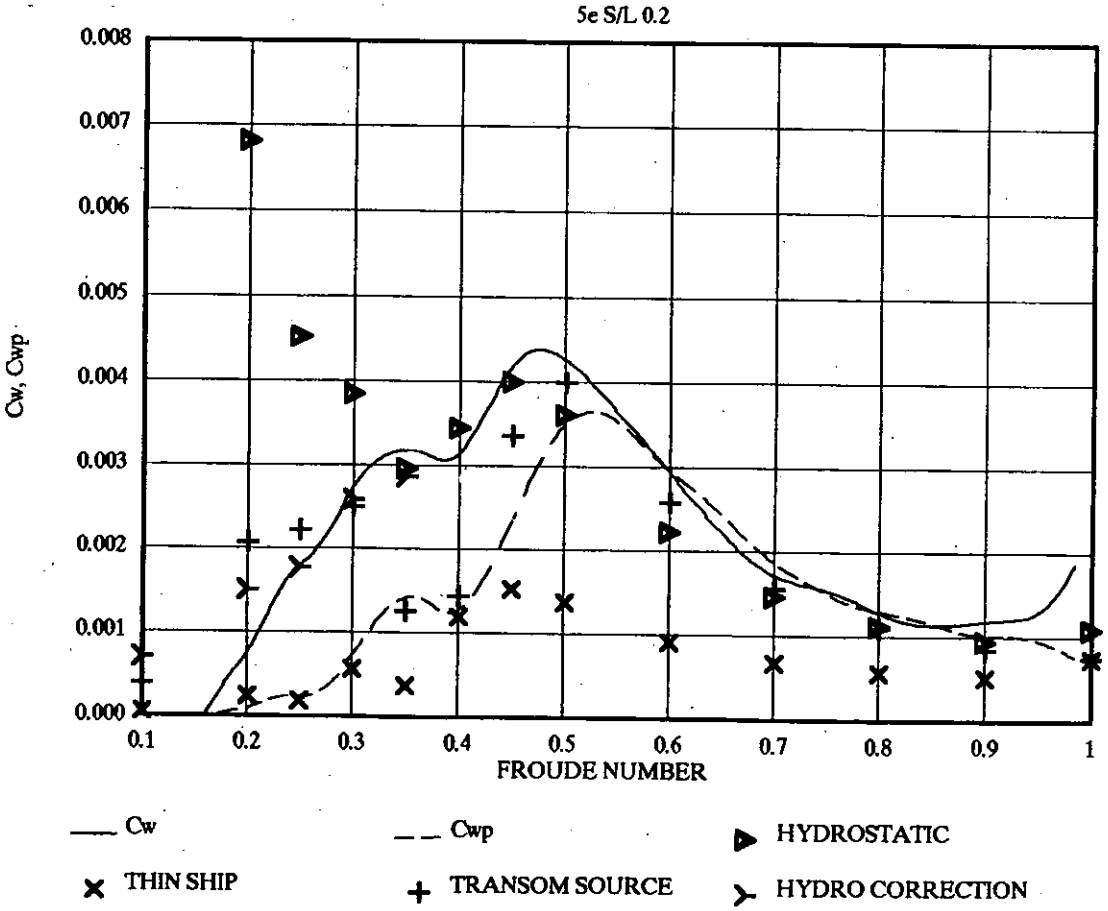

FIGURE 34

THEORETICAL WAVE RESISTANCE
5e S/L 0.3

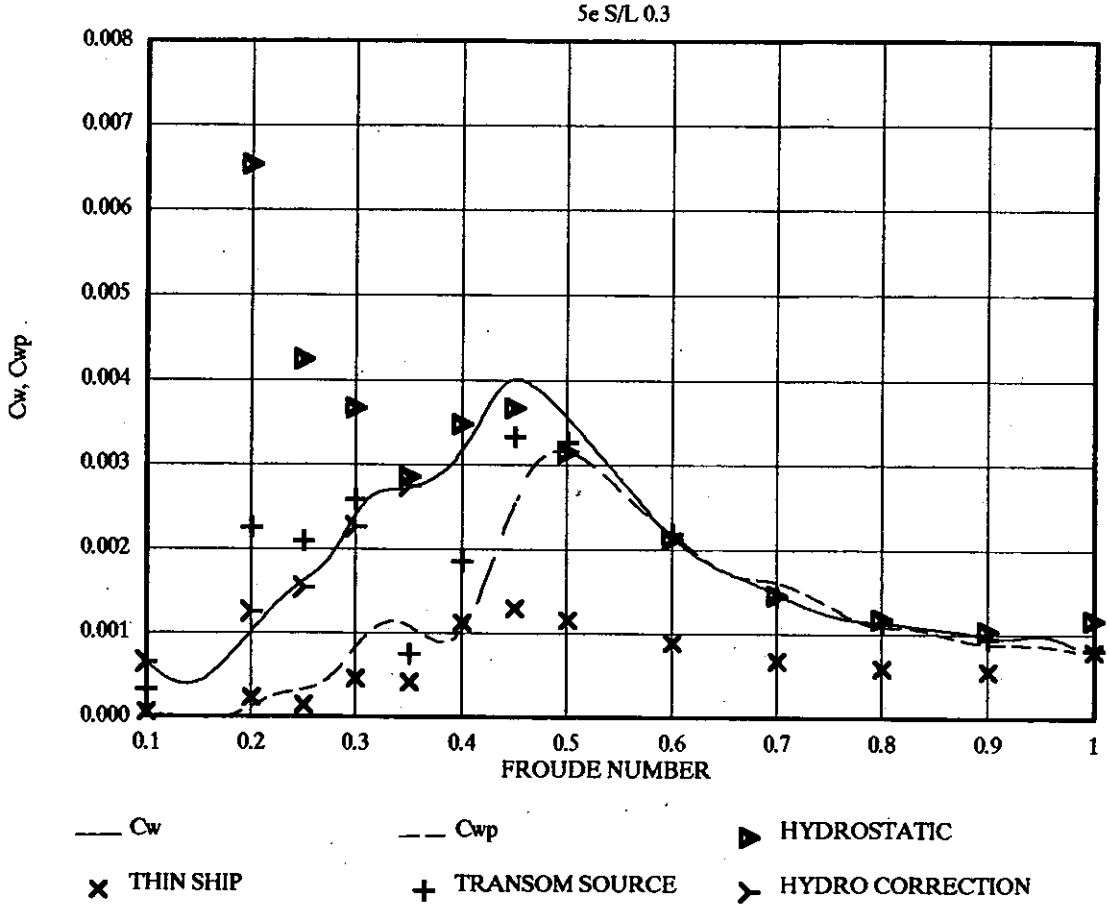

FIGURE 35

THEORETICAL WAVE RESISTANCE
5e S/L 0.4

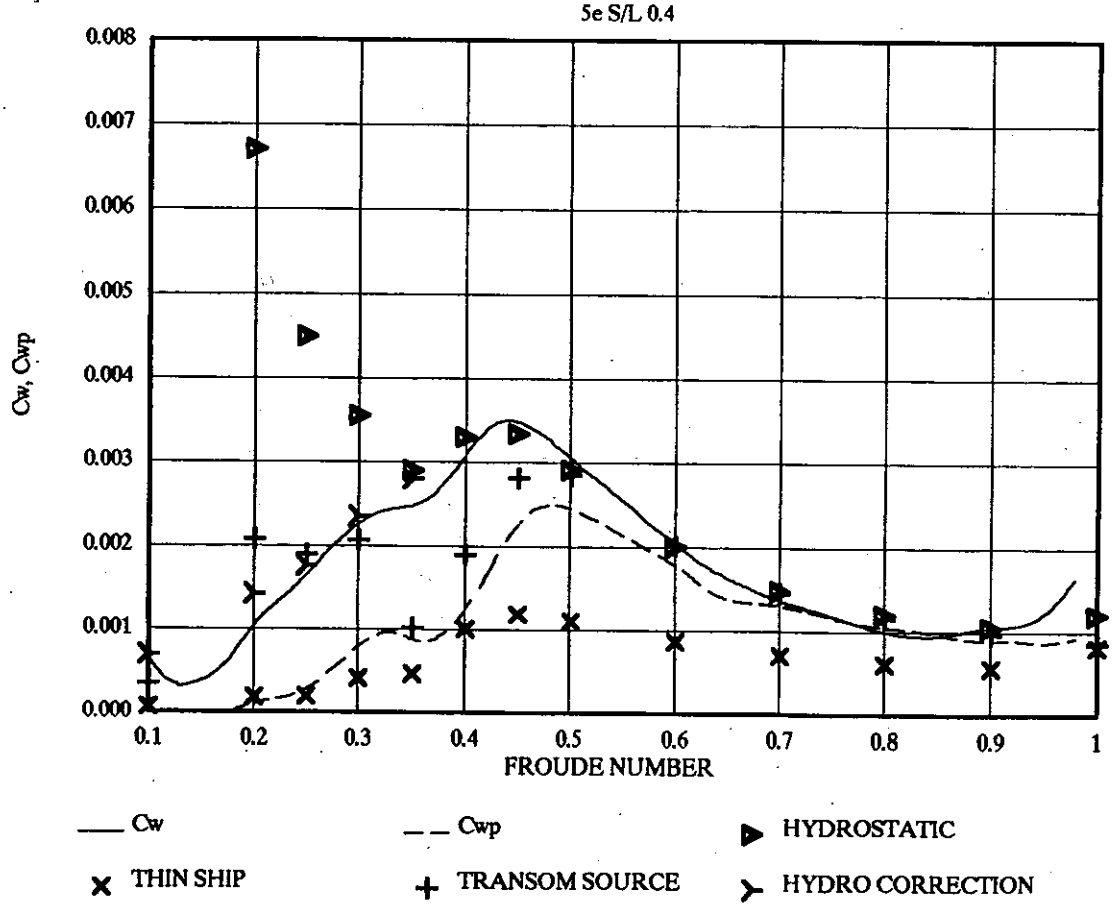

FIGURE 36

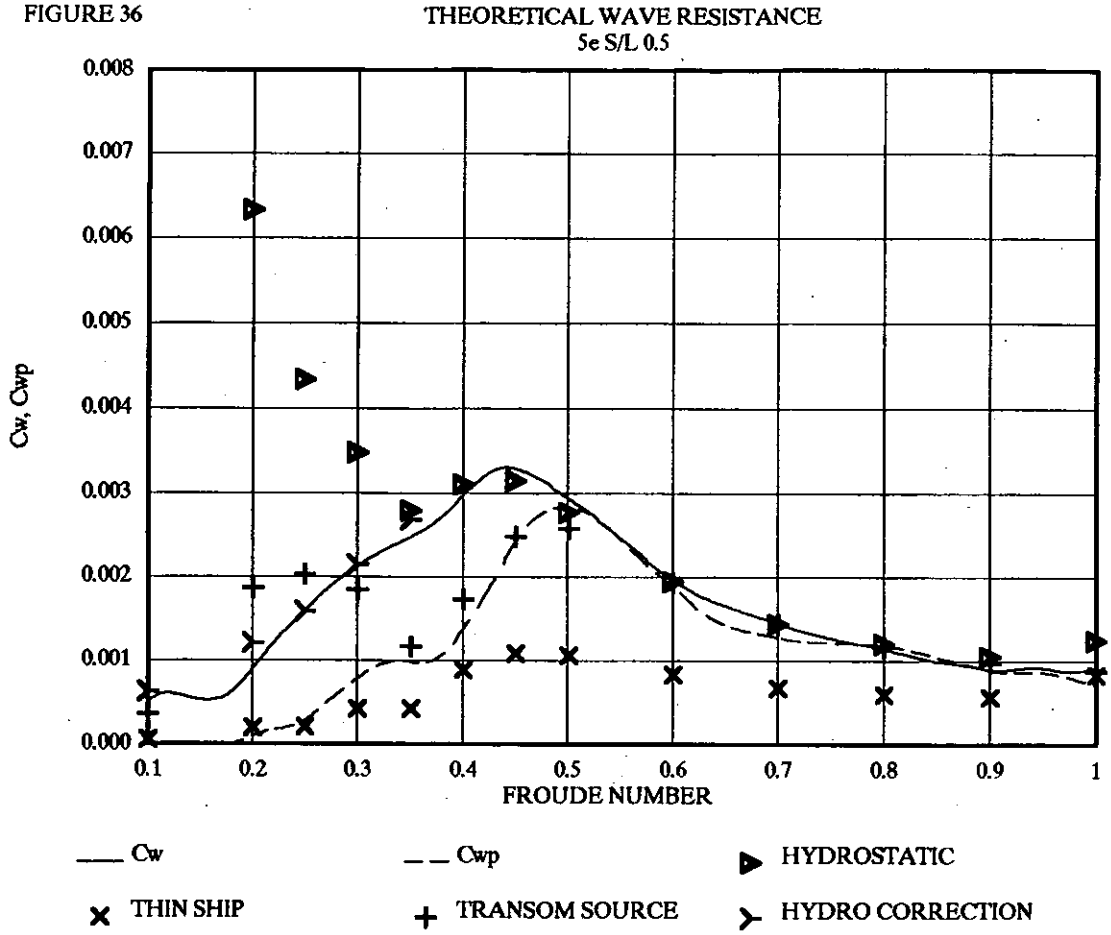

FIGURE 37

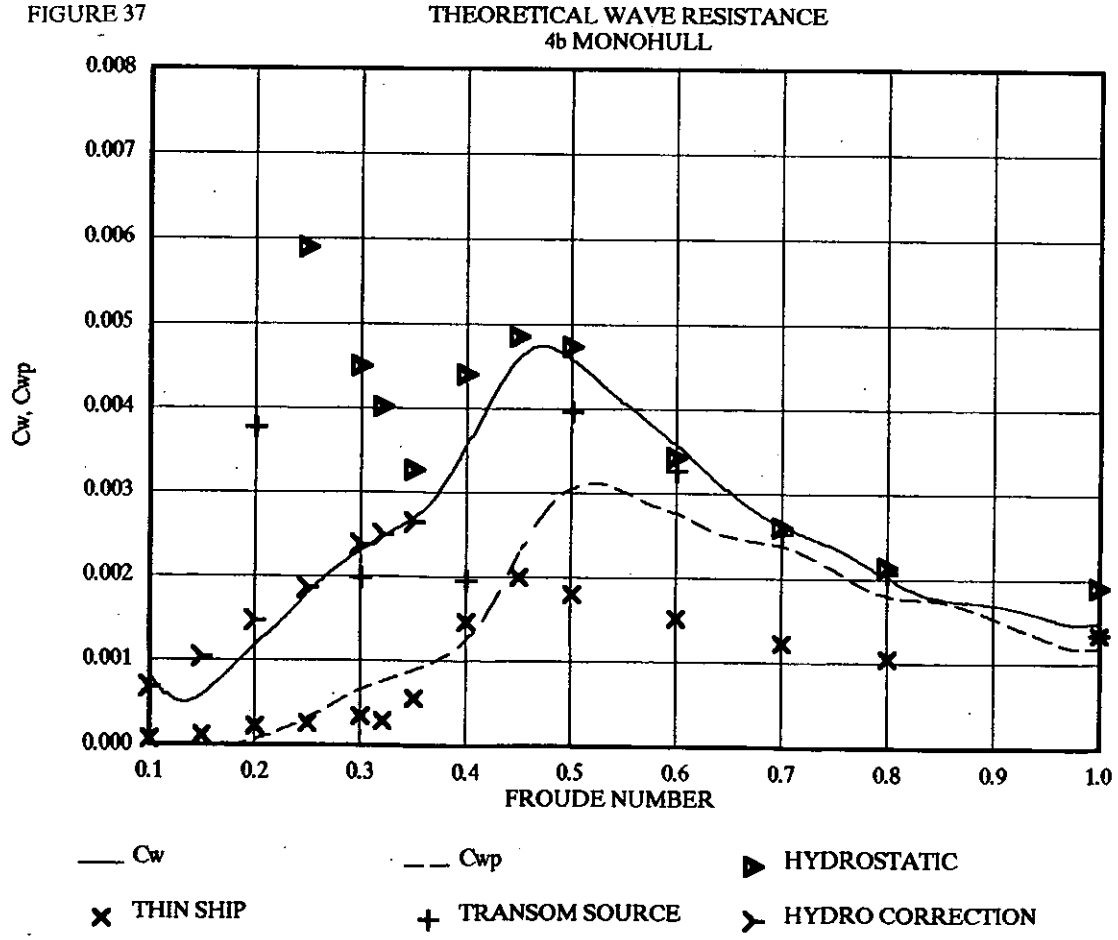

FIGURE 38

THEORETICAL WAVE RESISTANCE
4b S/L 0.3 NORMAL DISPLACEMENT

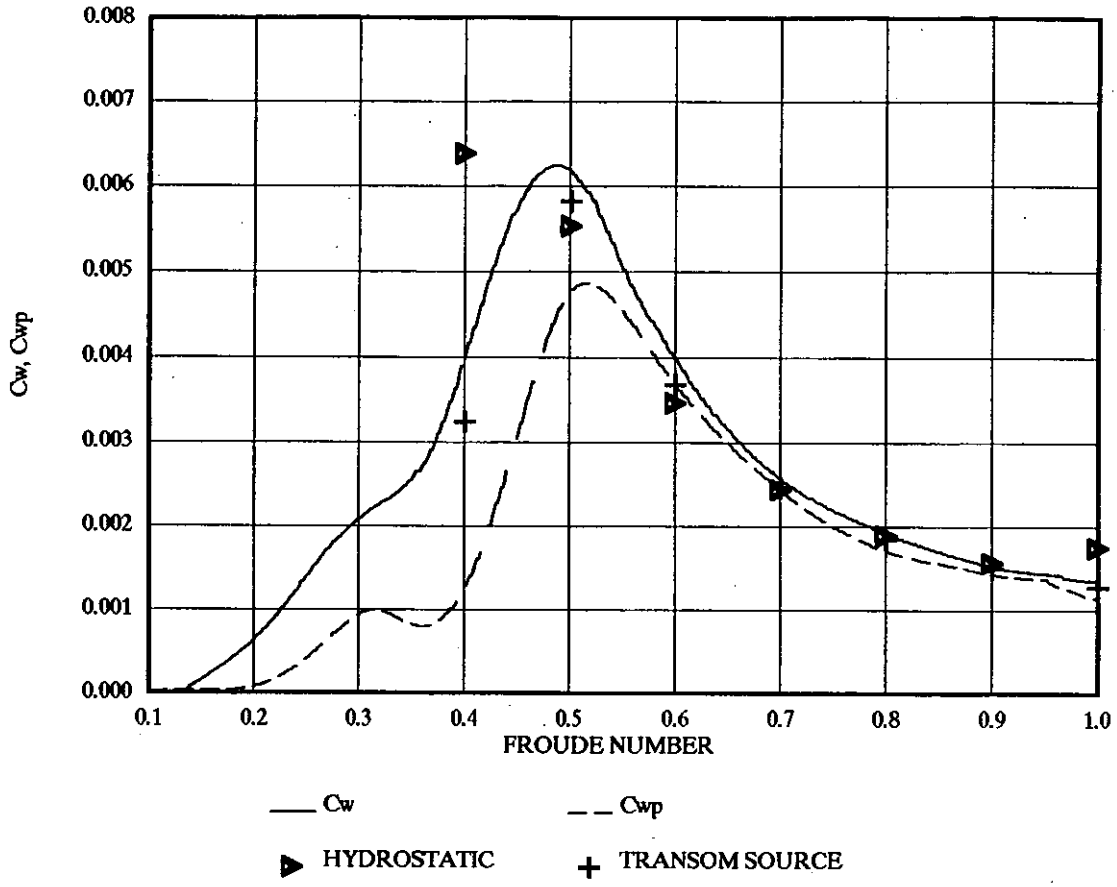

FIGURE 39

THEORETICAL WAVE RESISTANCE
4b S/L 0.5 NORMAL DISPLACEMENT

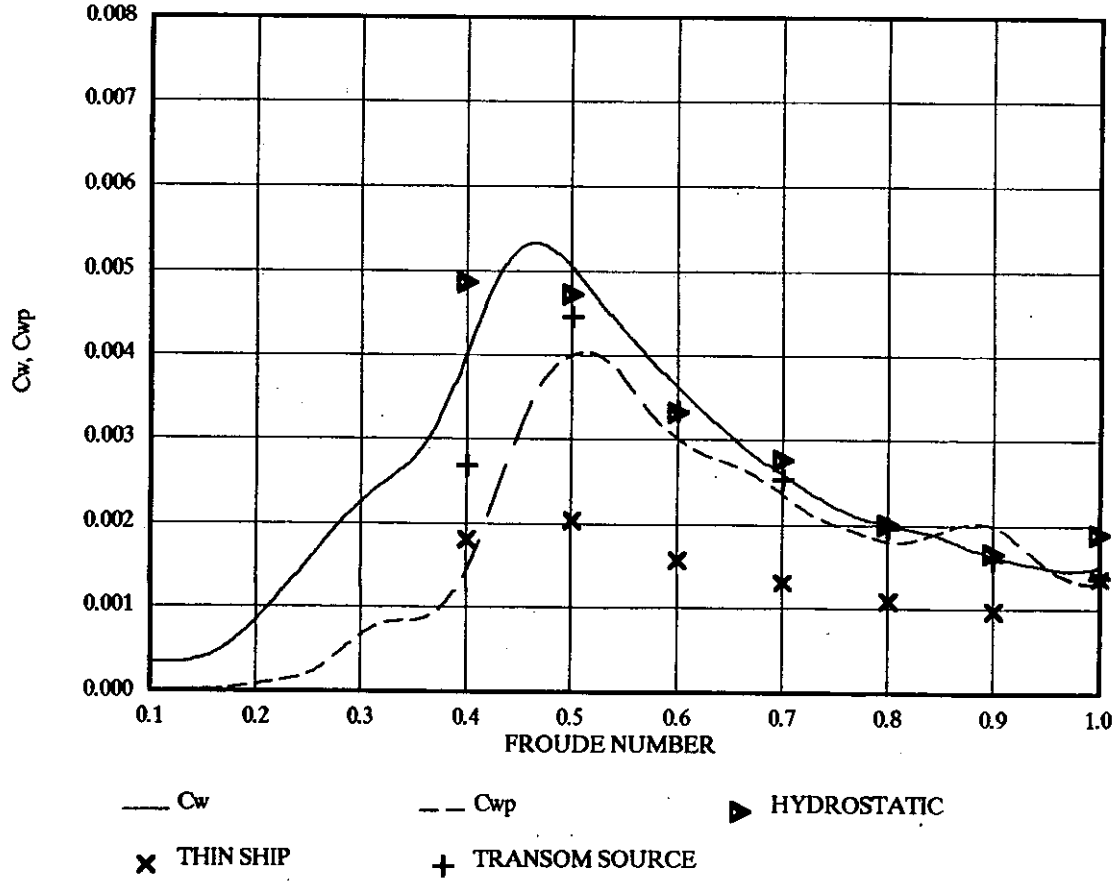

FIGURE 40

THEORETICAL WAVE RESISTANCE
4b MONOHULL LIGHT DISPLACEMENT

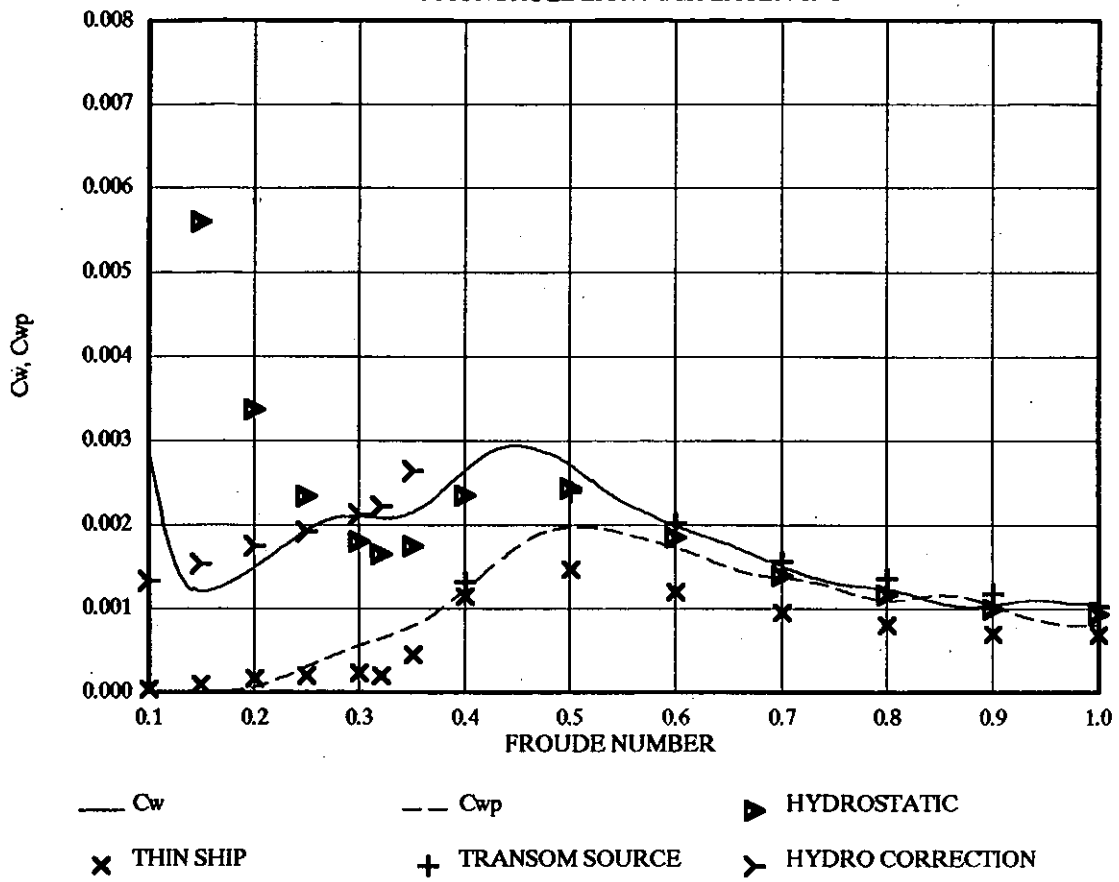

FIGURE 41

THEORETICAL WAVE RESISTANCE
4b S/L 0.3 LIGHT DISPLACEMENT

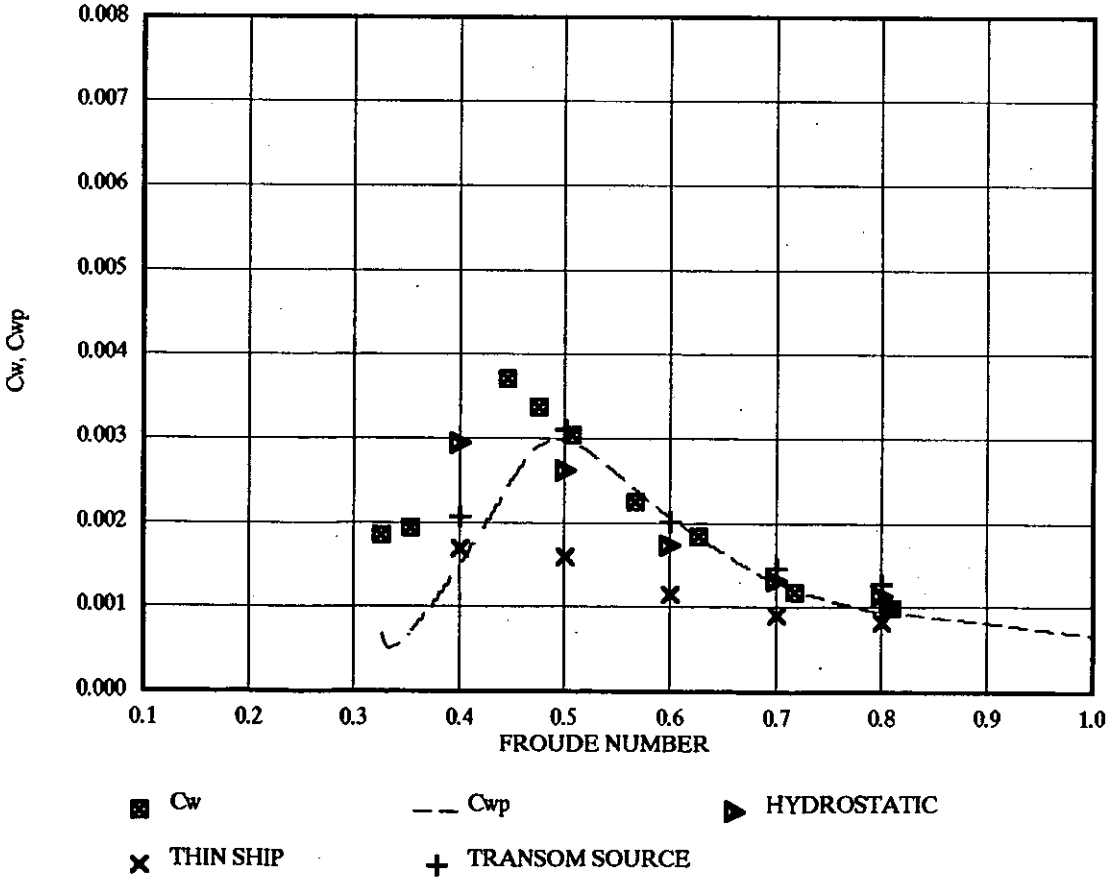

FIGURE 42

THEORETICAL WAVE RESISTANCE
4b S/L 0.5 LIGHT DISPLACEMENT

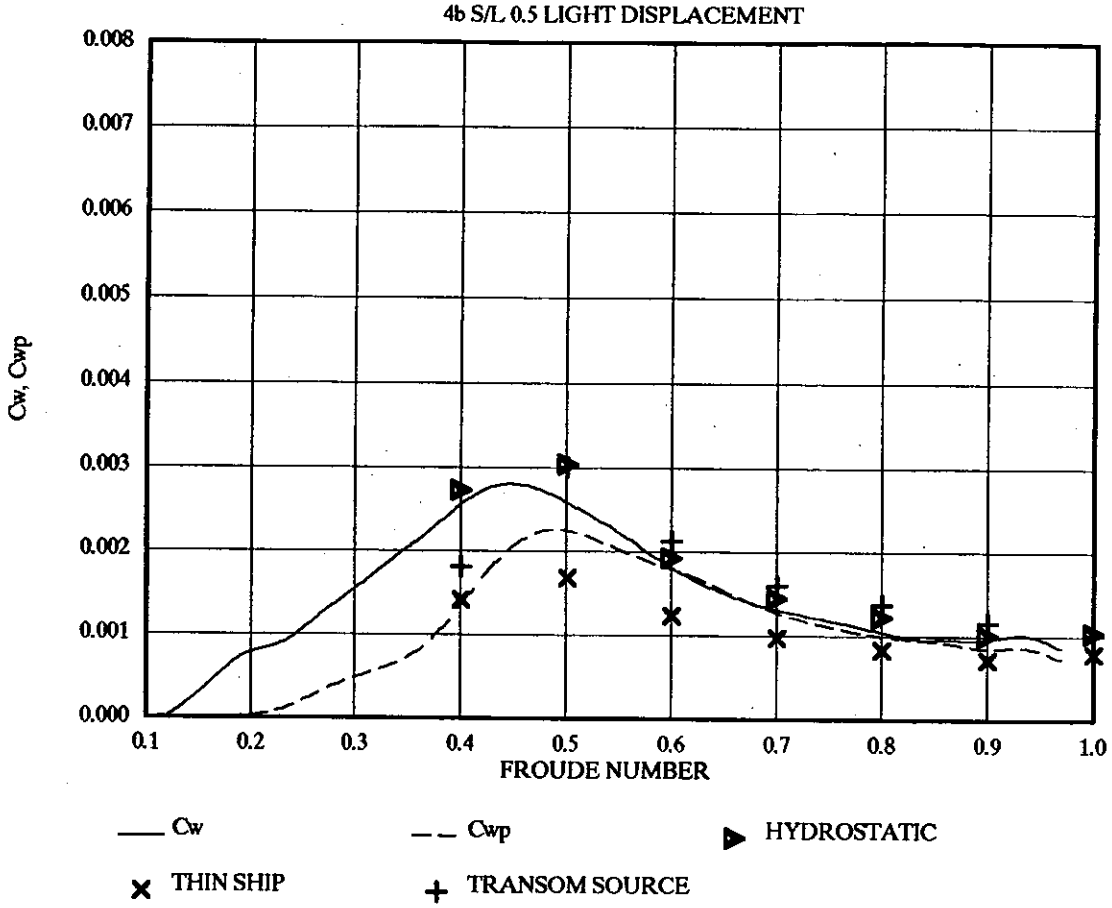

FIGURE 43 THEORETICAL WAVE RESISTANCE FOR 4b (HYDROSTATIC CORRECTED) USING SINKAGE AND TRIM FROM EXPERIMENTAL RESULTS

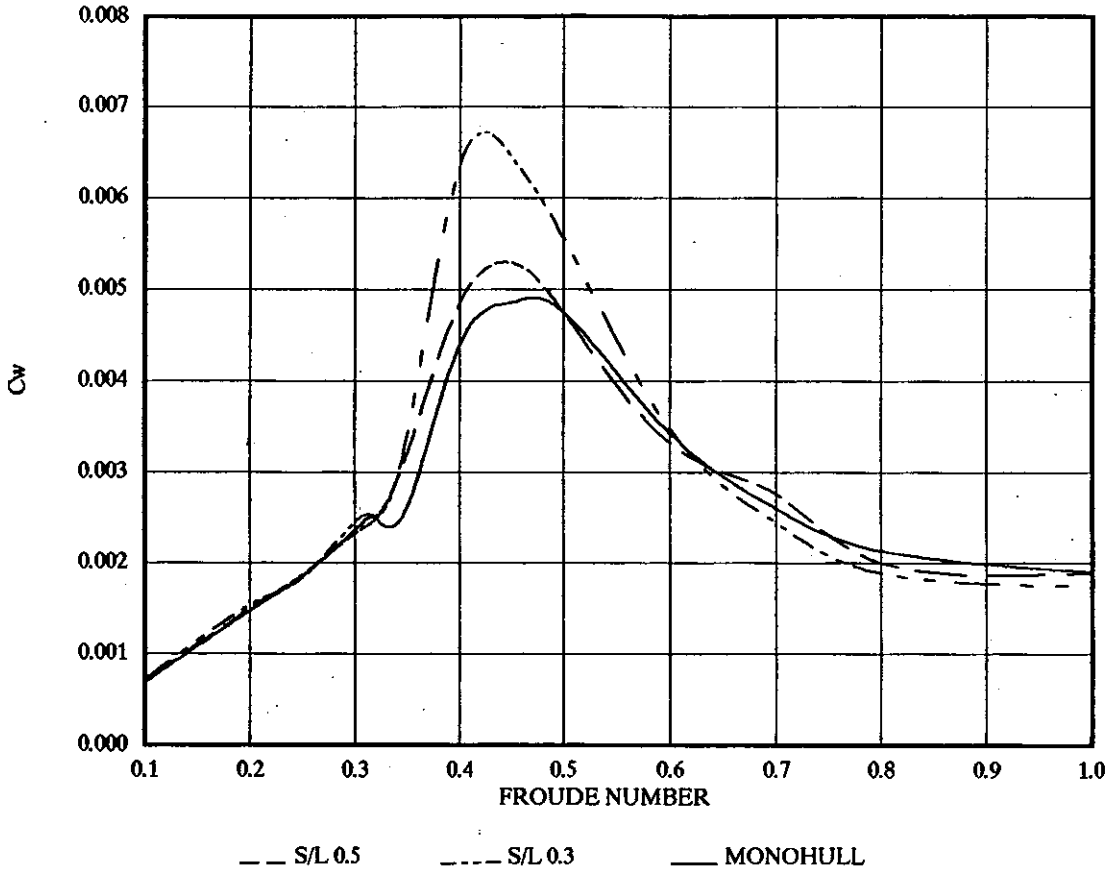

FIGURE 44 THEORETICAL WAVE RESISTANCE FOR 4b (TRANSOM SOURCE) USING SINKAGE AND TRIM FROM EXPERIMENTAL RESULTS

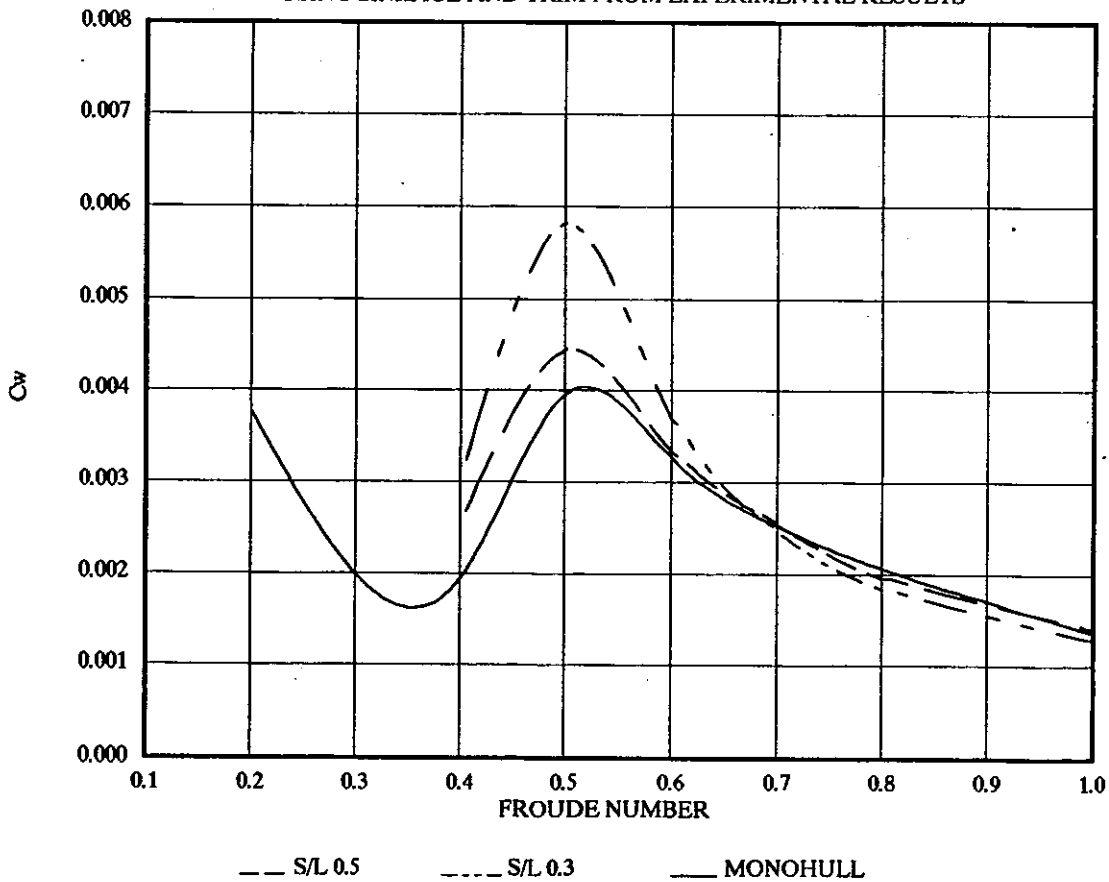

FIGURE 45 THEORETICAL WAVE RESISTANCE FOR 4b LIGHT(HYDROSTATIC CORRECTED) USING SINKAGE AND TRIM FROM EXPERIMENTAL RESULTS

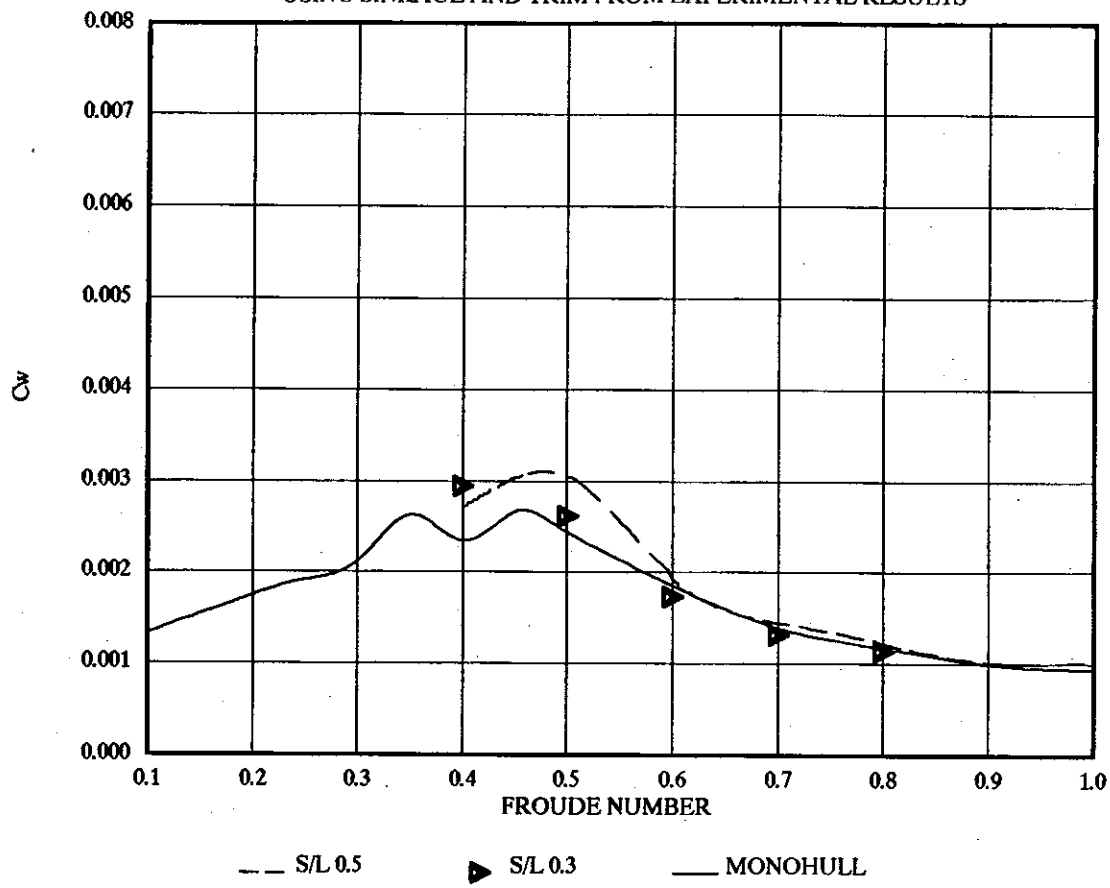

FIGURE 46 THEORETICAL WAVE RESISTANCE FOR 4b LIGHT(TRANSOM SOURCE) USING SINKAGE AND TRIM FROM EXPERIMENTAL RESULTS

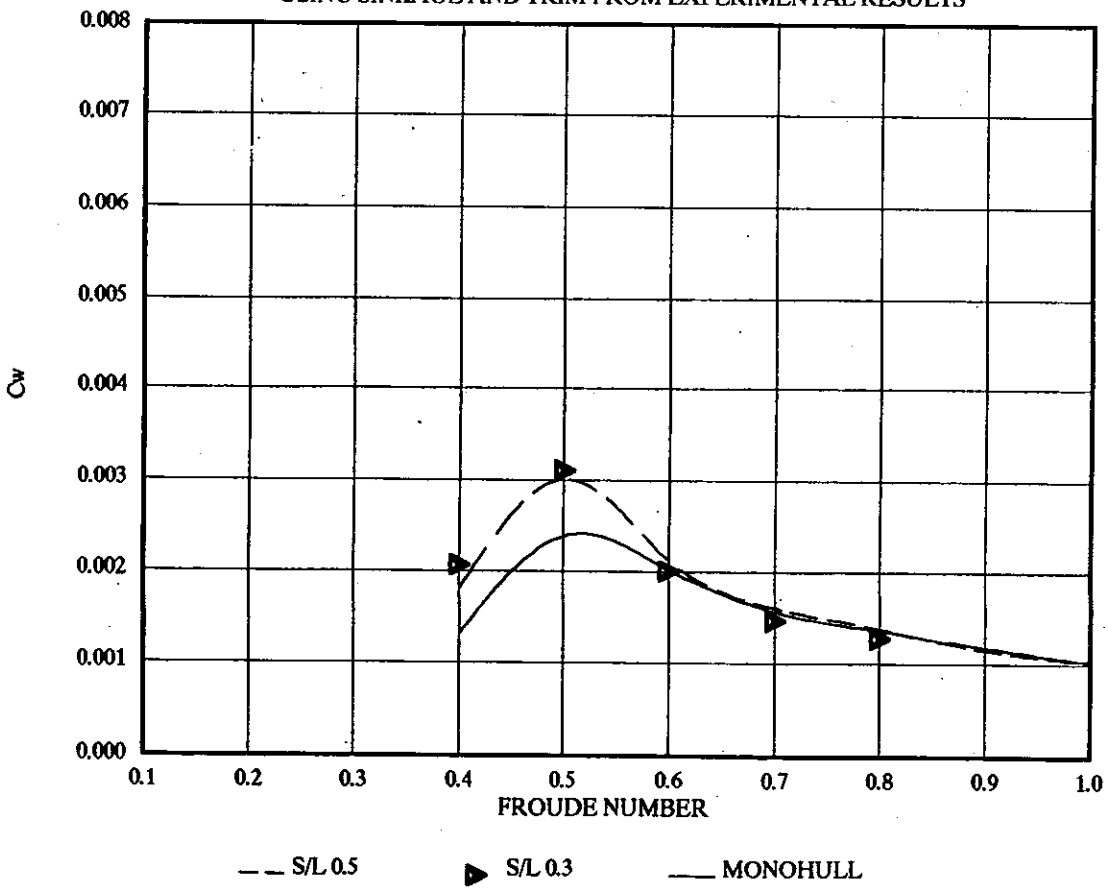

FIGURE 47

THEORETICAL WAVE RESISTANCE
5a, 5b, 5c MONOHULL

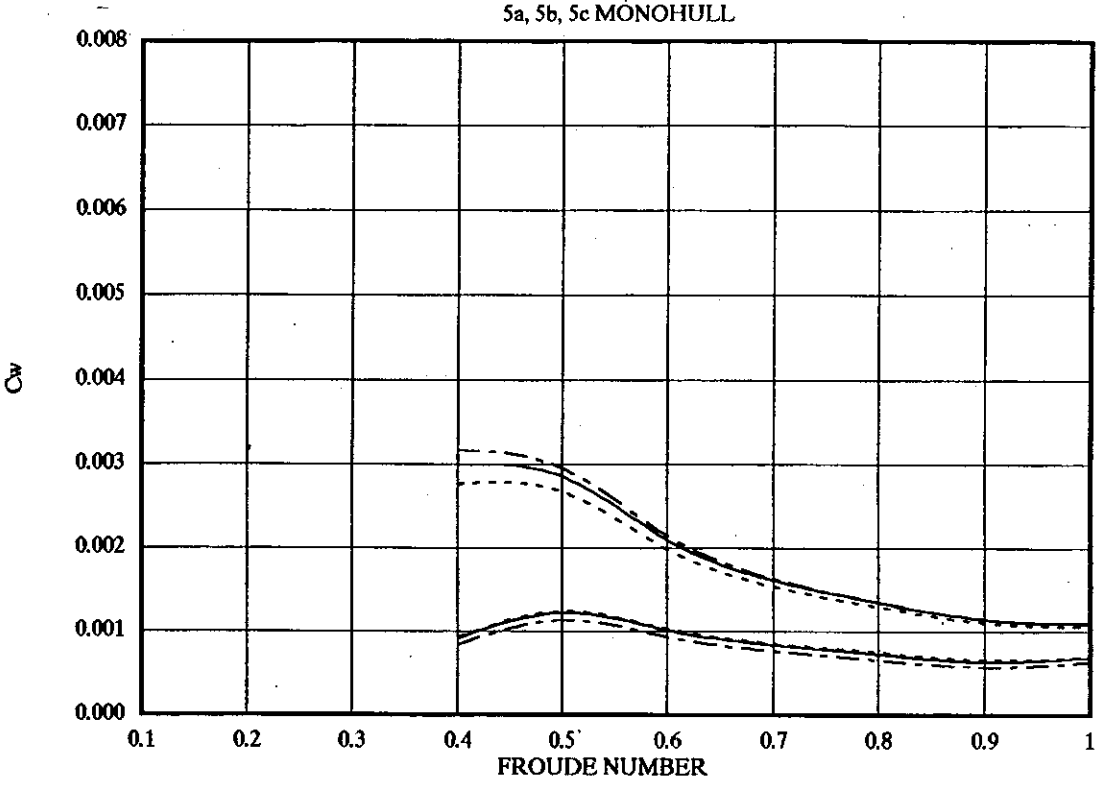

5a THIN SHIP 5b THIN SHIP 5c THIN SHIP

5a HYDRO 5b HYDRO 5c HYDRO

FIGURE 48

THEORETICAL WAVE RESISTANCE
5a, 5b, 5c MONOHULL

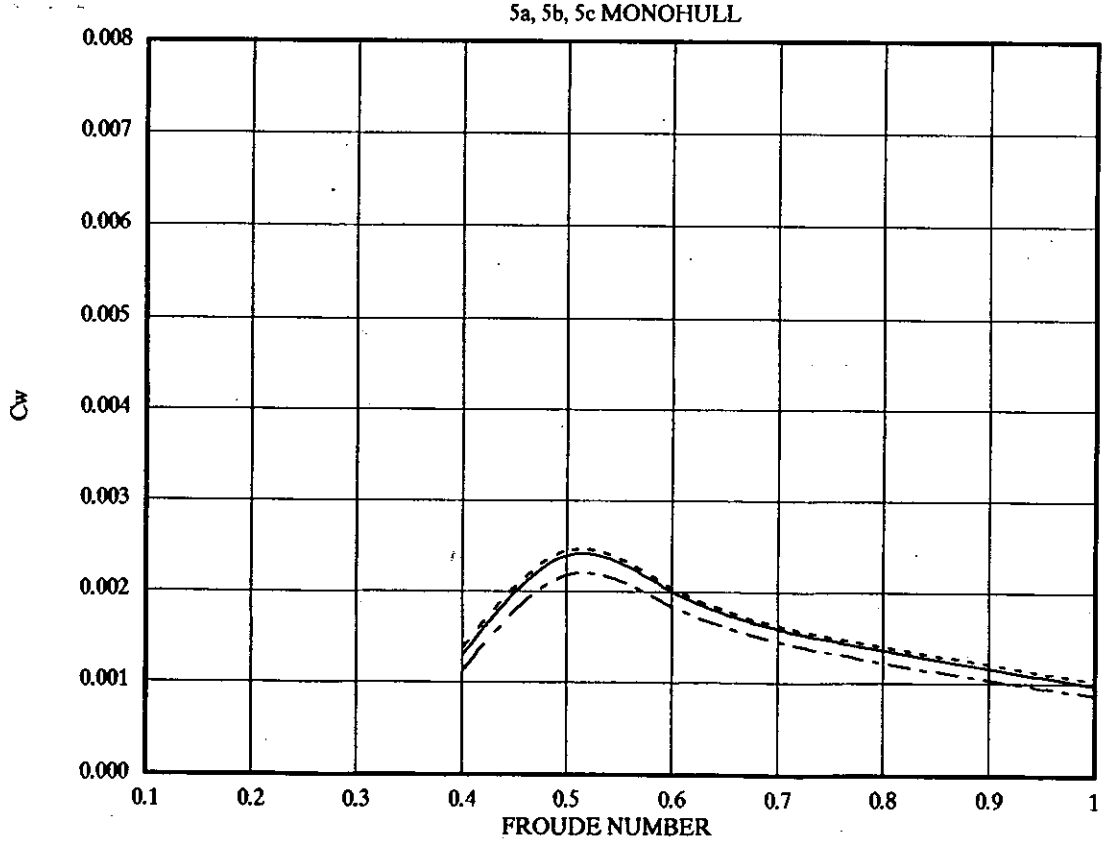

5a SINGLE SOURCE 5b SINGLE SOURCE 5c SINGLE SOURCE

FIGURE 49

THEORETICAL WAVE RESISTANCE
5a, 5b, 5c S/L 0.3

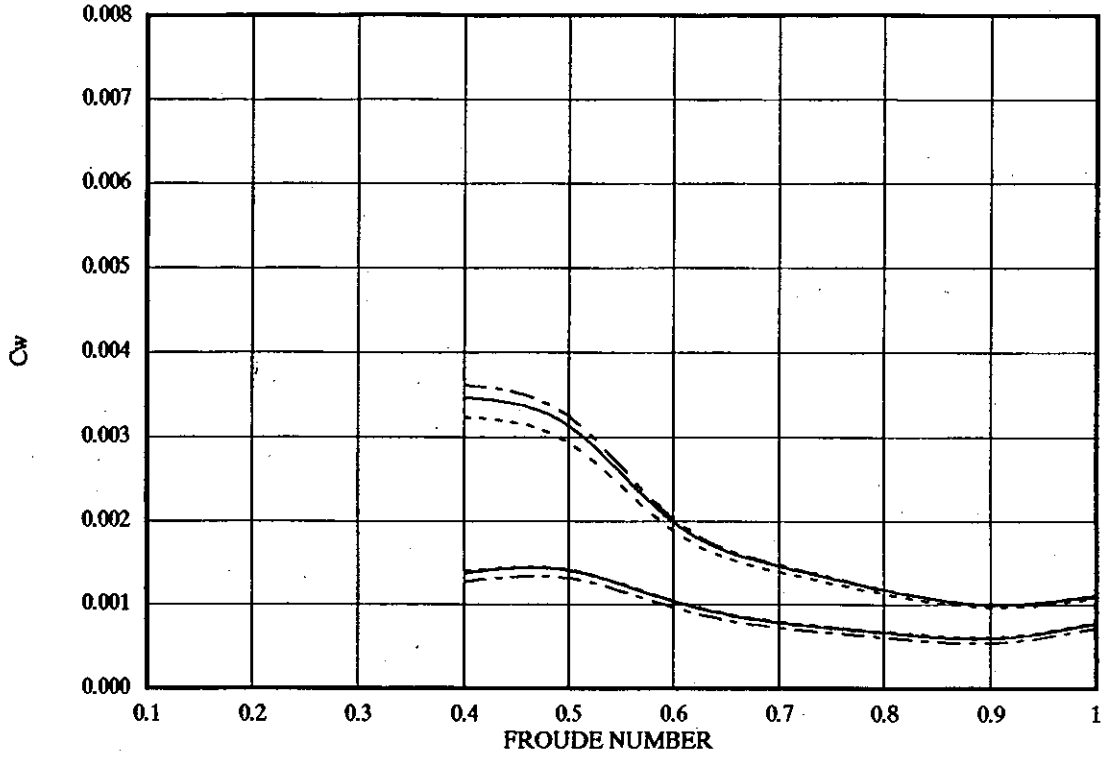

_ _ _ 5a THIN SHIP ___ 5b THIN SHIP - - - - 5c THIN SHIP

_ _ _ 5a HYDRO ___ 5b HYDRO - - - - 5c HYDRO

FIGURE 50

THEORETICAL WAVE RESISTANCE
5a, 5b, 5c S/L 0.3

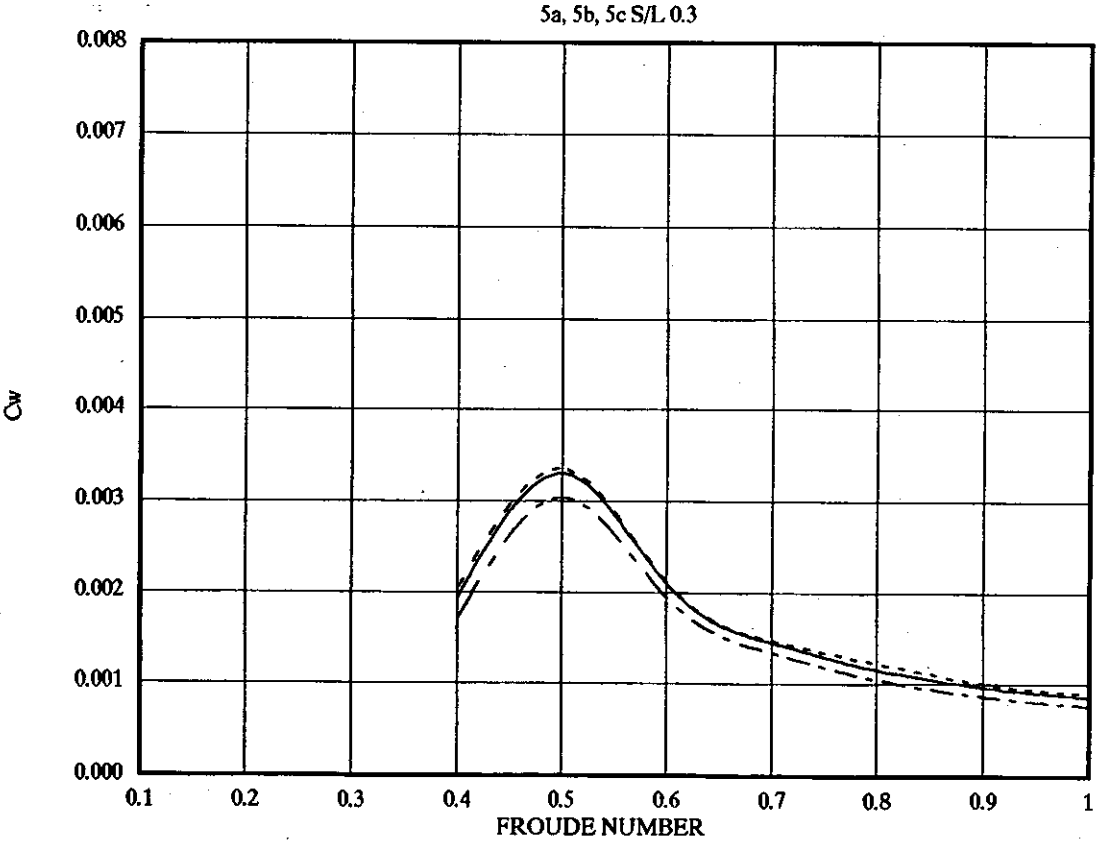

_ _ _ 5a SINGLE SOURCE ___ 5b SINGLE SOURCE - - - - 5c SINGLE SOURCE

FIGURE 51

THEORETICAL WAVE RESISTANCE
5a, 5b, 5c S/L 0.5

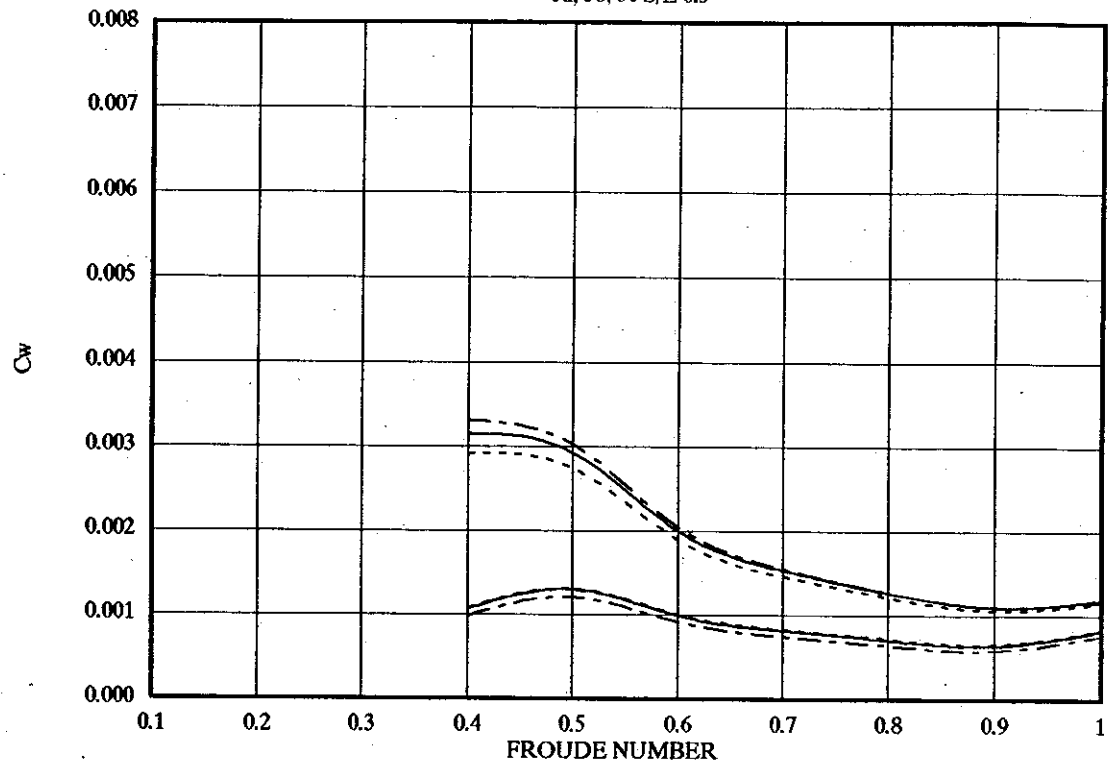

5a THIN SHIP 5b THIN SHIP 5c THIN SHIP

5a HYDRO 5b HYDRO 5c HYDRO

FIGURE 52

THEORETICAL WAVE RESISTANCE
5a, 5b, 5c S/L 0.5

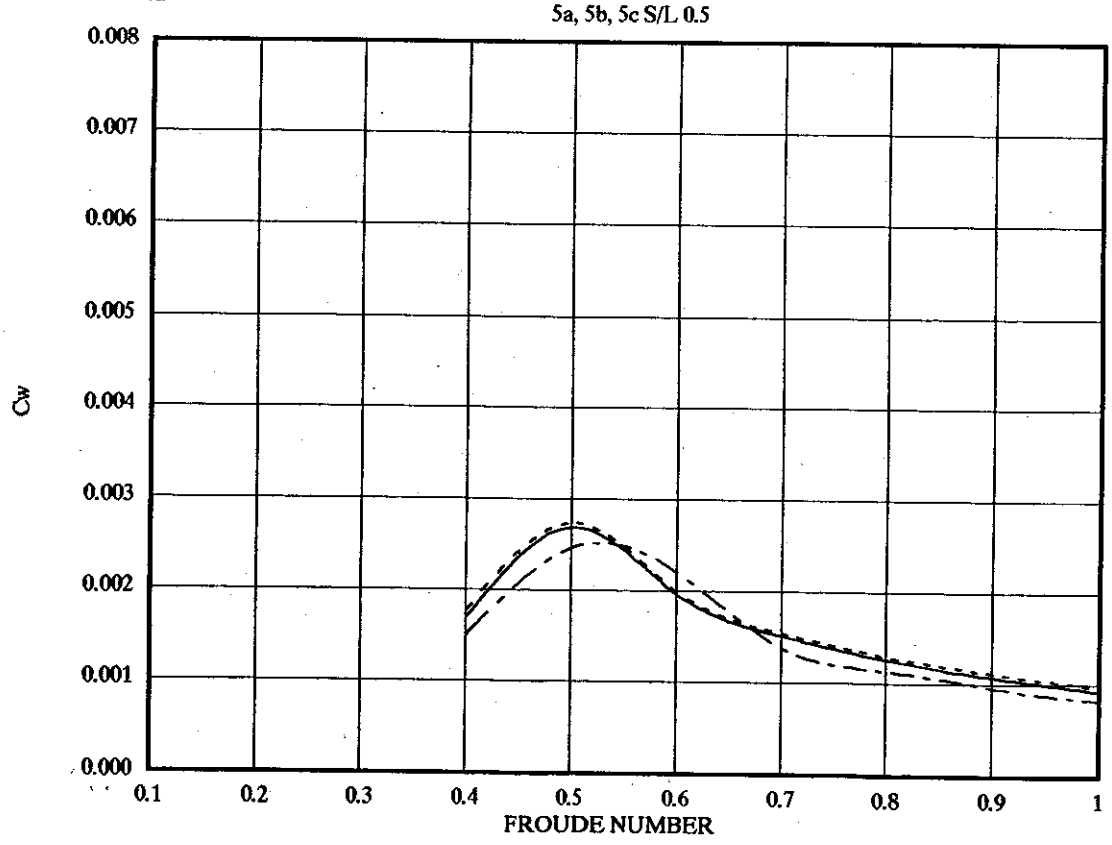

5a T–SOURCE 5b T–SOURCE 5c T–SOURCE

FIGURE 53

THEORETICAL WAVE RESISTANCE
5b, 5d, 5e MONOHULL

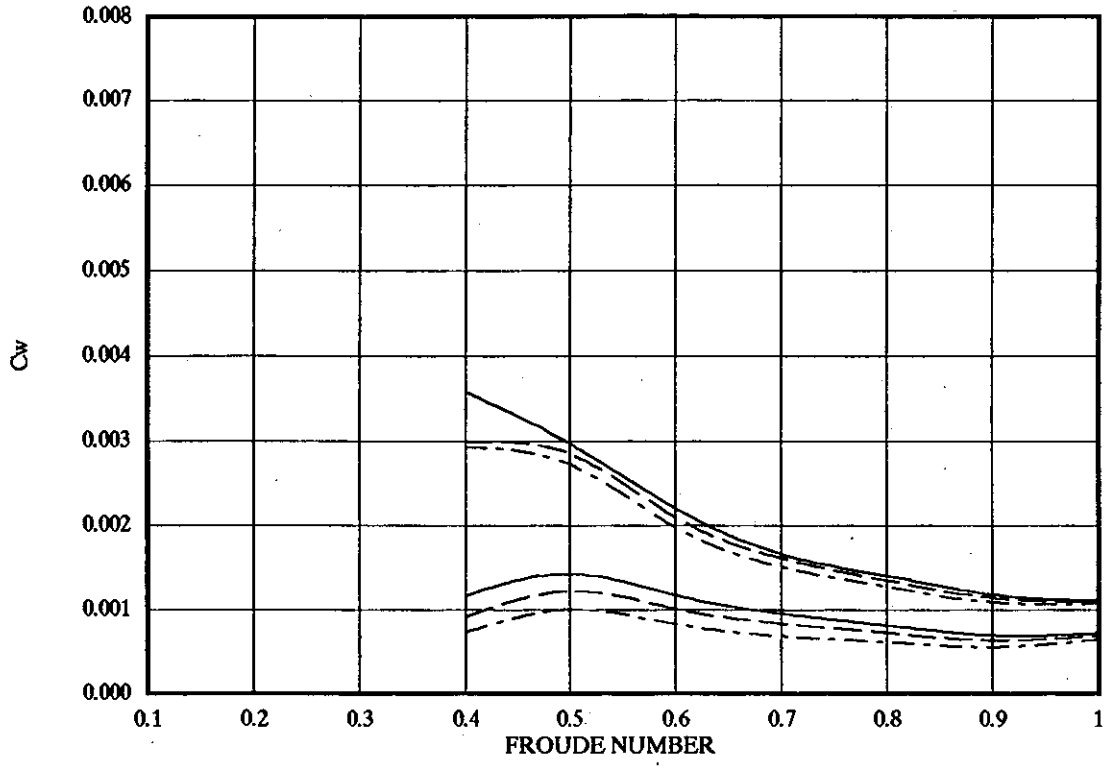

_ _ 5b THIN SHIP ___ 5d THIN SHIP _ _ _ 5e THIN SHIP

_ _ 5b HYDRO ___ 5d HYDRO _ _ _ 5e HYDRO

FIGURE 54

THEORETICAL WAVE RESISTANCE
5b, 5d, 5e MONOHULL TRANSOM SOURCE

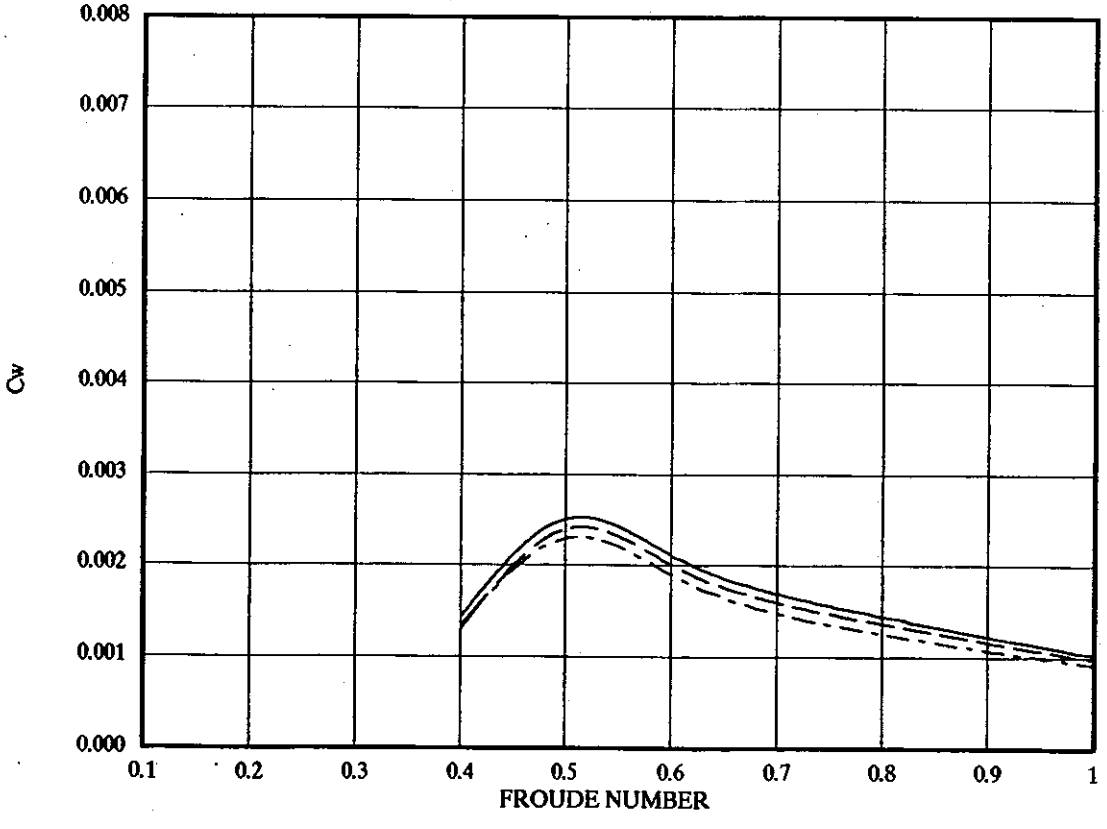

_ _ 5b ___ 5d _ _ _ 5e

FIGURE 55

THEORETICAL WAVE RESISTANCE
5b, 5d, 5e S/L 0.2 FANNED WATERLINES

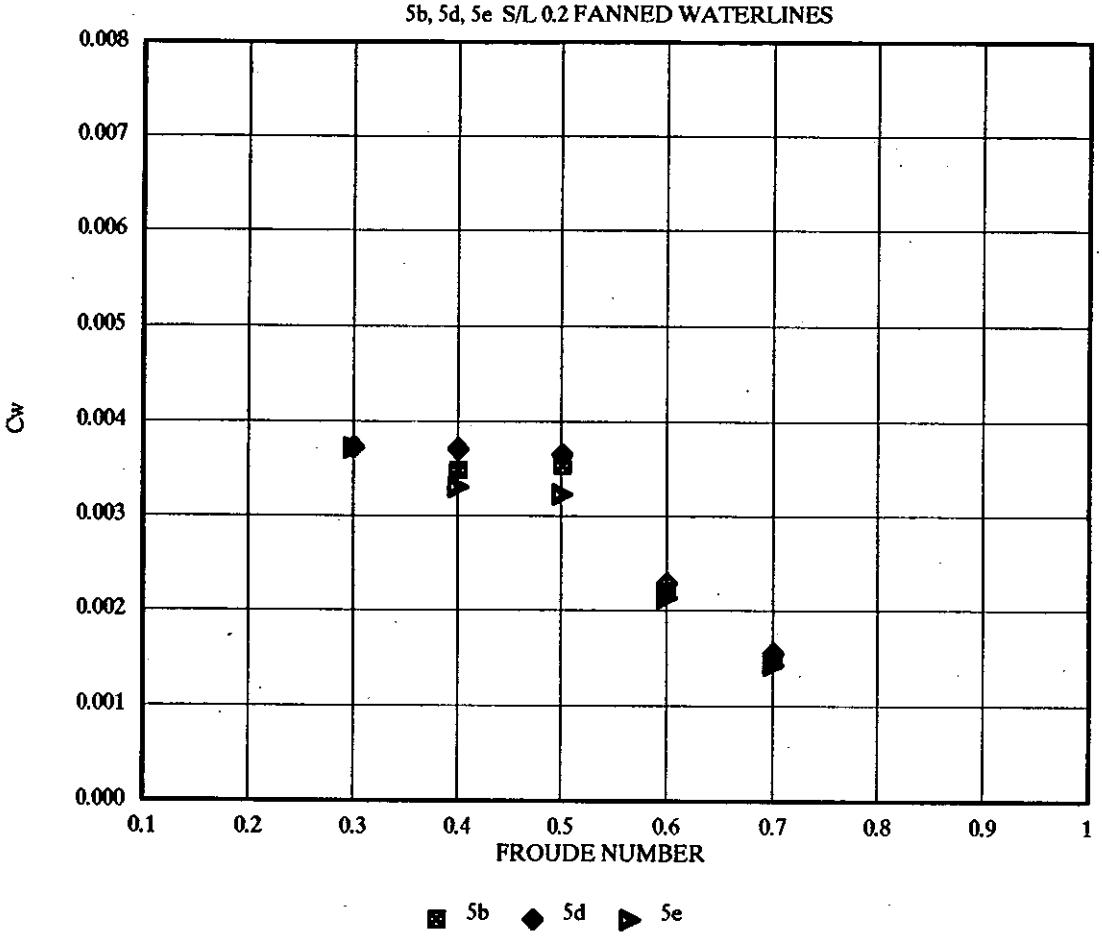

FIGURE 56

THEORETICAL WAVE RESISTANCE
5b, 5d, 5e S/L 0.3

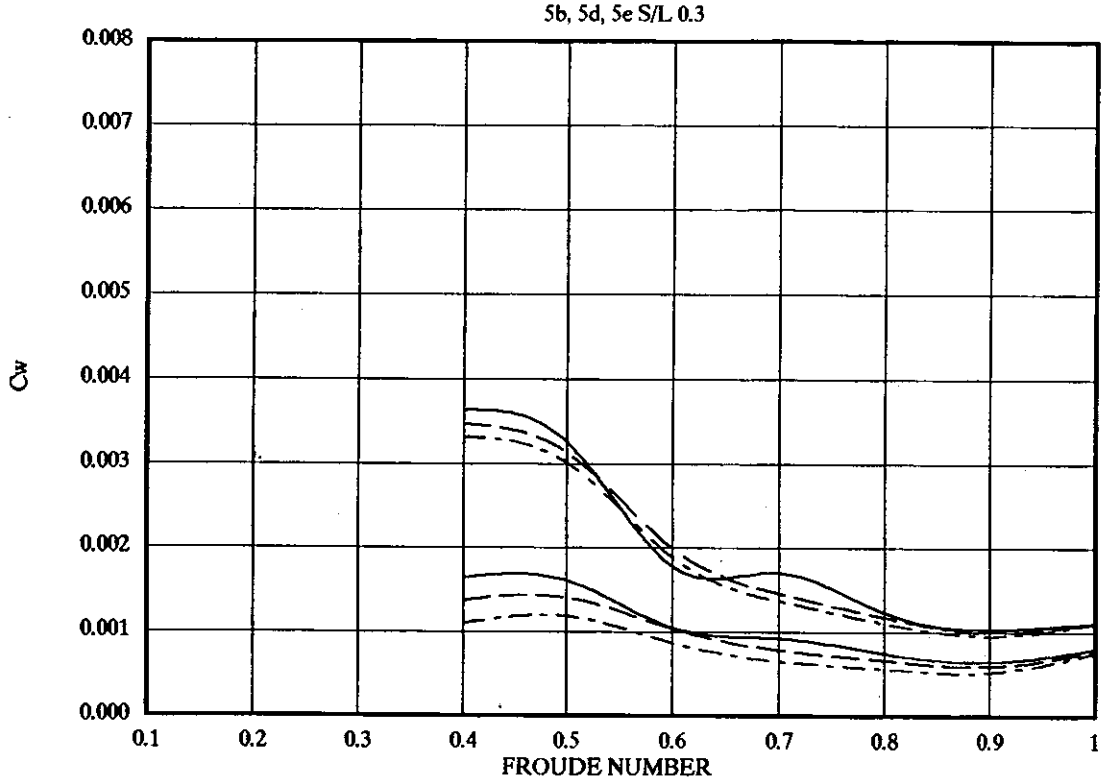

_ _ 5b THIN SHIP ____ 5d THIN SHIP _ _ _ 5e THIN SHIP

_ _ 5b HYDRO ____ 5d HYDRO _ _ _ 5e HYDRO

FIGURE 57

THEORETICAL WAVE RESISTANCE
5b, 5d, 5e S/L 0.3 TRANSOM SOURCE

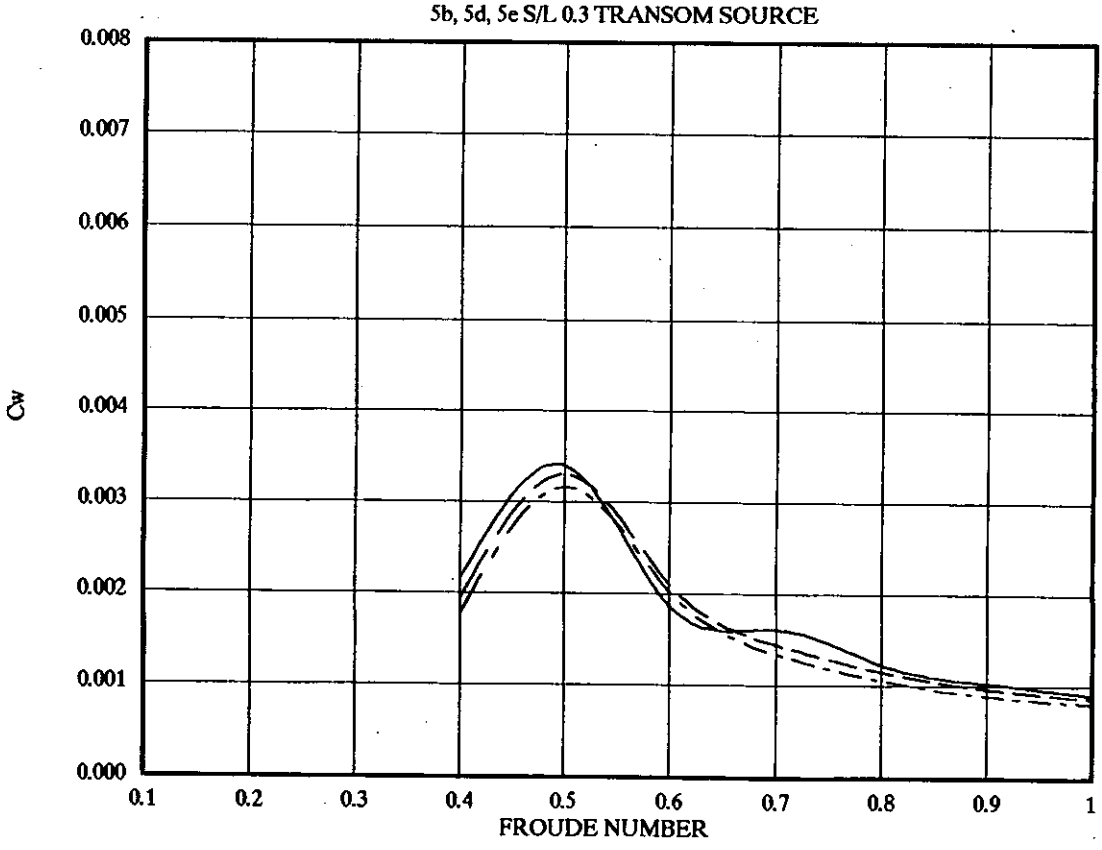

_ _ 5b ____ 5d _ _ _ 5e

FIGURE 58

THEORETICAL WAVE RESISTANCE
5b, 5d, 5e S/L 0.5

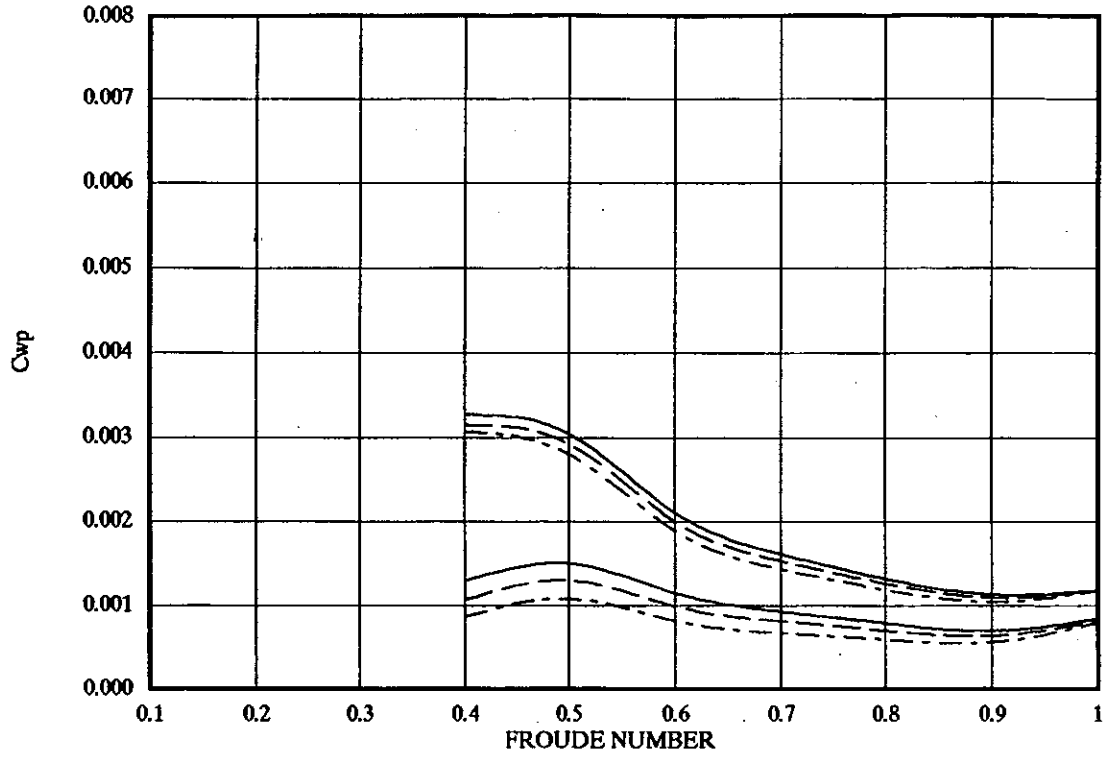

_ _ 5b THIN SHIP ___ 5d THIN SHIP _ _ _ 5e THIN SHIP

_ _ 5b HYDRO ___ 5d HYDRO _ _ _ 5e HYDRO

FIGURE 59

THEORETICAL WAVE RESISTANCE
5b, 5d, 5e S/L 0.5 TRANSOM SOURCE

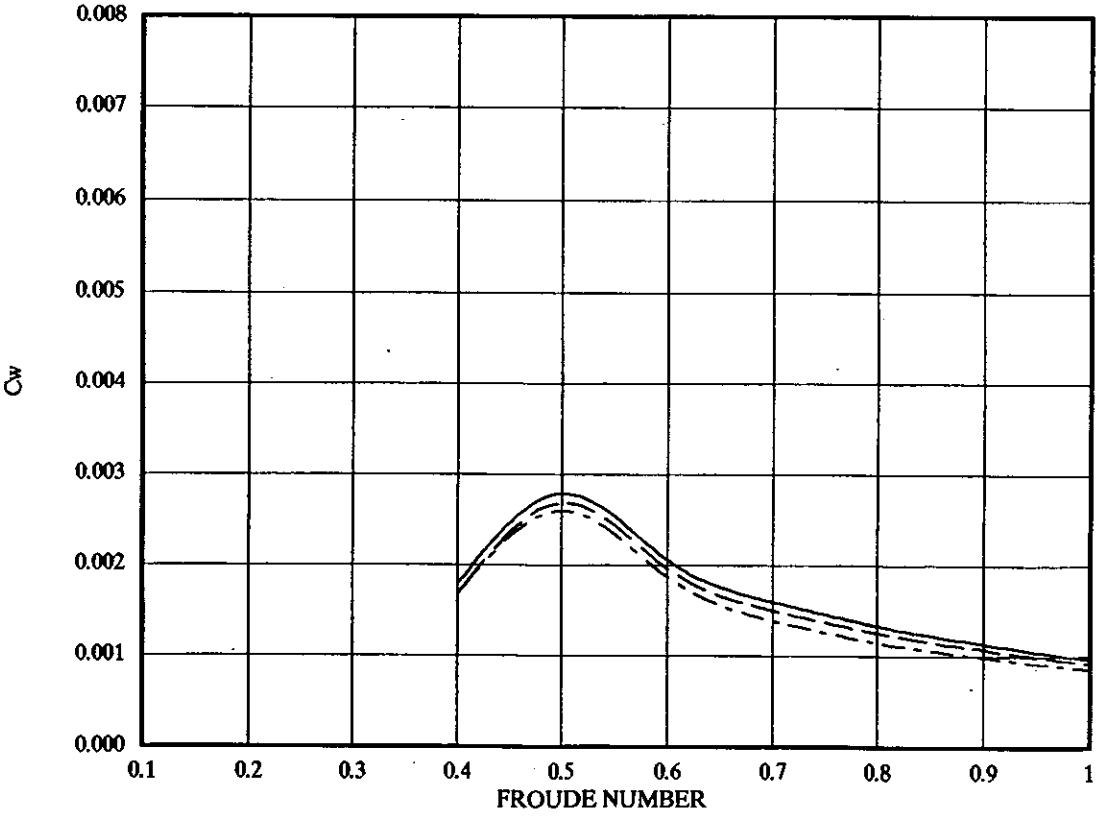

_ _ 5b ___ 5d _ _ _ 5e

FIGURE 60 THEORETICAL WAVE RESISTANCE FOR (HYDROSTATIC CORRECTED) 5b, 5d, 5e USING SINKAGE AND TRIM FROM EXPERIMENTAL RESULTS MONOHULL

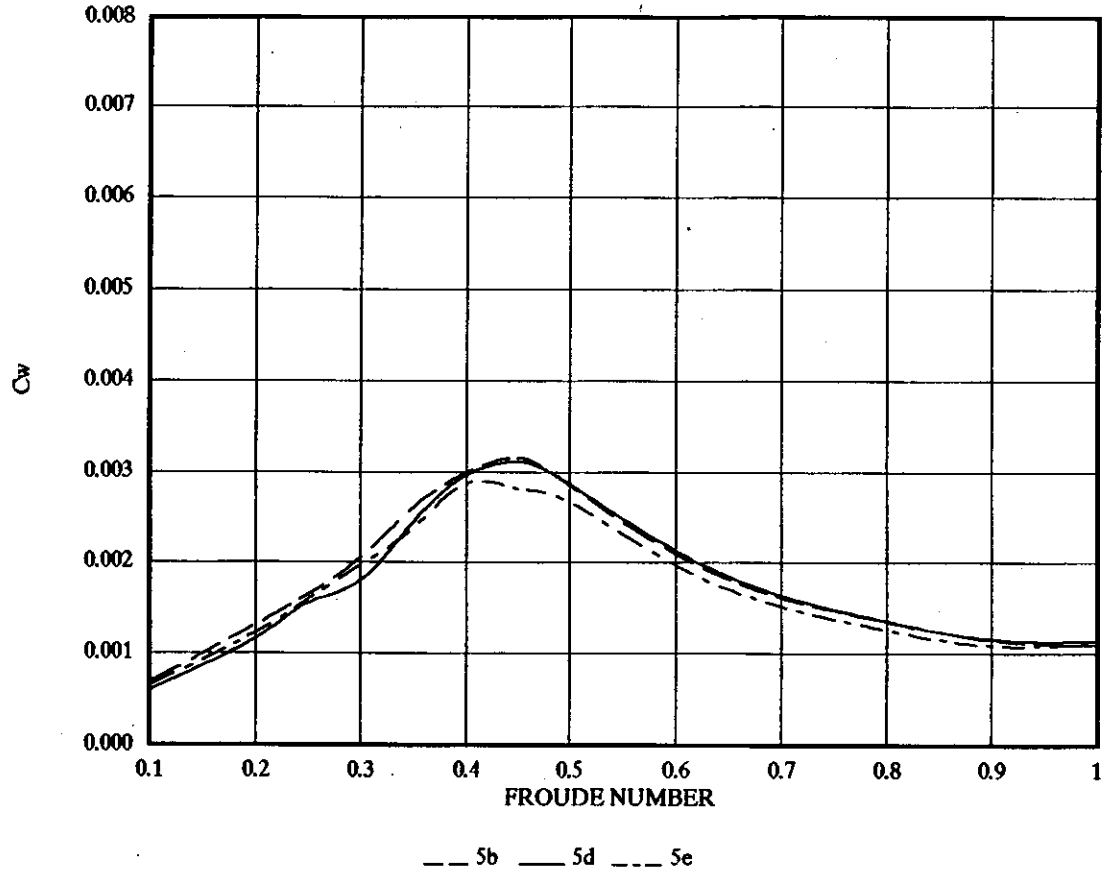

FIGURE 61 THEORETICAL WAVE RESISTANCE (TRANSOM SOURCE) 5b, 5d, 5e USING SINKAGE AND TRIM FROM EXPERIMENTAL RESULTS MONOHULL

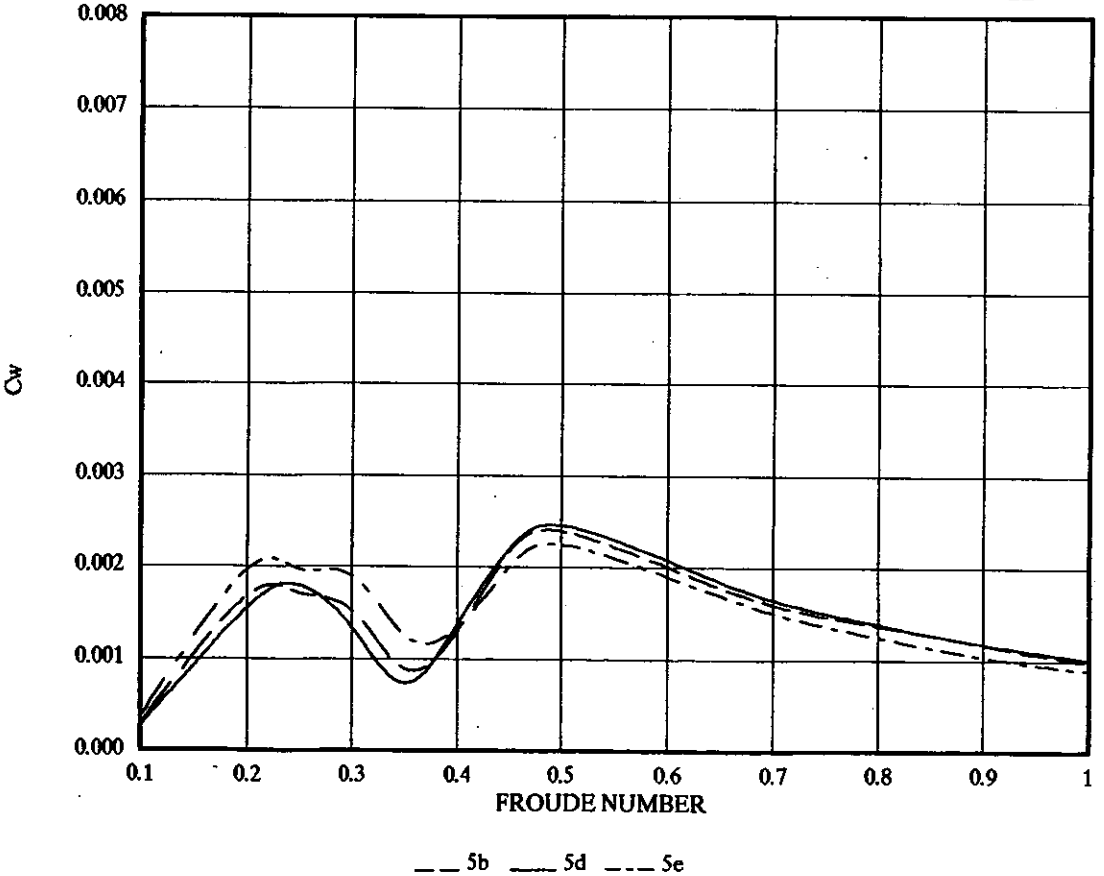

FIGURE 62 THEORETICAL WAVE RESISTANCE (HYDROSTATIC CORRECTED) 5d, 5e
USING SINKAGE AND TRIM FROM EXPERIMENTAL RESULTS S/L 0.2

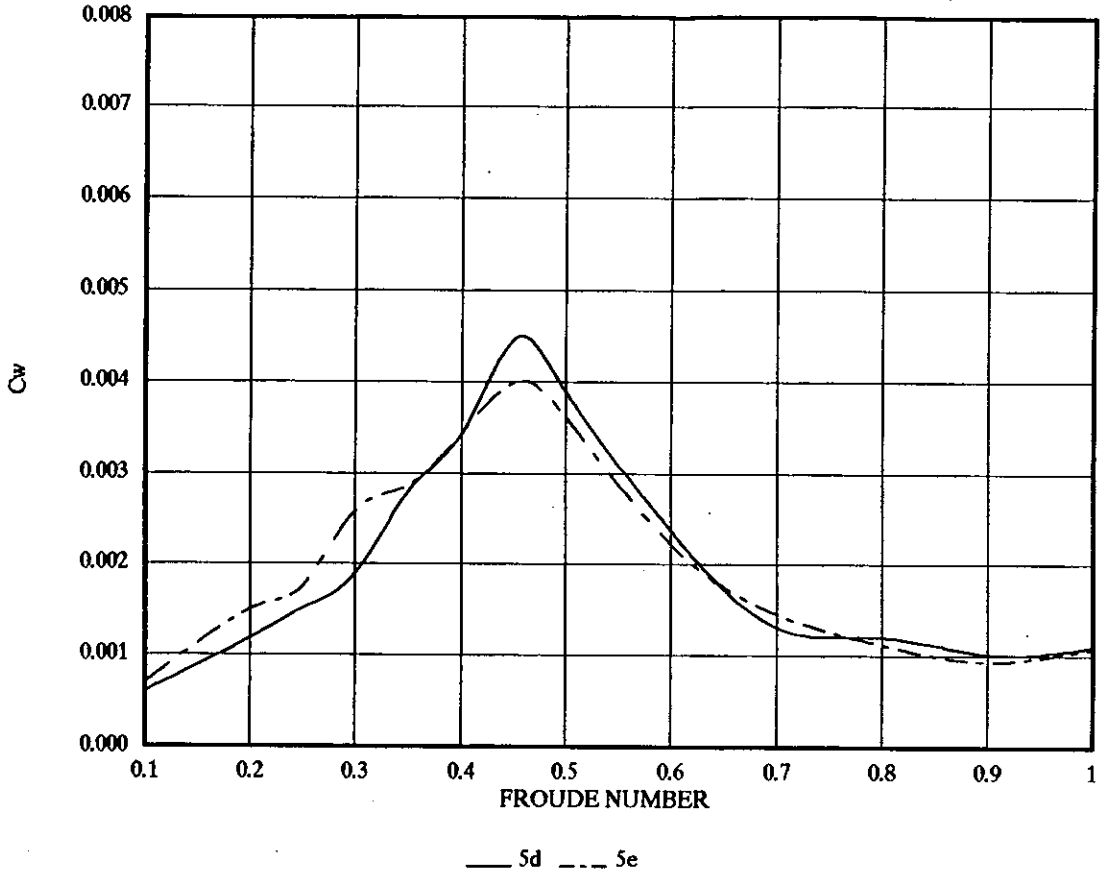

FIGURE 63 THEORETICAL WAVE RESISTANCE (TRANSOM SOURCE) 5d, 5e
USING SINKAGE AND TRIM FROM EXPERIMENTAL RESULTS S/L 0.2

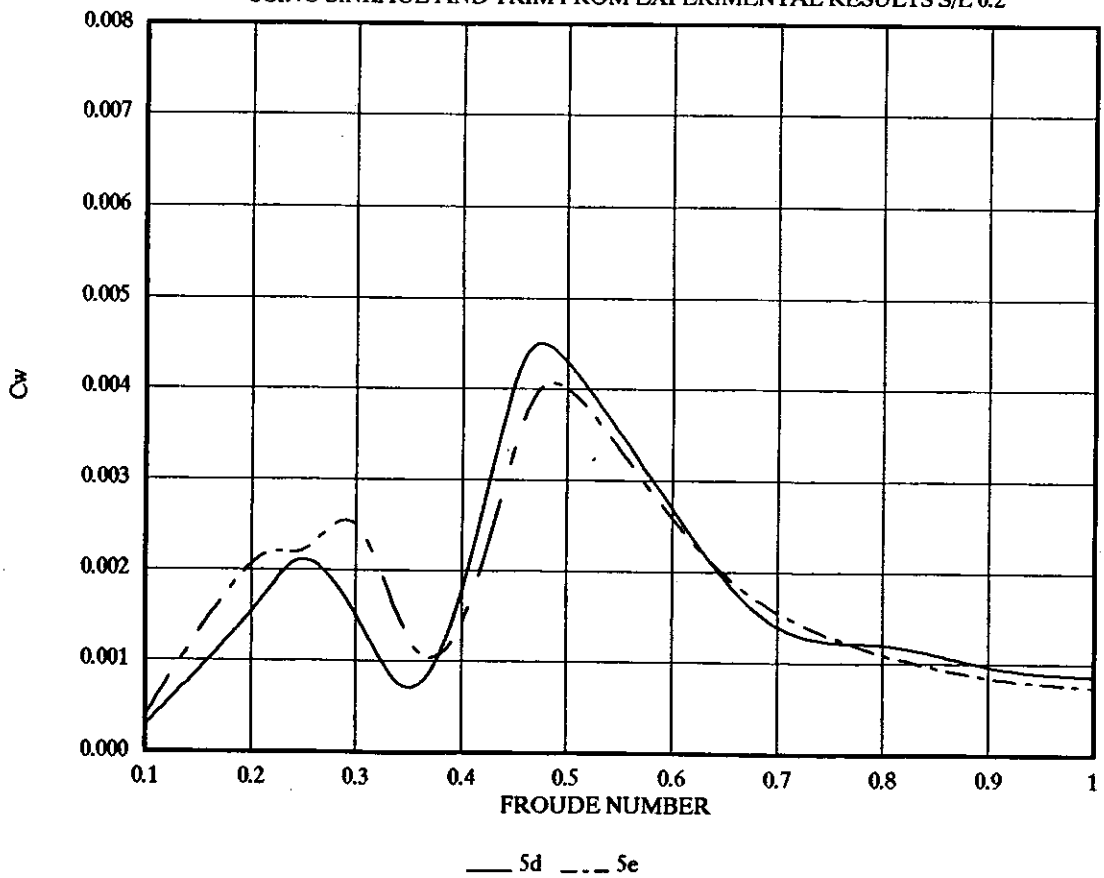

FIGURE 64 THEORETICAL WAVE RESISTANCE (HYDROSTATIC CORRECTED) 5b, 5d, 5e
USING SINKAGE AND TRIM FROM EXPERIMENTAL RESULTS S/L 0.3

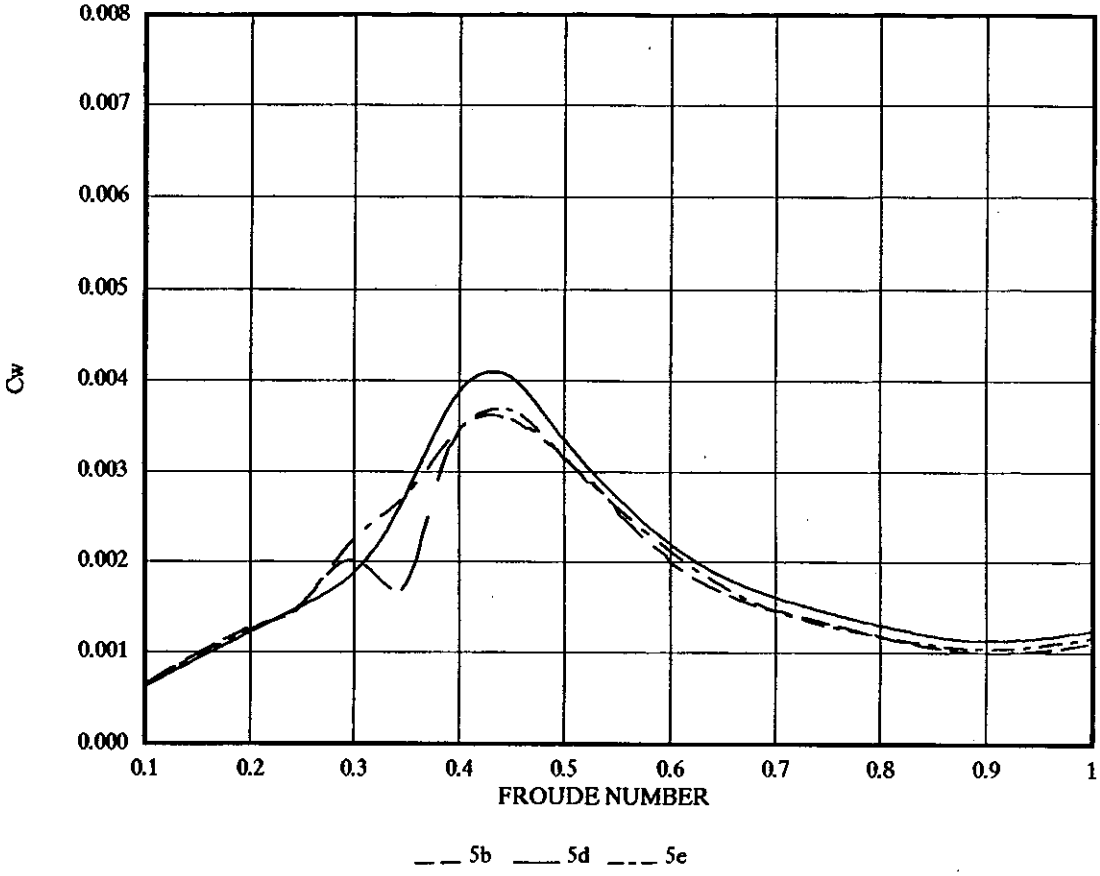

FIGURE 65 THEORETICAL WAVE RESISTANCE (TRANSOM SOURCE) 5b, 5d, 5e
USING SINKAGE AND TRIM FROM EXPERIMENTAL RESULTS S/L 0.3

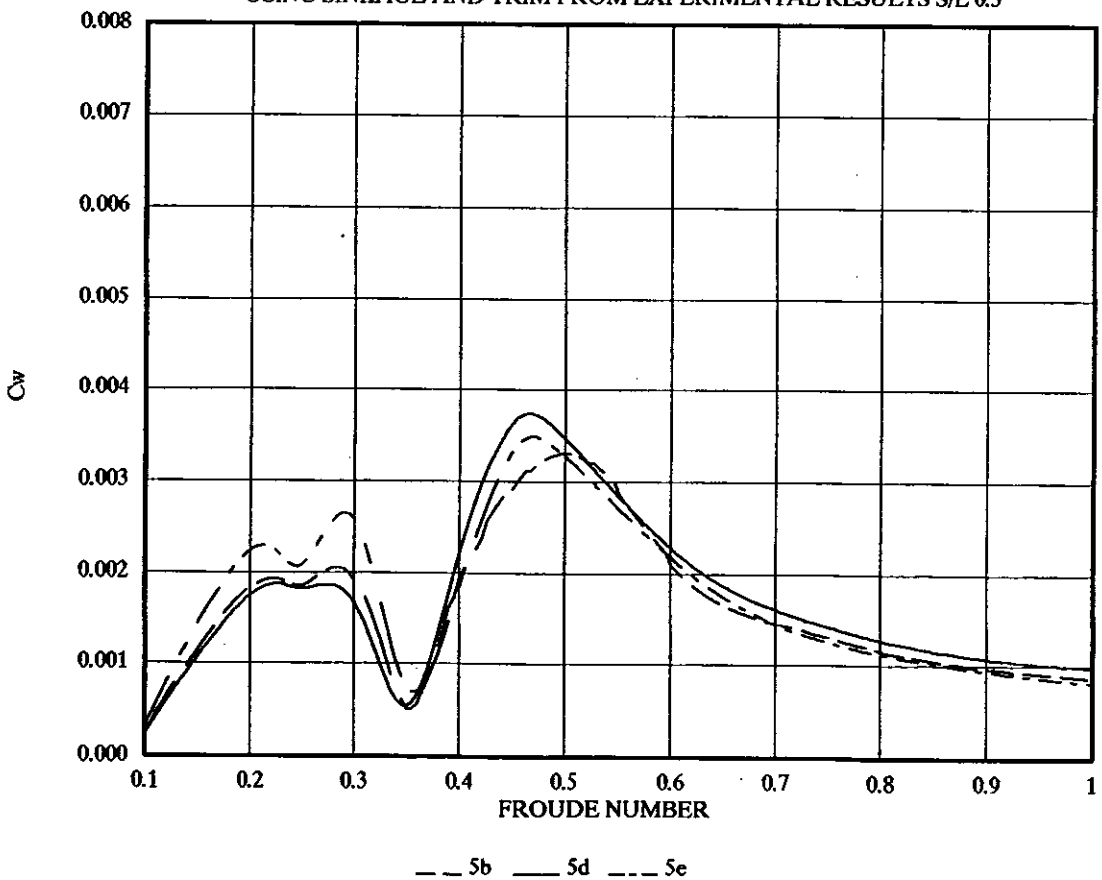

FIGURE 66 THEORETICAL WAVE RESISTANCE (HYDROSTATIC CORRECTED) 5d, 5e
USING SINKAGE AND TRIM FROM EXPERIMENTAL RESULTS S/L 0.4

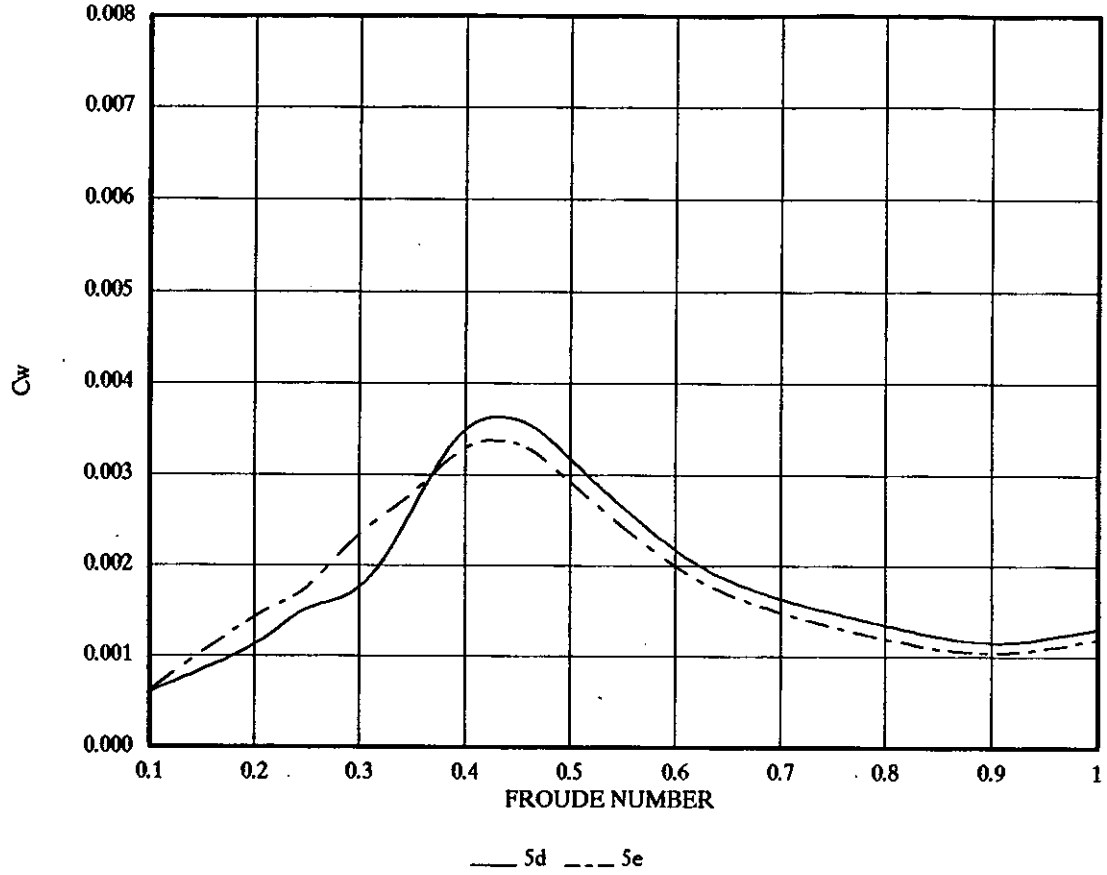

FIGURE 67 THEORETICAL WAVE RESISTANCE (TRANSOM SOURCE) 5d, 5e
USING SINKAGE AND TRIM FROM EXPERIMENTAL RESULTS S/L 0.4

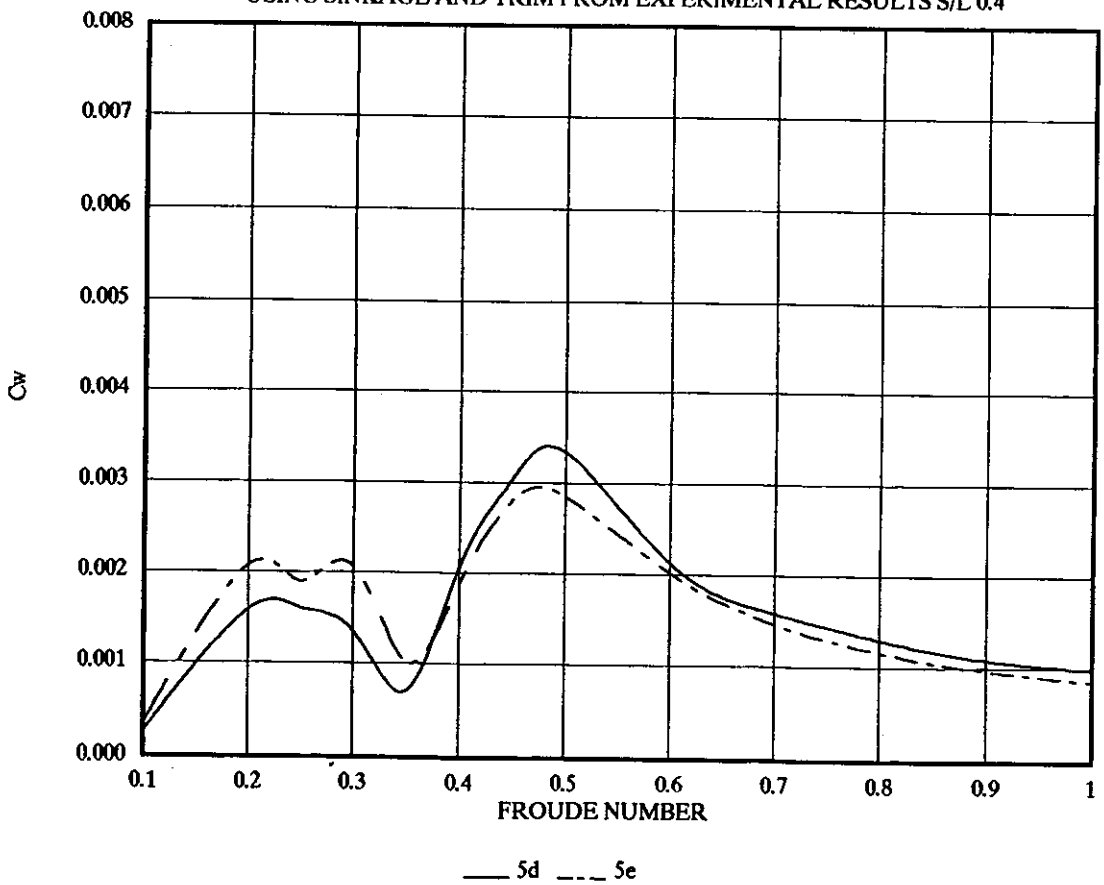

FIGURE 68 THEORETICAL WAVE RESISTANCE (HYDROSTATIC CORRECTED) 5b, 5d, 5e
USING SINKAGE AND TRIM FROM EXPERIMENTAL RESULTS S/L 0.5

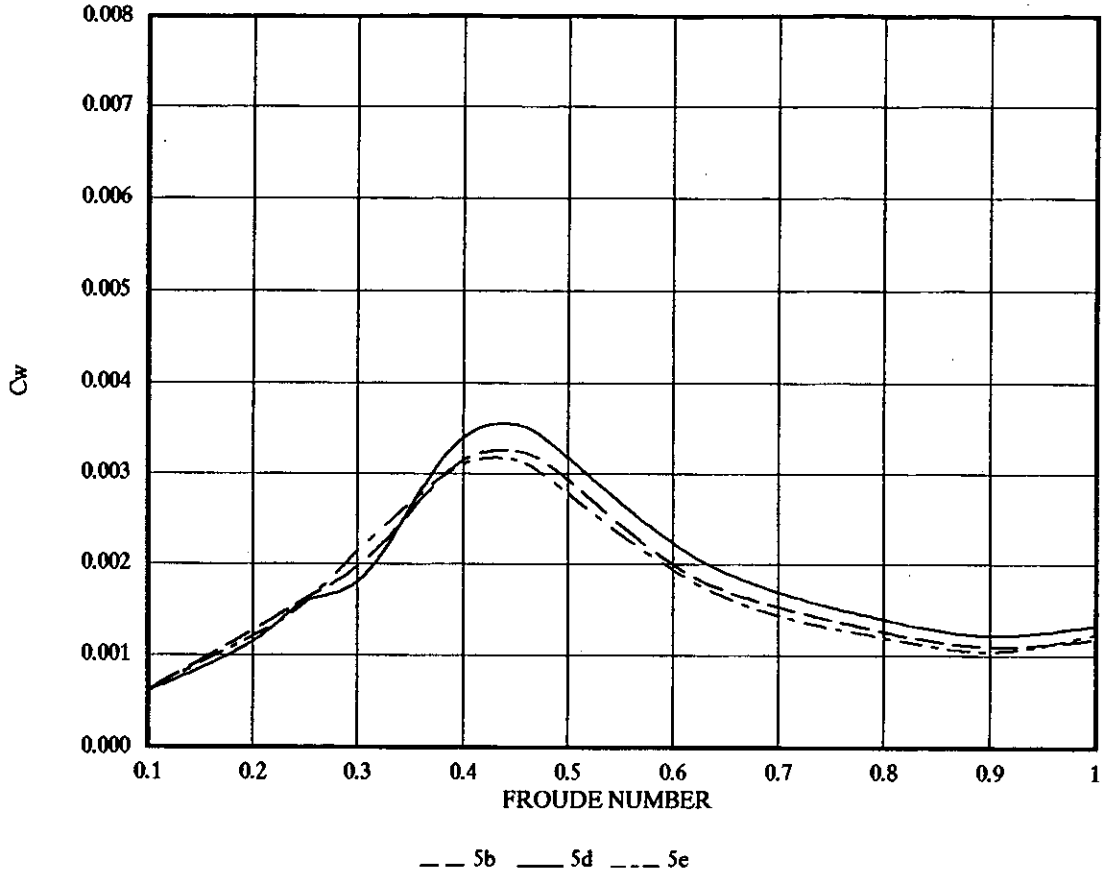

FIGURE 69 THEORETICAL WAVE RESISTANCE (TRANSOM SOURCE) 5b, 5d, 5e
USING SINKAGE AND TRIM FROM EXPERIMENTAL RESULTS FOR S/L 0.5

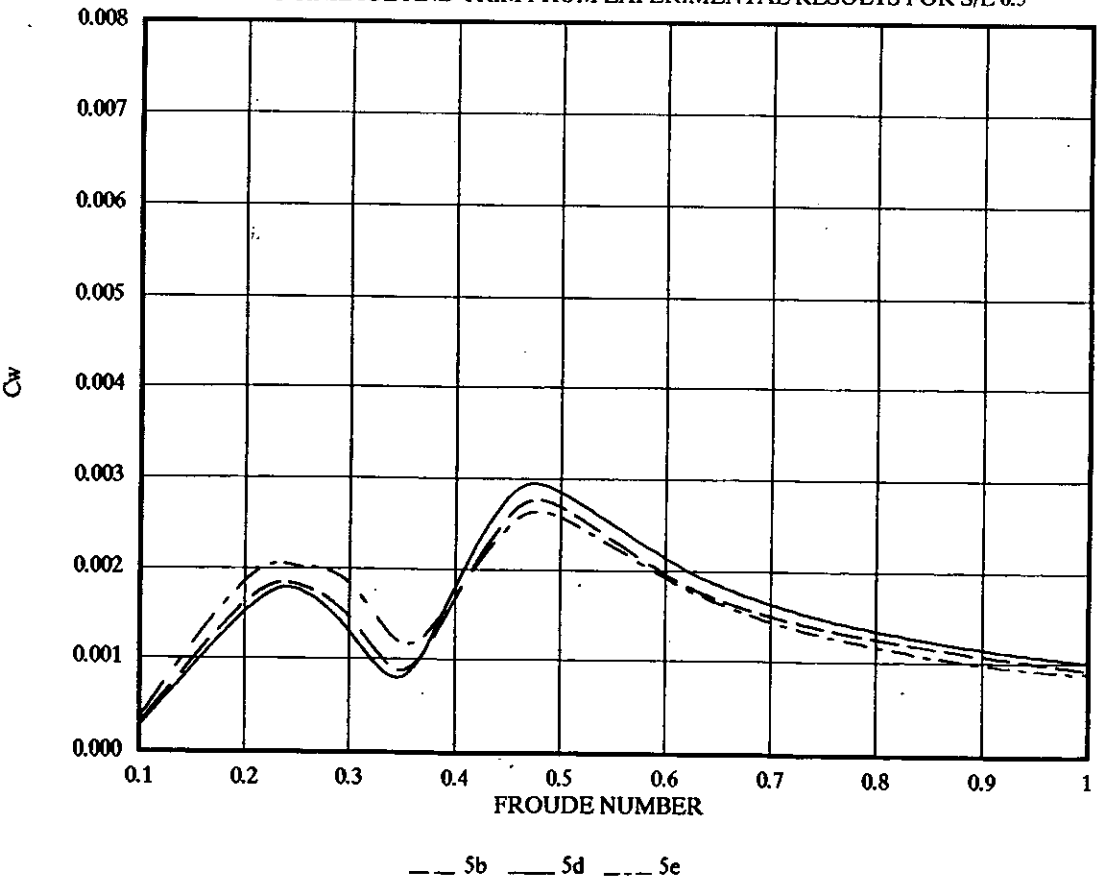

FIGURE 70 THEORETICAL WAVE RESISTANCE FOR 5d (HYDROSTATIC CORRECTED) USING SINKAGE AND TRIM FROM EXPERIMENTAL RESULTS

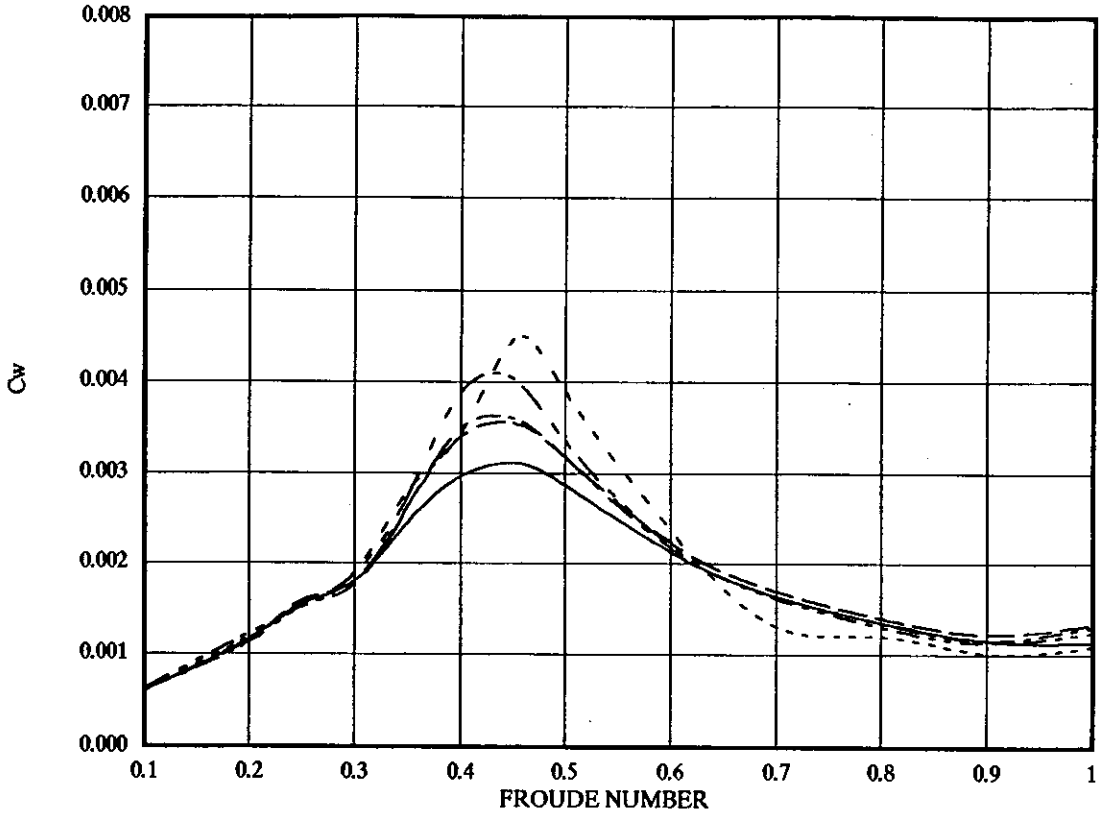

FIGURE 71 THEORETICAL WAVE RESISTANCE FOR 5d (TRANSOM SOURCE) USING SINKAGE AND TRIM FROM EXPERIMENTAL RESULTS

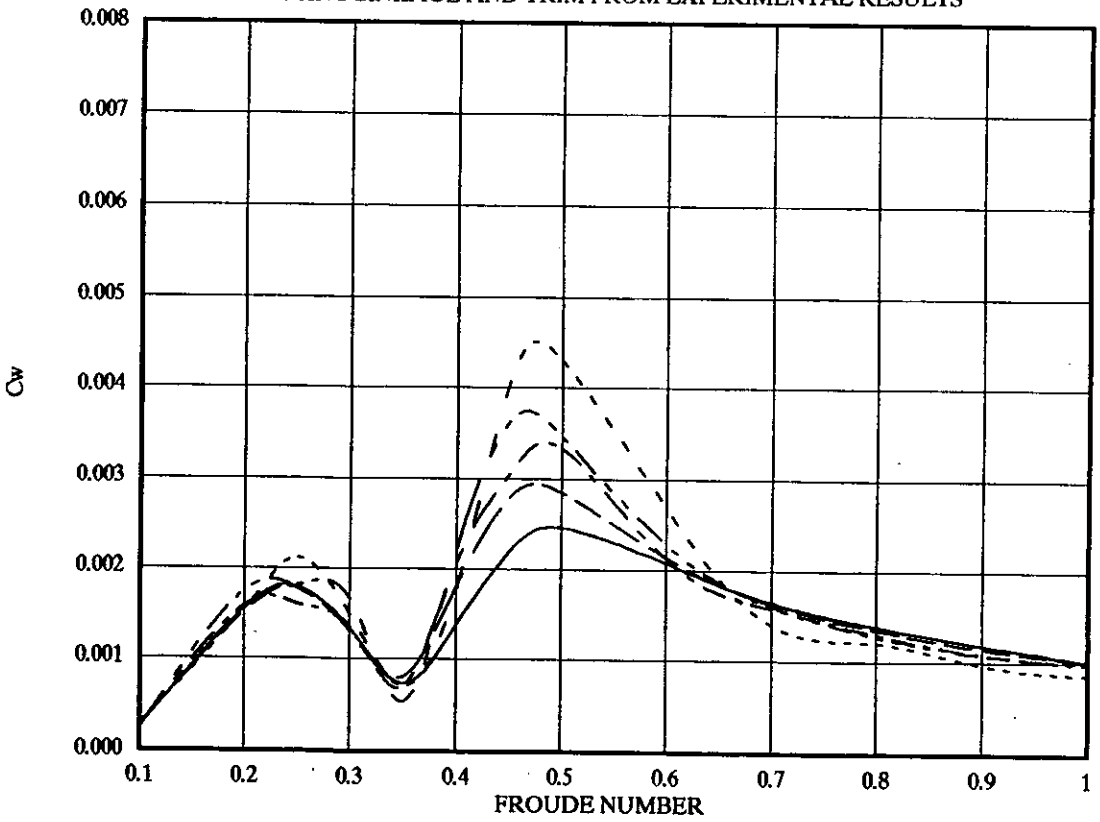

FIGURE 72 THEORETICAL WAVE RESISTANCE FOR 5e (HYDROSTATIC CORRECTED) USING SINKAGE AND TRIM FROM EXPERIMENTAL RESULTS

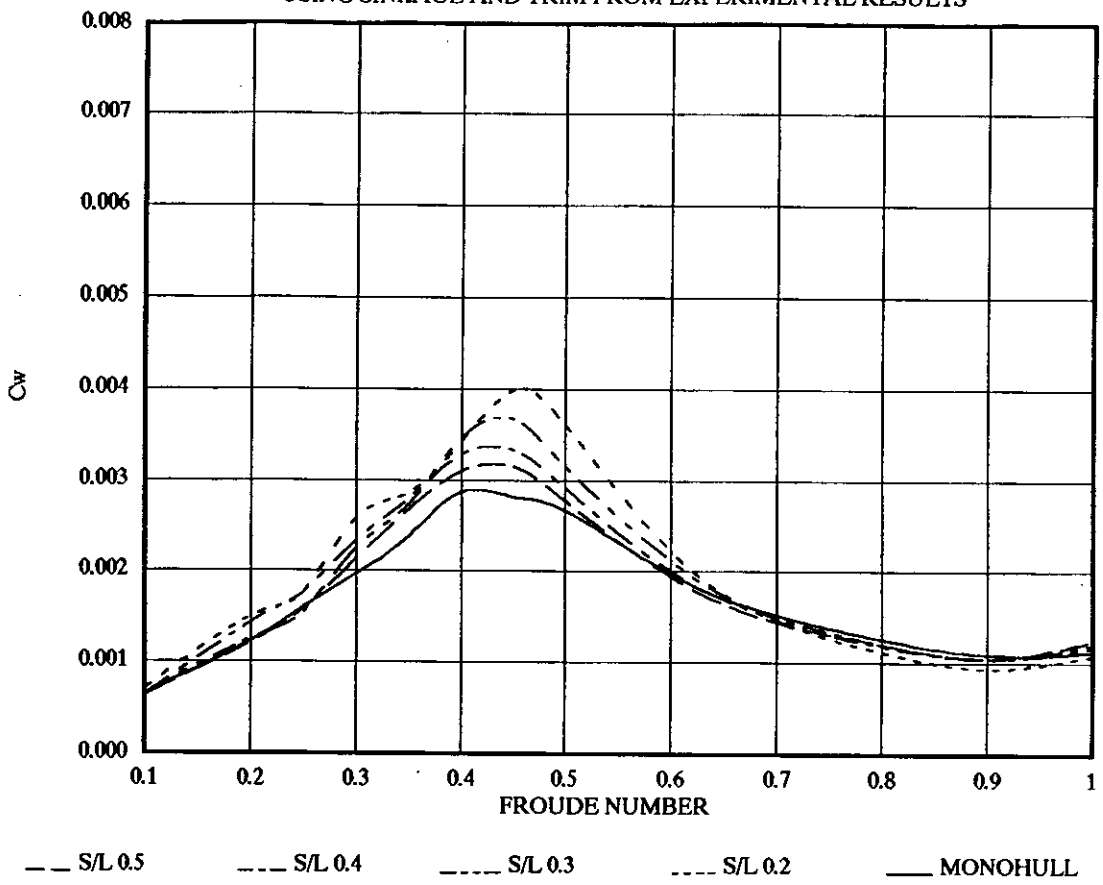

FIGURE 73 THEORETICAL WAVE RESISTANCE FOR 5e (TRANSOM SOURCE) USING SINKAGE AND TRIM FROM EXPERIMENTAL RESULTS

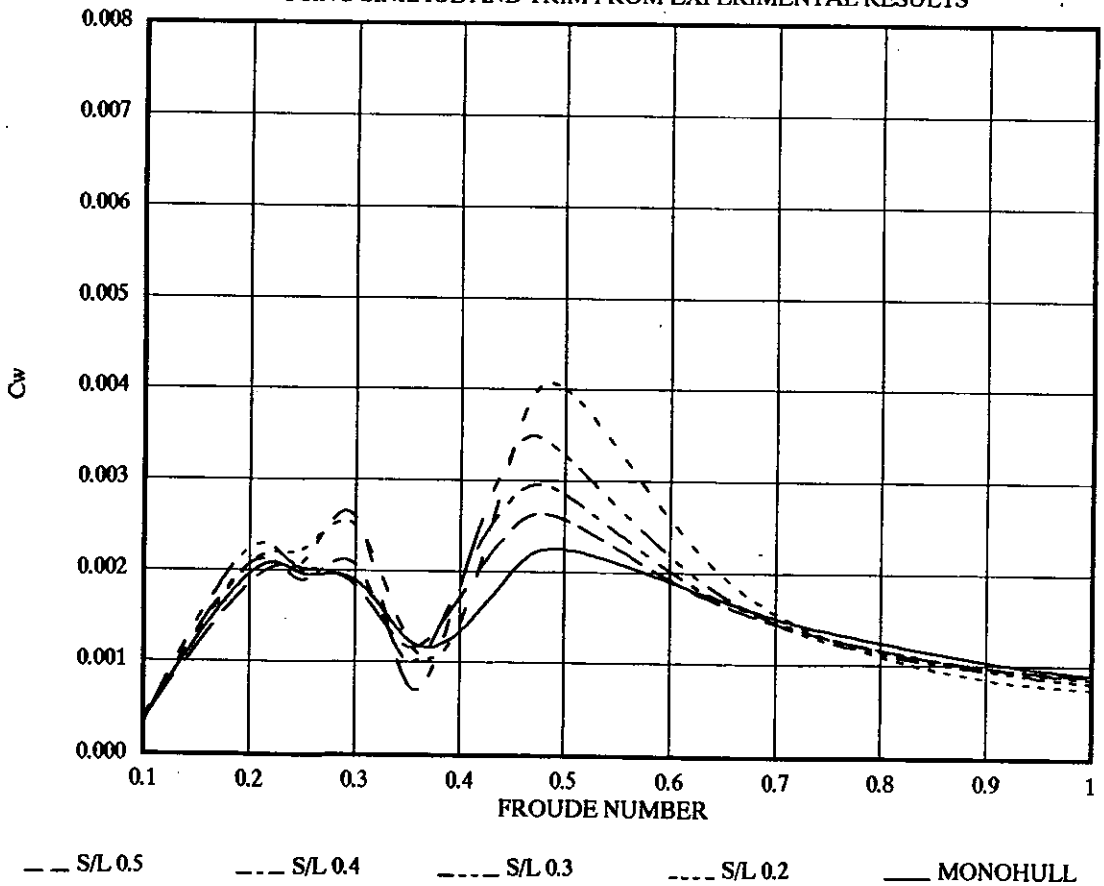

FIGURE 74 THEORETICAL WAVE RESISTANCE Cw (HYDROSTATIC CORRECTION)
5f AND 5g MONOHULL

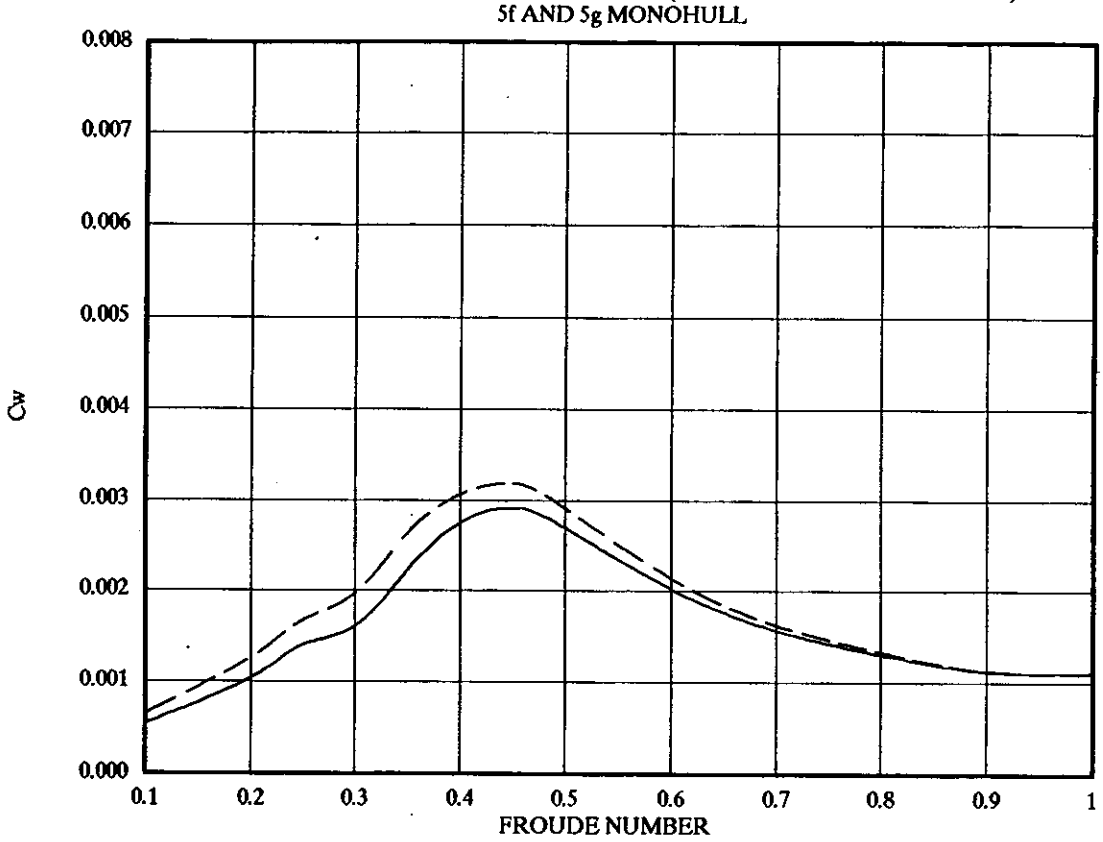

— — 5f (B/T 1.5) ——— 5g (B/T 2.5)

FIGURE 75 THEORETICAL WAVE RESISTANCE Cw (HYDROSTATIC CORRECTION)
5h AND 5i MONOHULL

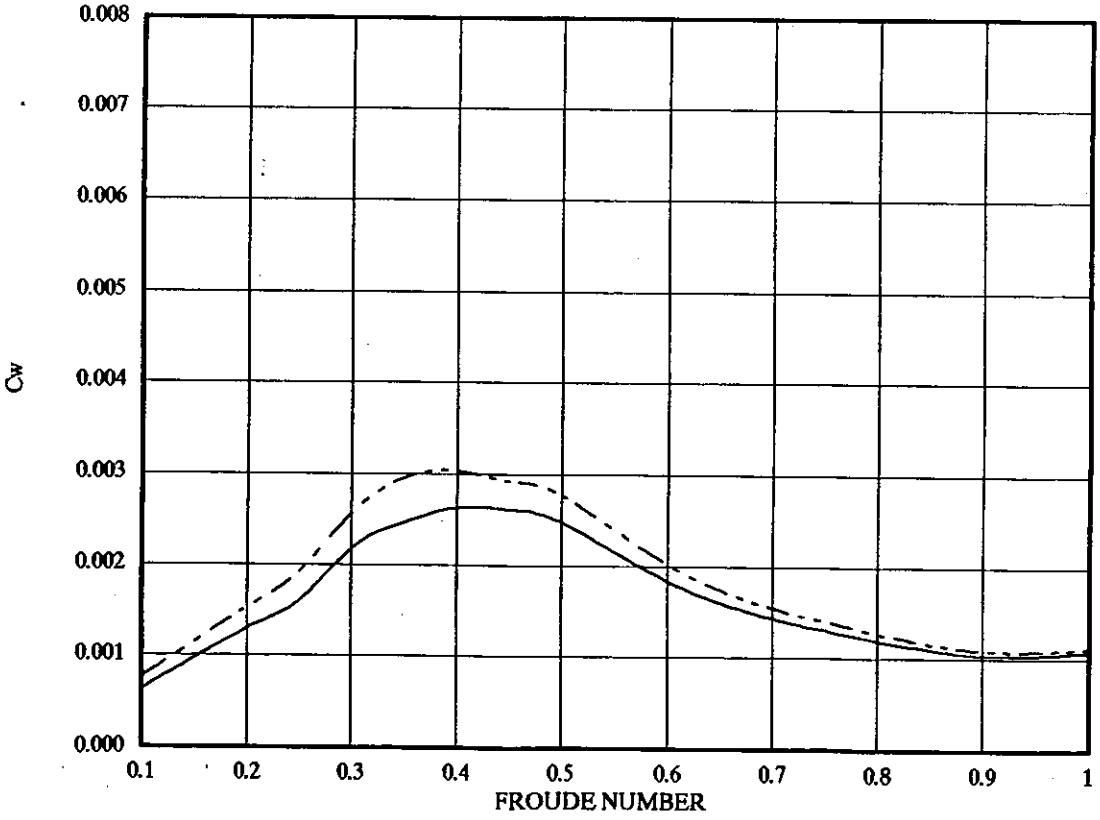

— — — — 5h (B/T 1.5) ——— 5i (B/T 2.5)

FIGURE 76 THEORETICAL WAVE RESISTANCE Cw (HYDROSTATIC CORRECTION)
5f AND 5g S/L 0.3

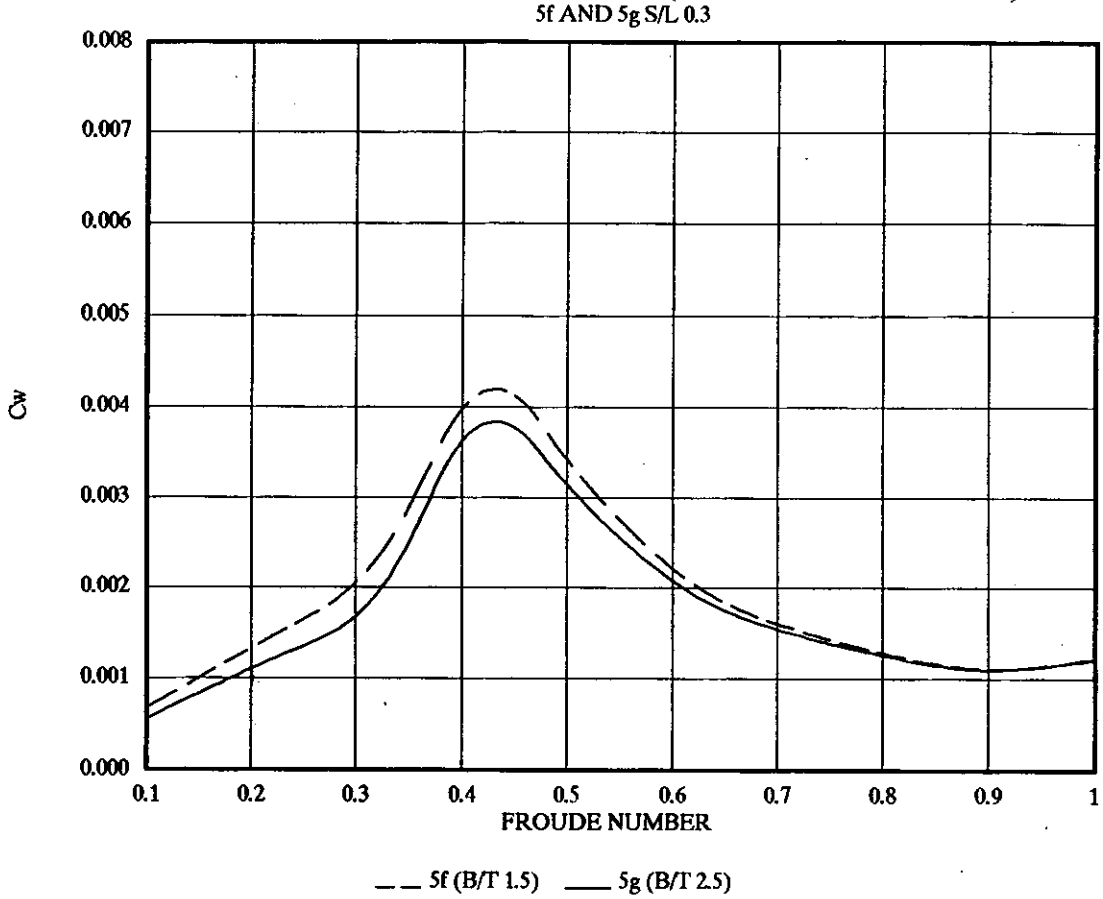

FIGURE 77 THEORETICAL WAVE RESISTANCE Cw (HYDROSTATIC CORRECTION)
5h AND 5i S/L 0.3

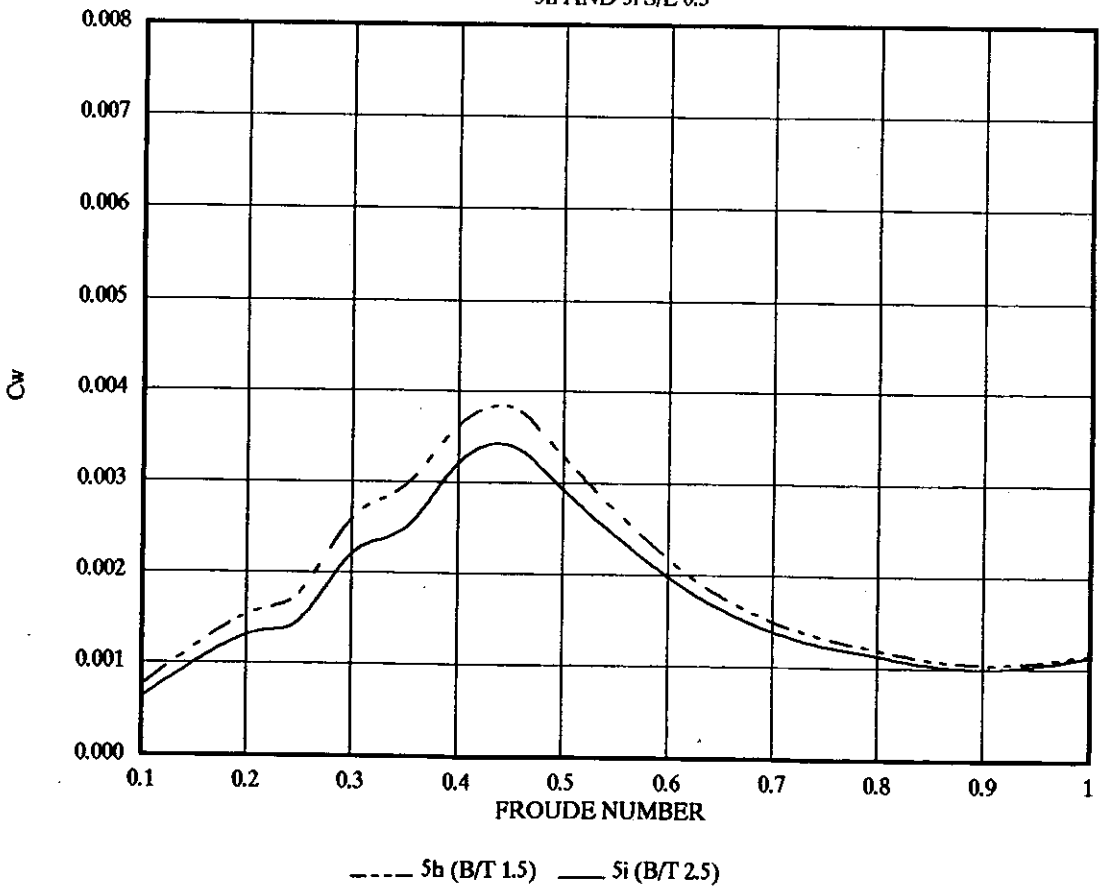

FIGURE 78 THEORETICAL WAVE RESISTANCE Cw (HYDROSTATIC CORRECTION)
5f AND 5g S/L 0.5

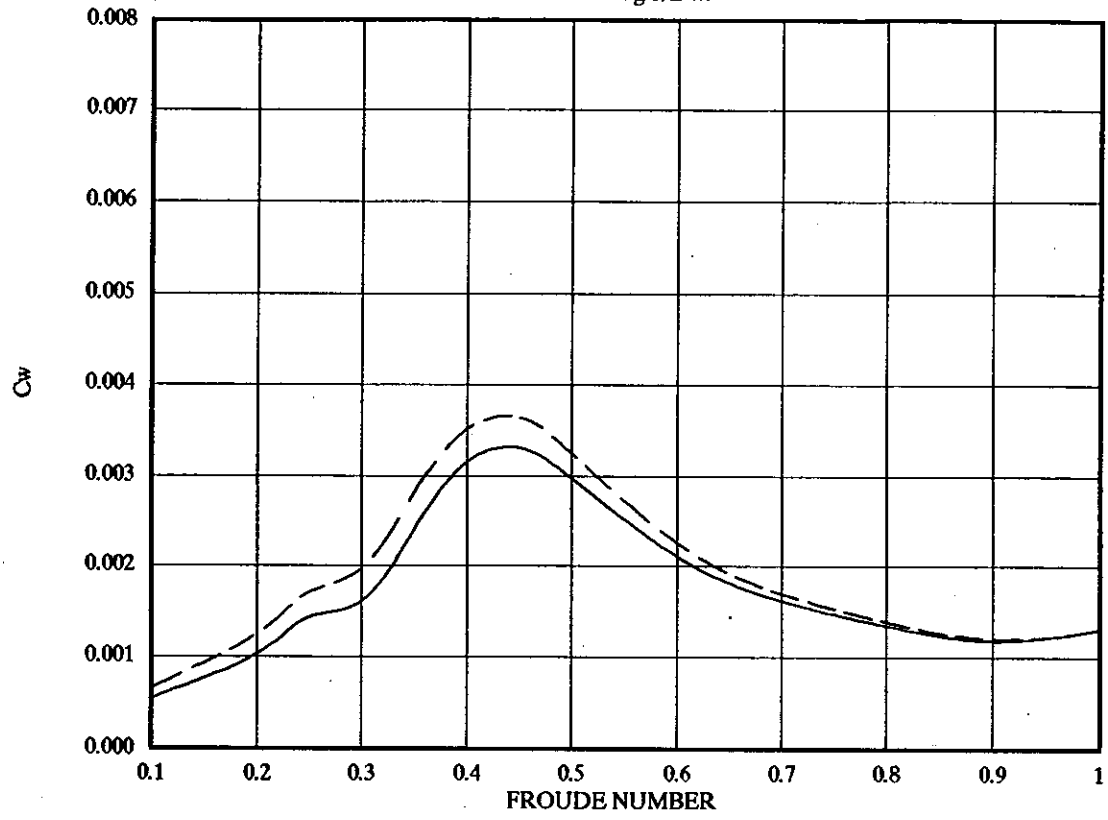

— — 5f (B/T 1.5) ——— 5g (B/T 2.5)

FIGURE 79 THEORETICAL WAVE RESISTANCE Cw (HYDROSTATIC CORRECTION)
5h AND 5i S/L 0.5

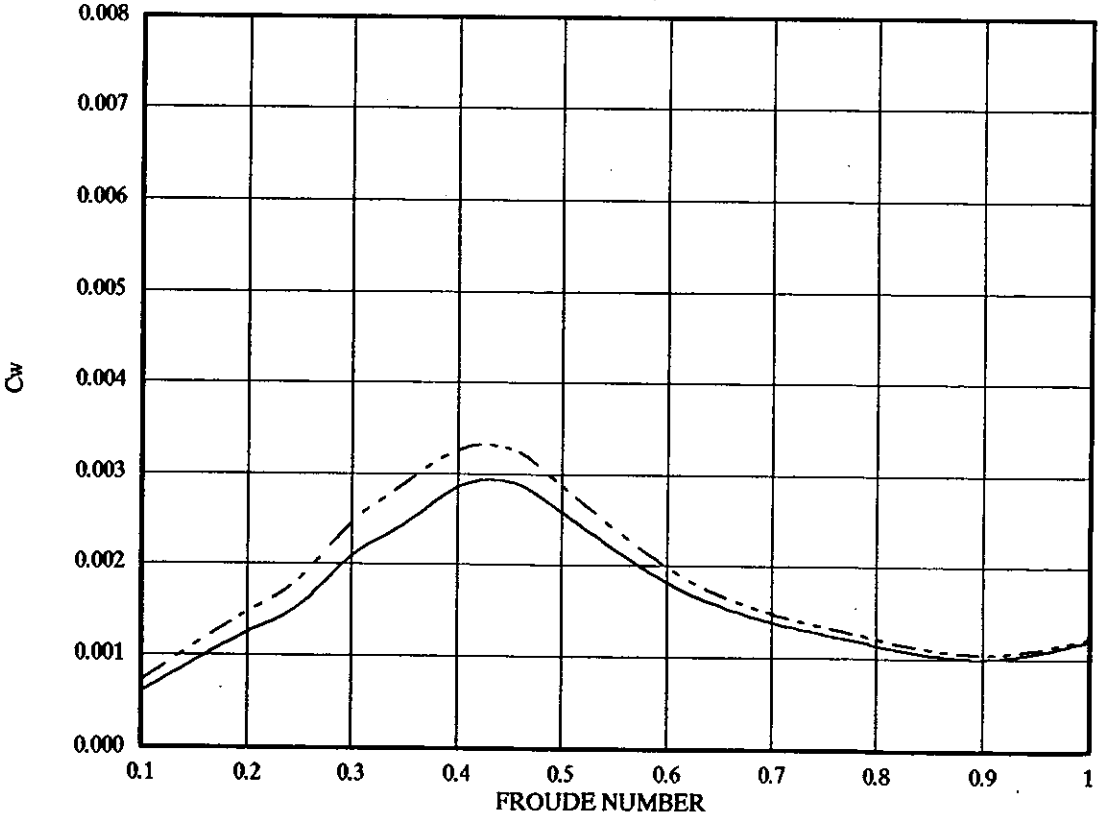

— — — — 5h (B/T 1.5) ——— 5i (B/T 2.5)

FIGURE 80 THEORETICAL WAVE RESISTANCE Cw (HYDROSTATIC CORRECTION)
6d AND 6e MONOHULL

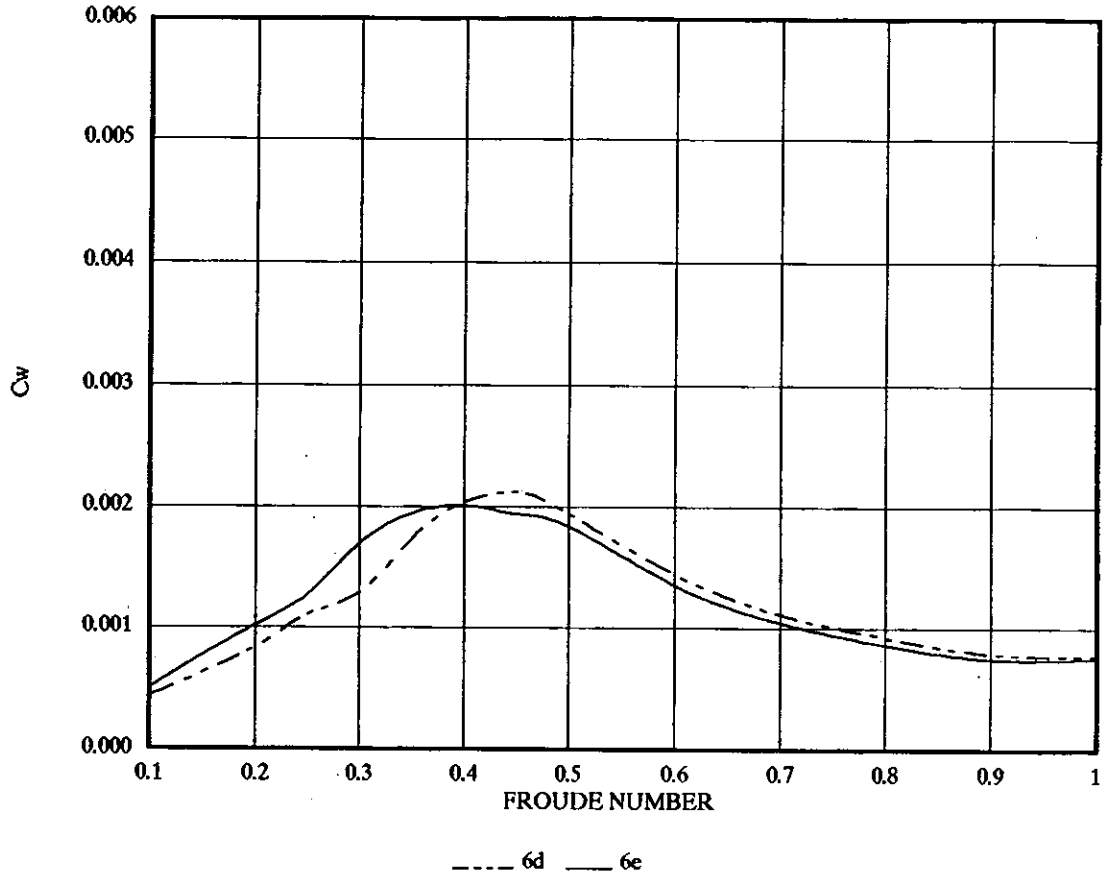

FIGURE 81 THEORETICAL WAVE RESISTANCE Cw (HYDROSTATIC COREECTION)
6d AND 6e S/L 0.3

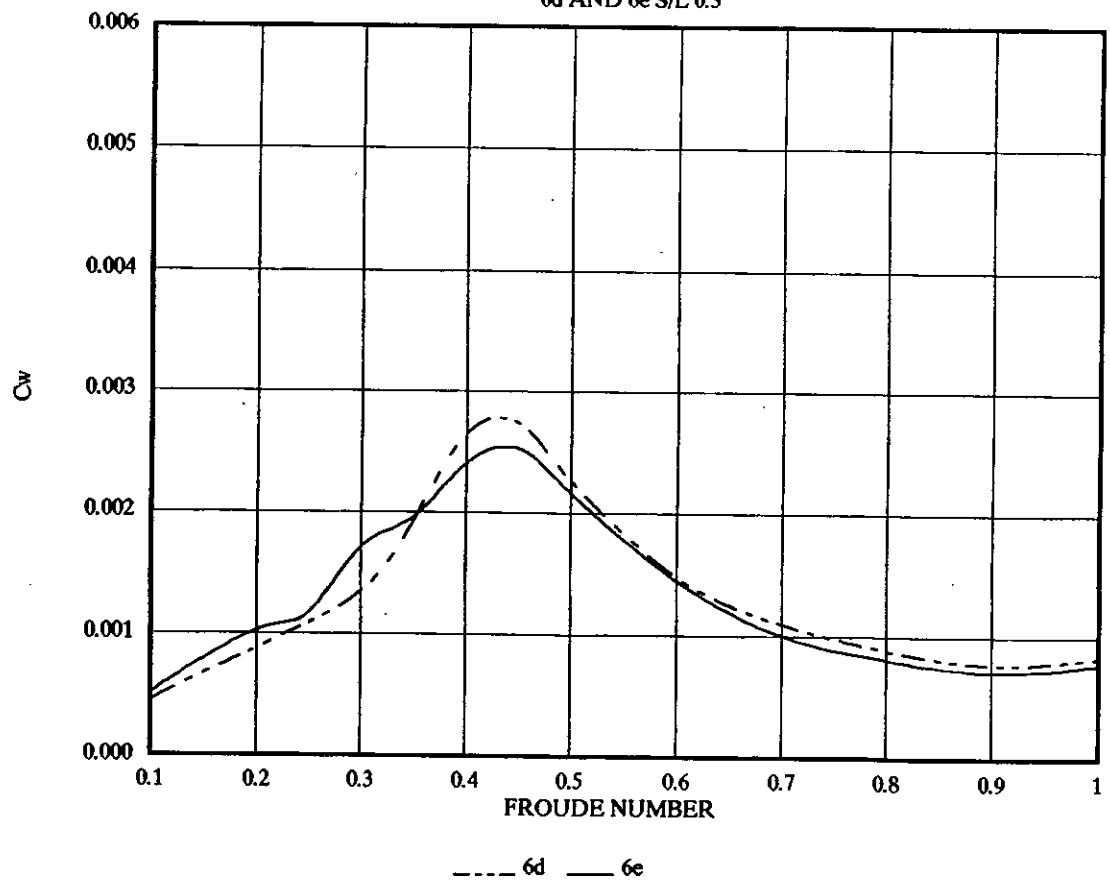

FIGURE 82 THEORETICAL WAVE RESISTANCE Cw (HYDROSTATIC CORRECTION)
6d AND 6e S/L 0.5

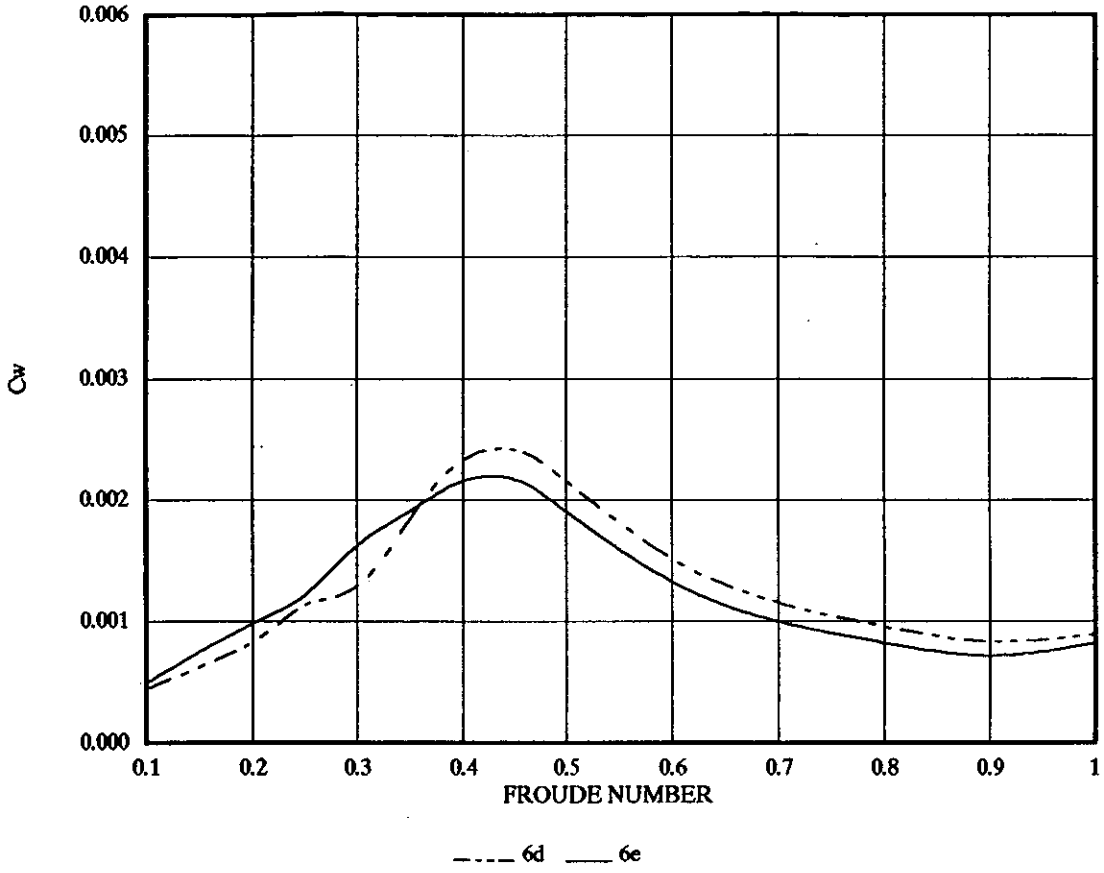

FIGURE 83 TRANSOM SOURCE STRENGTH
MONOHULL

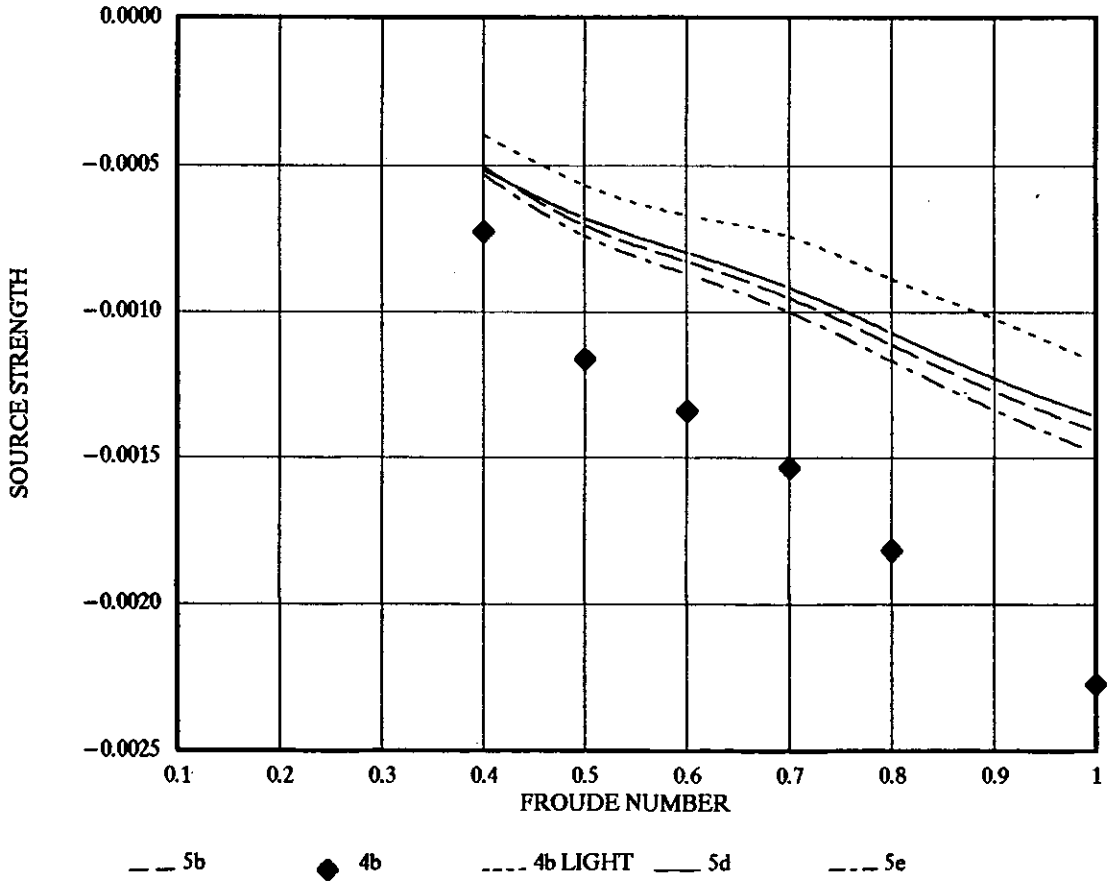

FIGURE 84

THEORETICAL WAVE RESISTANCE
6B MONOHULL

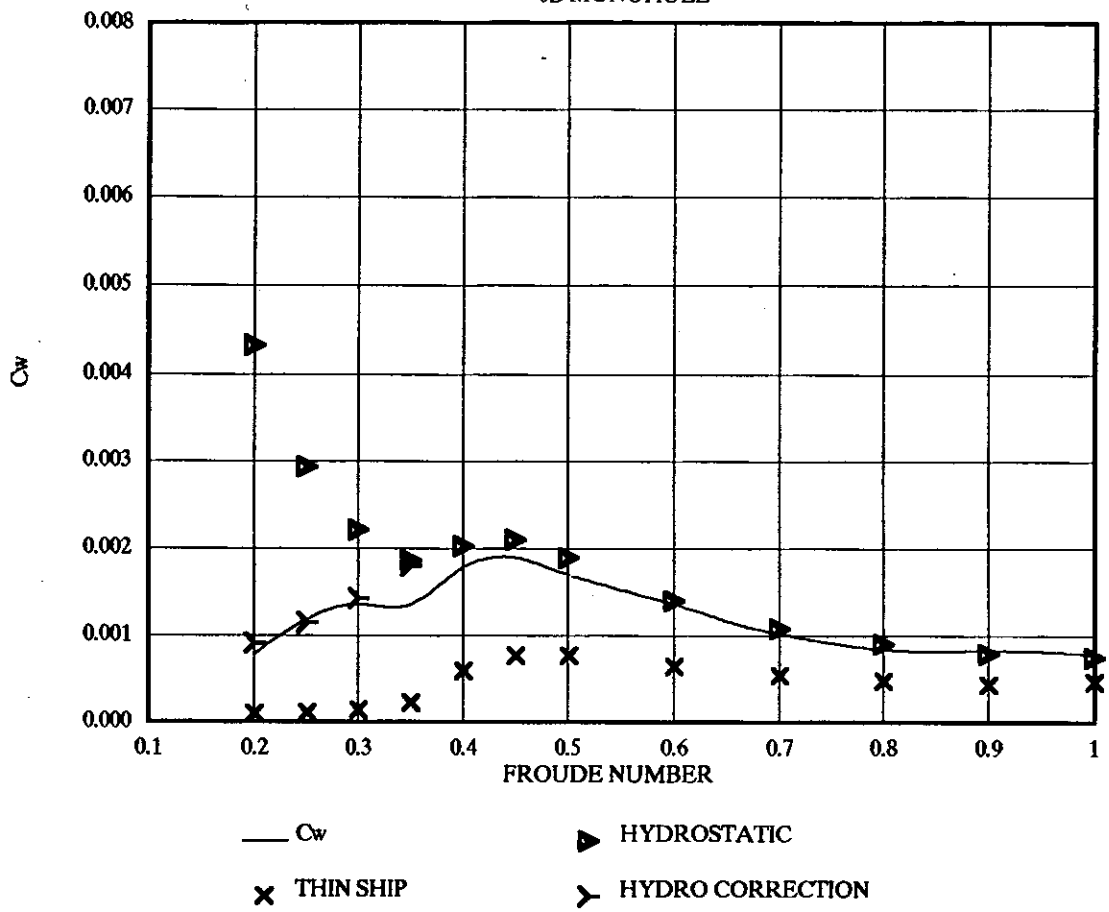

FIGURE 85

THEORETICAL WAVE RESISTANCE
6B S/L 0.3

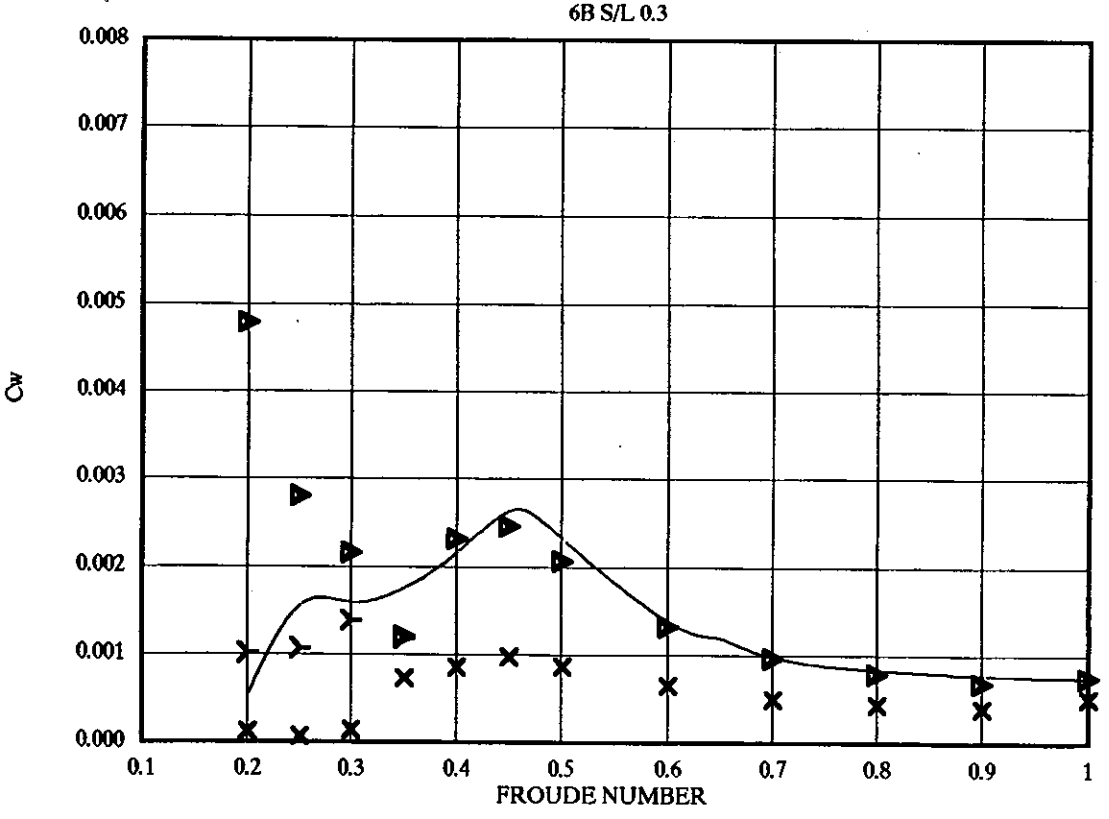

FIGURE 86

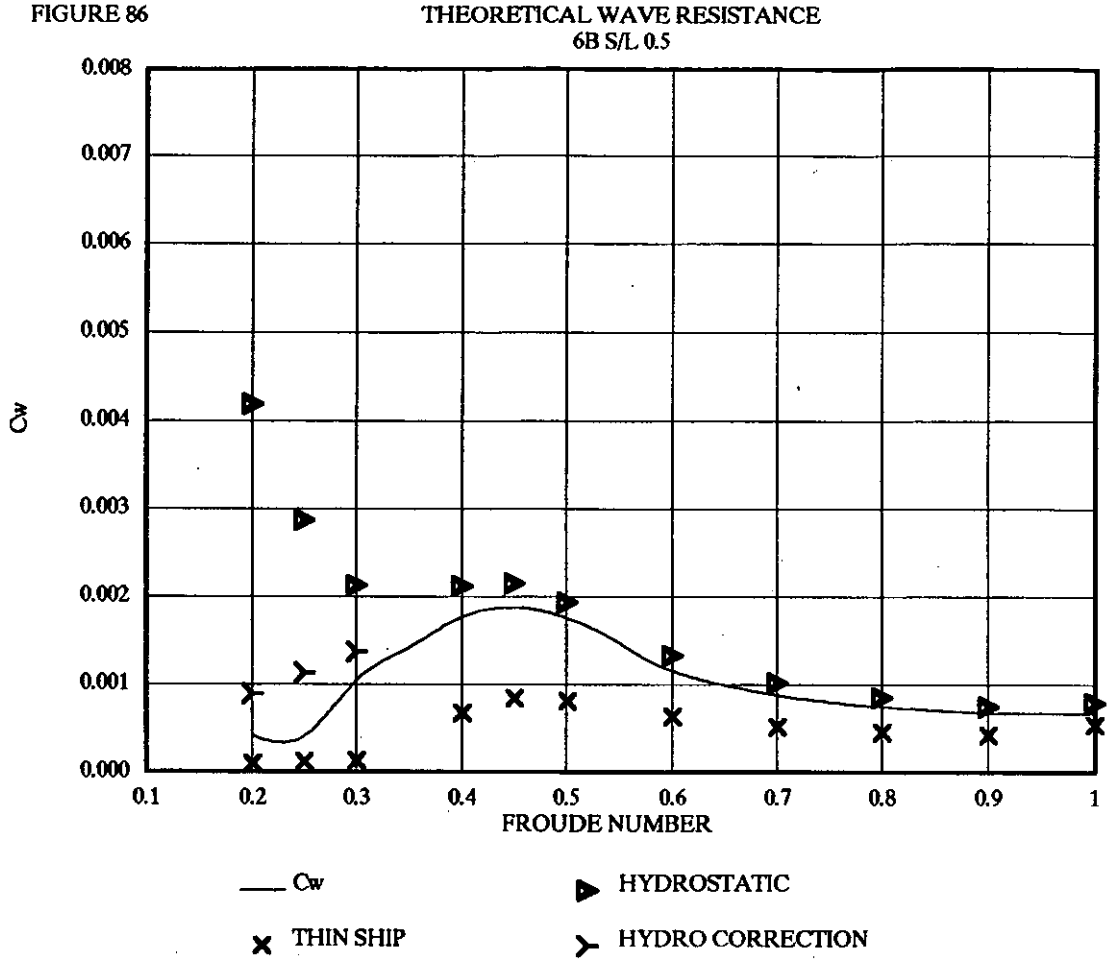
THEORETICAL WAVE RESISTANCE
6B S/L 0.5
Cw
0.008
0.007
0.006
0.005
0.004
0.003
0.002
0.001
0.000
0.1
0.2
0.3
0.4
0.5
0.6
0.7
0.8
0.9
1
FROUDE NUMBER
Cw
HYDROSTATIC
THIN SHIP
HYDRO CORRECTION